

2015

Rational design and characterization of electron-deficient heterocycles for organic photovoltaic materials

Dana Lynn Drochner
Iowa State University

Follow this and additional works at: <https://lib.dr.iastate.edu/etd>

 Part of the [Organic Chemistry Commons](#)

Recommended Citation

Drochner, Dana Lynn, "Rational design and characterization of electron-deficient heterocycles for organic photovoltaic materials" (2015). *Graduate Theses and Dissertations*. 14793.
<https://lib.dr.iastate.edu/etd/14793>

This Dissertation is brought to you for free and open access by the Iowa State University Capstones, Theses and Dissertations at Iowa State University Digital Repository. It has been accepted for inclusion in Graduate Theses and Dissertations by an authorized administrator of Iowa State University Digital Repository. For more information, please contact digirep@iastate.edu.

Rational design and characterization of electron-deficient heterocycles for organic photovoltaic materials

by

Dana Drochner

A dissertation submitted to the graduate faculty
in partial fulfillment of the requirements for the degree of

DOCTOR OF PHILOSOPHY

Major: Organic Chemistry

Program of Study Committee:
Malika Jeffries-EL, Major Professor
Jason Chen
Javier Vela
Arthur Winter
Yan Zhao

Iowa State University

Ames, Iowa

2015

Copyright ©Dana Drochner, 2015. All rights reserved.

DEDICATION

This dissertation is dedicated in loving memory of Donna E. David.

TABLE OF CONTENTS

	Page
CHAPTER 1 INTRODUCTION TO CONDUCTING POLYMERS	1
1.1 Dissertation overview	1
1.2 Introduction to organic photovoltaics	3
1.3 Bulk heterojunction solar cells.....	6
1.4 Material design considerations	16
1.5 References.....	20
CHAPTER 2 SYNTHESIS OF ORTHOESTERS AND HETEROCYCLES FROM TRITHIORTHOESTERS.....	27
2.1 Introduction.....	27
2.2 Results & Discussion	30
2.3 Conclusion	36
2.4 Acknowledgements.....	36
2.5 Experimental	36
2.6 References	41
CHAPTER 3 TOWARD THE SYNTHESIS OF 2,6-ASYMMETRIC BENZOBISOXAZOLES.....	43
3.1 Introduction to benzobisoxazoles	43
3.2 Synthesis of asymmetric trans-BBOs	48
3.3 Conclusion	56
3.4 Acknowledgements.....	56
3.5 Experimental	56
3.6 References.....	64
CHAPTER 4 TUNING THE BANDGAP OF BENZOBISOXAZOLE SEMICONDUCTING MATERIALS BY 2,6-SUBSTITUTION..	67
4.1 Introduction.....	67
4.2 Results & Discussion	70
4.3 Conclusion	81
4.4 Acknowledgements.....	81
4.5 Experimental	81
4.6 References.....	95
CHAPTER 5 TUNING THE BANDGAP OF CONJUGATED POLYMERS BY N-ACYLATION OF ISOINDIGO CONJUGATED POLYMERS	97
5.1 Introduction.....	97

5.2	Results & Discussion	98
5.3	Conclusion	106
5.4	Acknowledgements.....	106
5.5	Experimental	107
5.6	References.....	112
CHAPTER 6 ISATIN-BASED SMALL MOLECULES FOR ORGANIC PHOTOVOLTAIC MATERIALS.....		114
6.1	Introduction.....	114
6.2	Results & Discussion	115
6.3	Conclusion	120
6.4	Acknowledgements.....	121
6.5	Experimental	121
6.6	References	127
CHAPTER 7 CONCLUSION.....		129
7.1	Conclusion	129
7.2	Future work.....	129
7.3	Acknowledgements.....	141
7.4	References.....	141
APPENDIX LIST OF ACRONYMS AND DESCRIPTIONS		145

CHAPTER 1

INTRODUCTION TO CONDUCTING POLYMERS

1.1. Dissertation overview

This dissertation is comprised of work performed primarily by the author while in the Jeffries-EL research group from 2009-2015. The main goal of the research is to design, synthesize, and characterize new electron accepting constituents for organic photovoltaic (OPV) materials by analyzing the structure-property relationships arising from such structural modifications. Design of the materials is guided by the results of previous research and fundamental physical organic principles. The following overviews the composition of this dissertation and the role of each contributor toward the project.

Chapter 1 introduces organic semiconductors, with an emphasis on organic photovoltaic materials by exploring the operation principles of a bulk heterjunction (BHJ) solar cell, from the nanoscale to macroscale level. Chapter 1 concludes by discussing the various elements to consider when designing an organic photovoltaic material; concepts which are implemented in the following chapters.

New transformations of trithioorthoesters are studied in Chapter 2. The initial motivation was to develop a new route for synthesis of orthoesters, an important intermediate of benzobisoxazole (BBO) based compounds used in our group. We optimized this transformation and studied the scope of reactivity by synthesizing various orthoesters. The reaction was then expanded by synthesizing other heterocycles, demonstrating the utility of this versatile reaction which can have applications toward synthesis of other organic electronic building blocks. The concept for this

research was proposed by Dr. Jeffries-EL and implemented by the author of this dissertation along with James Klimavicz.

Chapter 3 introduces the properties and synthesis of benzobisoxazoles as used for OPV materials to preface the experimental attempts to synthesize 2,6-asymmetric *trans*-benzobisoxazoles.

The goal of Chapter 4 is to improve the electron accepting ability of benzobisoxazoles in conjugated polymers by altering the conjugation pathway and varying the substitution at the 2,6-position. Donor-acceptor-donor small molecules are used as a platform to study the structure-property effects of the 2,6-substitutions and then a polymer is synthesized with the benzobisoxazole which resulted in the lowest bandgap of the small molecules.

Having demonstrated in Chapter 4 that strategic addition of electron-withdrawing groups can lower the bandgap of the material, Chapter 5 continues that pursuit by focusing on substitution of another heterocycle, isodindigo. A new synthesis of an *N*-acyloyl isodindigo is presented and the structure-property effects of *N*-alkyl vs. *N*-acyloyl isodindigos are compared when incorporated into a donor-acceptor conjugated polymer.

Chapter 6 studies an electron-deficient heterocycle, isatin, used for the first time herein for the synthesis of a solution processable small molecule for organic photovoltaics. The structure is modified by a Knoevenagel condensation with the goal of decreasing the bandgap. Both molecules are characterized and their performance in the active layer of a bulk heterjunction solar cell is evaluated.

This dissertation concludes with general remarks and ideas of future research for benzobisoxazoles and donor-acceptor small molecules, followed by acknowledgements.

1.2. Introduction to organic photovoltaics

Energy demand is expected to increase by 56% by 2040¹, yet the supply of traditional fossil fuels is expected to be depleted within the next 120 years². This inversely proportional relationship of fossil fuel availability to global energy demand highlights the urgent need for practical, renewable sources of energy. The largest source of energy in our solar system by far is the sun itself and it has the potential to be harnessed in some capacity in most environments. While the greatest solar resource in the United States is located in the southwest, even the northern states can, on average, receive about 4 kWh/m²/day³. Future energy models predict that solar will become one of the prominent renewable energy sources, accounting for up to 14% of the global supply by 2040⁴. The development of cost-efficient photovoltaic devices would help open more markets for renewable energy and, in recent years, the cost of silicon based solar panels has reached a level of practical affordability for most consumers⁵, but continuing development of organic electronics holds the promise of obtaining the most economical devices⁶.

Unlike inorganic semiconductors, semiconducting organic molecular or polymeric materials offer the advantages⁷ of not only cheaper overall cost, but easier fabrication via conventional printing techniques⁸, flexibility⁹, and a variety of synthetic techniques can be utilized to tune the material for any desired application or property. With these unique properties, organic electronics could find niche applications such as integration into apparel, customer electronics, and off-grid power generation¹⁰, as well as hybrid organic/inorganic tandem solar cells¹¹. While the latest certified organic photovoltaic device achieved a 12% efficiency in 2013¹², more research progress is needed to further advance the efficiencies of organophotovoltaics to compete with the dropping prices of traditional solar.

The photoconductivity properties of organic compounds have long been known, beginning with the small molecules and then conjugated polymers. Heeger, MacDiarmid, and Shirakawa discovered in 1977 that doping of polyacetylene enhanced its photoconductivity¹³, for which they received the Nobel Prize in 2000. Tang reported the first bilayer organic heterojunction¹⁴ solar cell by 1986 and the field of organic photovoltaics has expanded ever since¹⁵. The combinations of organic structures that can be utilized for devices, ranging from the semiconducting backbone units to solubilizing or functional side groups, is seemingly infinite and in an effort to increase device performance, research strategically focuses on such structure-property relationships and the underlying physics of the processes involved as well as improved device engineering methods. With the increase in efficiency gained in the last few years, ongoing research can contribute to even better device performances.

1.2.1. Origin of organic semiconductors

Before exploring the variety of structures used for organic electronics, we will discuss the origin of their semiconducting properties in the context of conjugated polymers. Solution processable conjugated small molecules are emerging as popular materials and certainly many of the properties discussed below apply to them as well.

The property of conductivity determines whether a material is a metal (10^6 to 10^4 (Ωcm)⁻¹), semiconductor (10^4 to 10^{-10} (Ωcm)⁻¹), or insulator ($< 10^{-10}$ (Ωcm)⁻¹)¹⁶. The semiconducting nature of a material depends on its bandgap, defined as the difference in the conduction and valence bands, with the bands being the summation of the energy levels occupied (valence) and unoccupied (conduction) by electrons. When there is no gap the material is a conductor and electrons can flow freely, such as in metals (Figure 1.1). A small gap gives the material semiconducting properties such that electrons can be excited to the conduction band by electrical, chemical, or thermal

stimulation. Larger bandgaps result in insulating materials which cannot conduct charges under normal operating conditions.

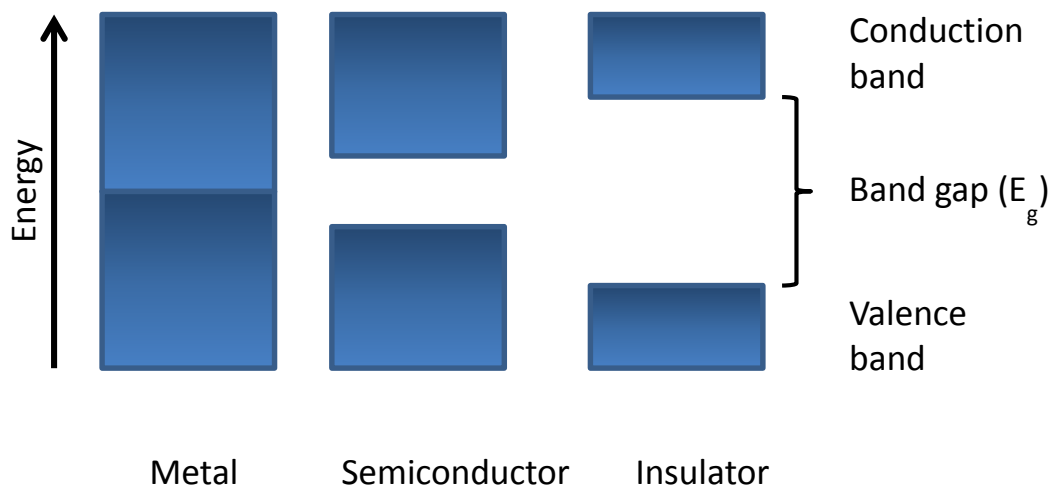


Figure 1.1. Band diagram of metallic, semiconducting and insulating materials.

The nature of organic semiconductors is based on an increasing degree of conjugation¹⁷ within the molecule. When conjugation, the alternation of double and single bonds, in an organic molecule increases, the filled bonding and antibonding pi molecular orbitals of the structure builds up to a state that they resemble the valence and conduction bands of traditional inorganic semiconductors. The bandgap is the energy gap between the highest occupied molecular orbital (HOMO) and lowest unoccupied molecular orbital (LUMO).

One might imagine that as the degree of conjugation increases, the bandgap continuously decreases to a point where it vanishes and the material obtains metallic properties; however this does not occur. It is true that the bandgap decreases up to a certain point at which the material has reached its so-called effective conjugation¹⁸ and no further decrease can be obtained by extending conjugation. Due to Peierl's distortion¹⁹, organic metals do not exist. For example, consider the material polyacetylene which is comprised of alternating double and single bonds. At first glance,

it appears that a resonance form can be drawn by exchanging the position of these bonds, and therefore can be denoted with equal bond lengths similarly to that of a benzene ring (Figure 1.2). In actuality, it has been observed by NMR and X-ray crystallography²⁰ that the alternating bonds differ by approximately 0.08 \AA ²¹, resulting in a bandgap of 1.5-2.0 eV²².

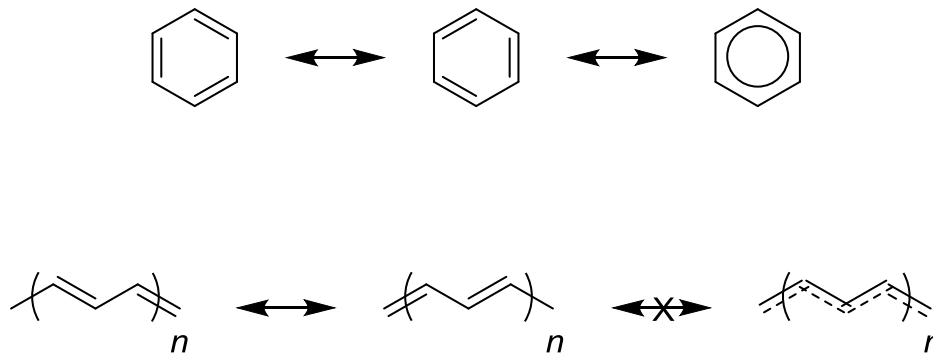


Figure 1.2. Resonance forms of benzene and polyacetylene.

1.3. Bulk Heterojunction Solar Cells

1.3.1. Solar cell architecture

Conventional OPV architecture layers the components of the device as shown in **Figure 1.3**, starting with an indium tin oxide (ITO) glass substrate as the anode, followed by a hole conducting layer of poly(3,4-ethylenedioxythiophene) polystyrene sulfonate (PEDOT:PSS). The active layer is a mixture of electron-donating polymer and electron accepting [6,6]-phenyl-C₆₁-butyric acid methyl ester (PCBM), a soluble fullerene derivative with good electron transport properties²³. Lastly, an electron transport layer followed by a metal anode are applied. The polymer and PCBM are analogous to the p-type and n-type materials of inorganic semiconductors, but they operate in

a different way. Their mode of conduction will be explained in the following section.

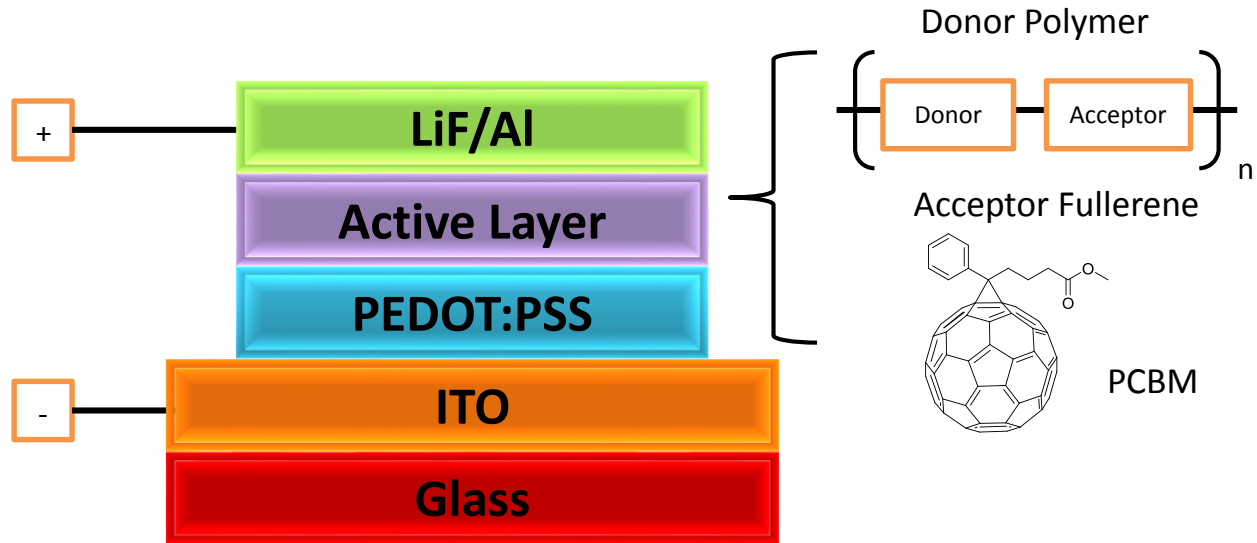


Figure 1.3. Architecture of an OPV device.

The composition of the active layer is a key component of device performance and it has evolved from original bilayer devices¹⁴ into the concept of a bulk heterojunction²⁴ with polymer and fullerene blended into one layer of intermixed materials to form networks for conduction (**Figure 1.4**). It is important to optimize the morphology of the polymer/PCBM mixture within 10 to 20nm to provide the pathways for conduction²⁵. This can be controlled through the design of the polymer structure, by solvent vapor²⁶ or thermal annealing²⁷, or the addition of solvent additives²⁸.

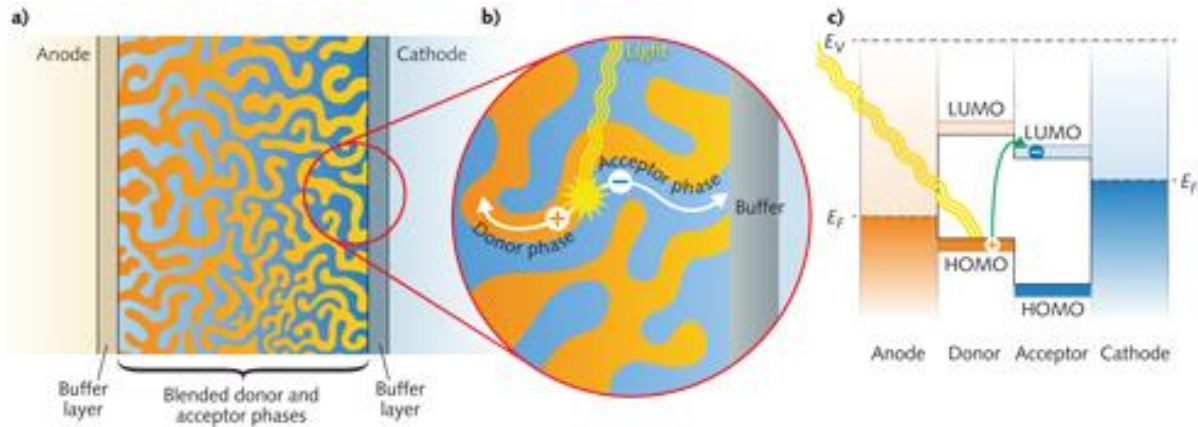


Figure 1.4. Close-up of the active layer in a bulk heterojunction solar cell.²⁹

1.3.2. Charge transport

In short, charge transport in an OPV occurs by stepwise charge generation, exciton diffusion, charge separation and transport to the electrodes, as illustrated in Figure 1.5. The conjugated polymer is the active material³⁰ which absorbs the solar photons (Step 1, **Figure 1.5**) to excite an electron from the HOMO to the LUMO, leaving behind a hole in the HOMO (Step 2, **Figure 1.5**). Because of the low dielectric constant of organic materials³¹, the resulting hole and electron are weakly bound by Coulombic forces to form a neutral species called an exciton. The neutral exciton is not influenced by external fields³², and thus can randomly travel down the chain via Förster resonant energy transfer³³. The exciton can travel a short distance (Step 3, **Figure 1.5**), before recombining or meeting with a material of a higher

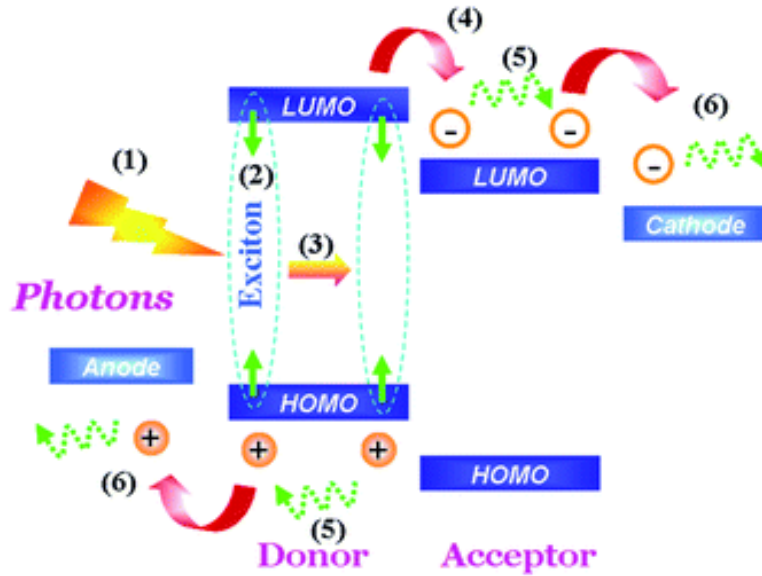


Figure 1.5. Charge formation and transport in a donor-acceptor material configuration.³⁴

electron affinity (usually PCBM)³⁵ onto which to donate the electron³⁶ (Step 4, **Figure 1.5**) to form a charge transfer species. Upon dissociation of the exciton onto the donor and acceptor materials, the hole and electron then each travel to their respective electrodes (Step 5 and 6, **Figure 1.5**).

1.3.3. Device performance characteristics

An OPV device is analyzed by measuring the current density (J) as the voltage (V) is varied, resulting in what is called a J - V curve. The working equation for calculating the power conversion efficiency (PCE or η) of an OPV (equation 1) is represented by the fraction of power generated (P_{out}) versus power input (P_{in}), or the ratio of the variables of fill factor (FF), short circuit current density (J_{sc}) and open circuit voltage (V_{oc}) over P_{in} .

$$\eta = \frac{P_{out}}{P_{in}} = \frac{FF \cdot J_{sc} \cdot V_{oc}}{P_{in}} \quad (1)$$

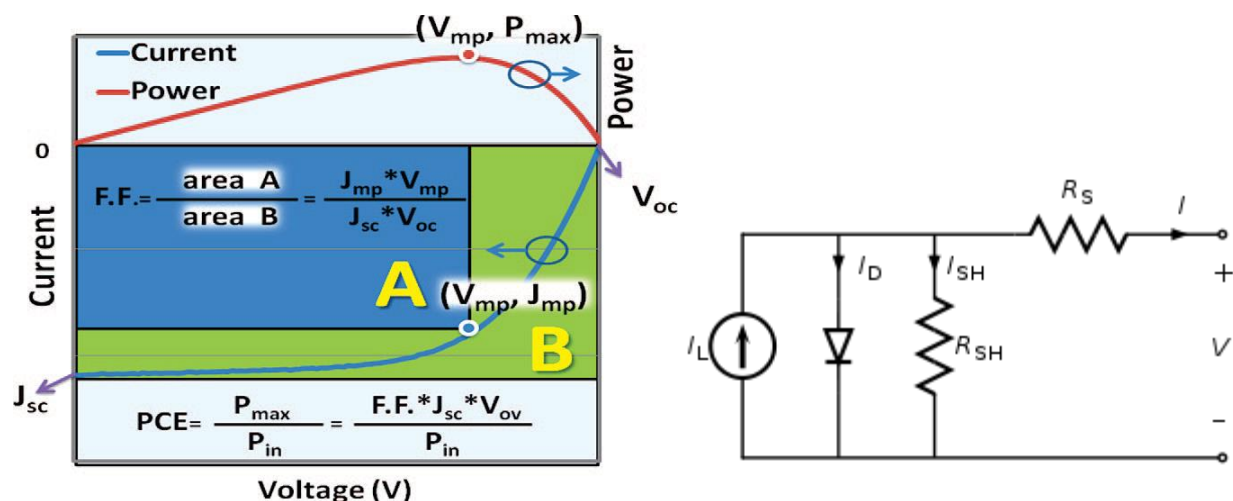


Figure 1.6. A J-V curve³⁷ and a circuit diagram of a solar cell.³⁸

The V_{oc} is the maximum voltage obtained under open circuit conditions. This is an intrinsic property of the active layer which is controlled by the offset of the LUMO of the PCBM acceptor and the HOMO of the polymer donor³⁹. The J_{sc} is the current per area under no applied bias. It depends on many factors such as charge generation, recombination, and mobility⁴⁰. Recombination can occur by decay of the charge transfer species (geminate recombination)⁴¹ or the charge separated species (bimolecular recombination)⁴².

Another variable is the fill factor which is the fraction of the graph extending from the axes to the point of V_{oc} at maximum power ($FF = (J_m V_m) / (J_{sc} V_{oc})$)⁴³. This represents the “squareness” of the J-V curve, and is influenced by a multitude of factors⁴⁴ that contribute to the overall shape of the curve. A summary of these features has been published by Qi & Wang⁴³. The slope of the curve near the Y-axis represents the inverse of the shunt resistance, R_{sh} , of the device. This resistance occurs from leakage currents either at the edge of the cell or material defects and impurities. R_{sh} can sometimes be improved after annealing, which is a strategy for generating higher ordered films and improving interlayer contacts⁴⁵. The effect of annealing and addition of buffer layers⁴⁶ upon

R_{sh} highlights the need for optimization of morphology not only between the donor and acceptor of the active layer, but also at layer interfaces. The slope of the line crossing near the X-axis represents the inverse of the series resistance (R_s), due to the bulk resistance of the active layer of the device, as well as that of the electrodes and every material interface of the device⁴⁷. Increasing the mobility of charge carriers, to a point⁴⁸, can improve the R_s and therefore the FF. Charge carrier balance is an important factor in performance. An imbalance of holes and electrons in the active layer will cause the formation of external fields and increased recombination, leading to a low FF, or even a characteristic S-shaped J-V curve⁴⁹.

1.4. Material design considerations

Some basic design principles have been developed to guide the selection of compounds for organic electronics to determine what type of device the material is best suited for, such as solar cells⁵⁰, light emitting diodes⁵¹, or transistors⁵². Additional structural modifications can tune the materials electronic properties to improve performance. The following looks at what techniques can lead to effective organic semiconducting materials for OPV applications. **Figure 1.7** graphically summarizes the main aspects which influence the bandgap of the material, including

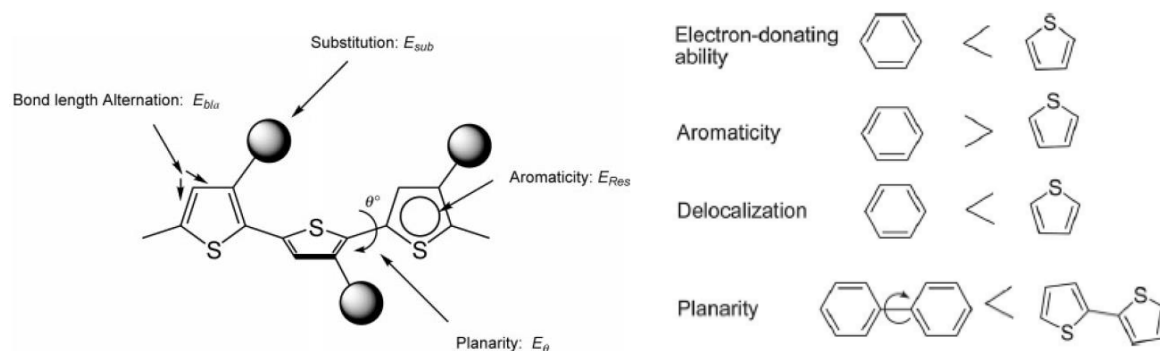


Figure 1.7. Illustration of structural factors that contribute to determination of the bandgap.^{53,54}

bond length alternation or quinoid form, addition of side groups, degree of planarity, and aromaticity. These topics will be discussed further in the following sections.

1.4.1. Conjugation and aromaticity

The first requirement of synthesizing organic electronics is establishing extended conjugation. This can be achieved by linking aromatic units together directly or between vinylene or alkynyl spacers. These aromatic structures have ground state nondegenerate resonance forms, known as quinoid forms³⁷, in which the double and single bonds are alternated. The units should be bonded together in such a way that there is a greater contribution of the quinoid resonance structure because the decrease of aromaticity in the quinoid form results in a higher energy state which can be an effective a strategy to lower the bandgap⁵⁵.

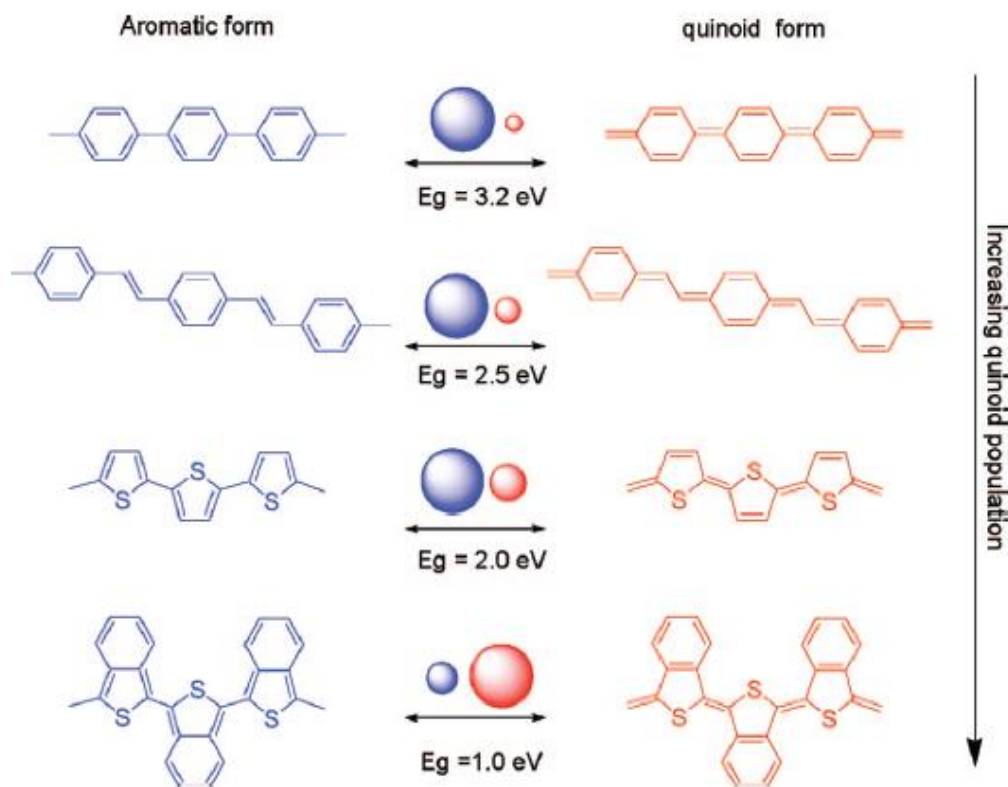


Figure 1.8. Greater contributions from the quinoid form lead to a lower bandgap.³⁷

1.4.2. Planarity

To obtain orbital overlap and extend the effective conjugation of the molecule, it is necessary to design planar materials for photovoltaic purposes. By considering the dihedral bond angles formed between units, torsional strain within the molecule can be avoided by placing complementary units next to each other. For example, a biphenyl system will have more torsional strain than bithiophene (see Figure 1.7). Placement of side groups must also be properly arranged, such that steric hindrance of neighboring alkyl chains does not lead to a disruption in planarity and decreased performance⁵⁶. Another strategy for obtaining planar materials is to fuse the rings into one rigid unit, whether it is a polycyclic aromatic unit such as fluorene or so-called ladder structures with fully fused units⁵⁷.

1.4.3. Solubility and morphology

While utilizing many aromatic units can extend the conjugation to improve conductivity, an undesired side effect of this is that a large degree of pi-stacking⁵⁸ can occur which will render the material insoluble in common organic solvents and limit processability. The solution to this is to place solubilizing groups along the molecule. Different groups such as amphiphilic⁵⁹, conjugated⁶⁰, or hydrogen bonding⁶¹ can solubilize and produce specialized properties⁶², but typically alkyl chains are affixed to the material to control solubility. Interdigitation of the alkyl chains changes the d-spacing of the polymer and can direct self-assembly⁶³ to produce higher order structures, such as lamellar formations as shown in **Figure 1.9** for poly-3-hexylthiophene (P3HT). The length and degree of branching of the alkyl chains can be varied to obtain a balance between solubility, morphology, and semiconducting performance. Often a step in the optimization of the material is the synthesis and evaluation of many chain variations.

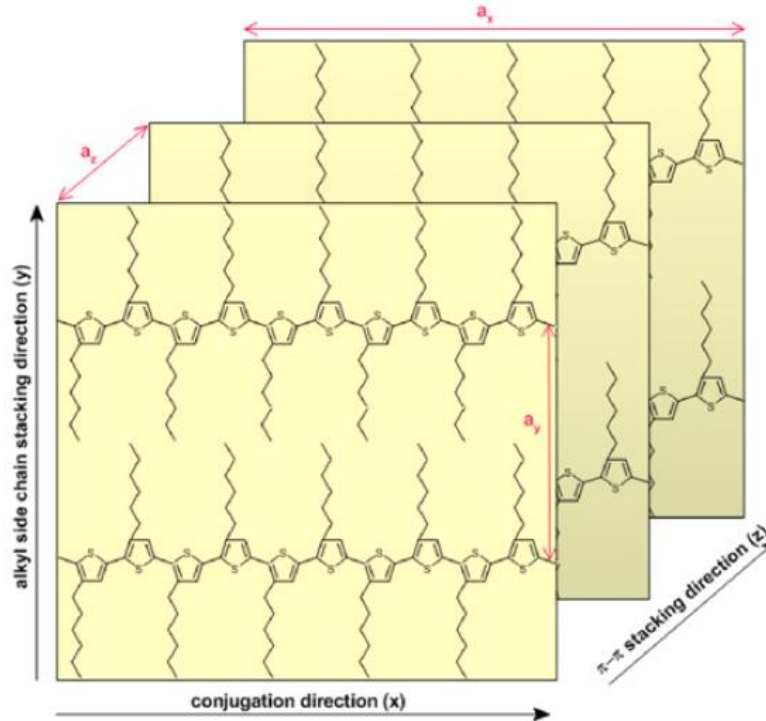


Figure 1.9. Lamellar formation of P3HT.⁶⁴

1.4.4. Optoelectronic properties

In addition to a conjugated and soluble material, it must also possess the proper optoelectronic properties to function in a photovoltaic device. For many years, poly-3-hexylthiophene (P3HT) was the most popular conjugated polymer because of its facile synthesis, excellent solubility and processability, as well as good crystallinity and charge transport properties. However, its relatively high-lying HOMO rendered it somewhat oxidatively unstable and its bandgap of about 2 eV was too large to capture the long wavelength portion of the visible spectrum. Despite extensive studies and engineering, devices thereof could only achieve efficiencies of about 4 to 5%⁶⁵.

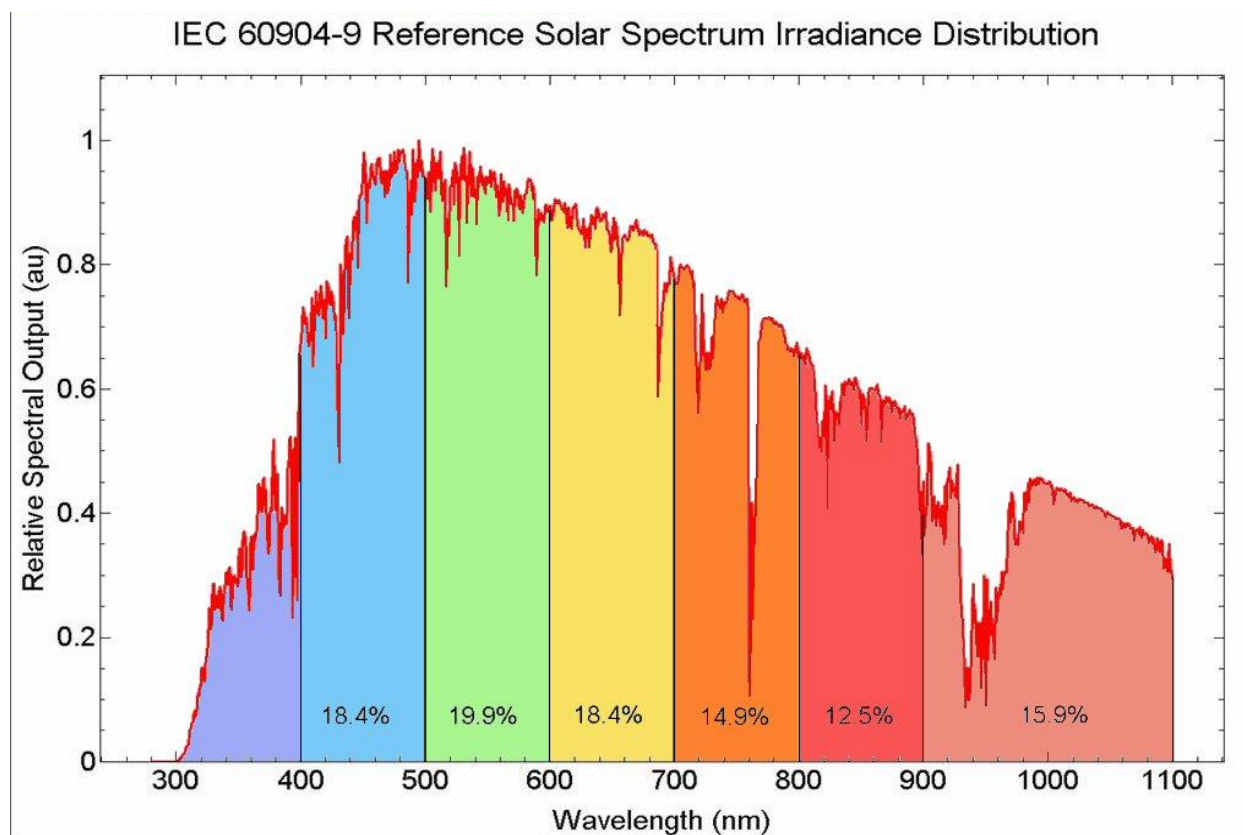


Figure 1.10. The solar spectrum⁶⁶.

An ideal polymer should efficiently absorb visible radiation of the solar spectrum, which mainly occurs within the visible range of 500-700 nm. Obtaining complementary absorption across this region is controlled by tuning the bandgap of the material due to the relationship $E=hc/\lambda$. A bandgap of 1.5 to 1.7 eV is desired³⁹, which is measured from the onset of absorption of the material in the solid state.

The polymer must also be oxidatively stable, and to ensure this a HOMO lower than -5.2 eV is necessary⁶⁷. While decreasing the HOMO will stabilize the material and increase the V_{oc} , going too low will also widen the bandgap. Positioning the LUMO at least 0.3 eV⁶⁸ above that of PCBM is desirable for efficient electron transfer^{39, 69} to overcome the Coulombic binding energy of the

exciton⁷⁰. When considering the “ideal” bandgap in an OPV device with PCBM as the acceptor component, a range of HOMO/LUMO values are therefore set as shown in **Figure 1.11**.

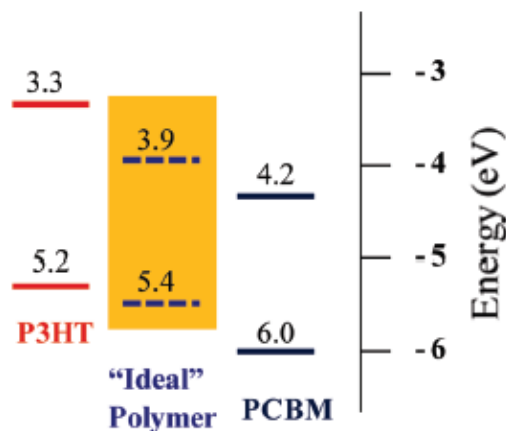


Figure 1.11. Illustration of energy levels of P3HT, an "ideal" polymer and PCBM.⁷¹

The next generation of conjugated materials after P3HT focused on reducing the bandgap to further increase device efficiencies. To tune the bandgap, electron-rich and electron-deficient monomers are copolymerized to form what is known as a donor-acceptor copolymer⁷². The donor and acceptor comonomers must be chosen according to the factors already overviewed such as planarity, solubility, and quinoid form, and also by the electron-donating/withdrawing strength of each aromatic unit. As shown in **Figure 1.12**, the donor material has a higher HOMO/LUMO relative to the acceptor unit. When polymerized, the combination of atomic orbitals produces new energy levels with an overall narrower bandgap⁵⁴, wherein the LUMO is dictated by the acceptor and the HOMO by the donor monomer. This enables fine-tuning of the bandgap by selective combinations of various comonomers. Stronger acceptors will lower the LUMO, and likewise, strong donors can raise the HOMO, while combining strong to medium acceptors with weak to medium donors can achieve the proper bandgap^{71, 72b, 73}. Research has focused on developing new

donor and acceptor units and exploring the properties resulting from the many combinations of monomers.

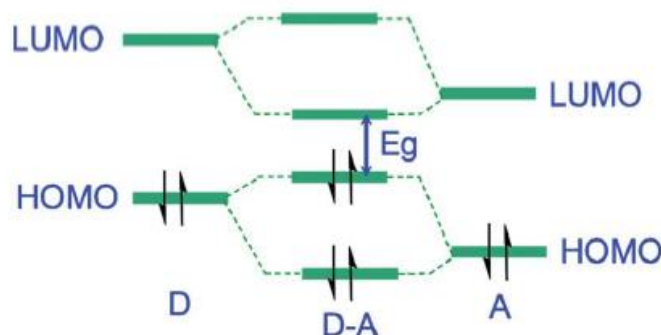


Figure 1.12. The bandgap of the polymer is tuned by the combination of the donor and acceptor components.⁵⁴

1.4.5. Donor and acceptor monomers used in organic electronics

Much of the discussion has emphasized the importance of proper monomer selection to tune the optoelectronic properties. Donor monomers, some of which are shown in **Figure 1.13**, often contain electron-rich heteroatoms, such as sulfur, oxygen, and sp^3 -hybridized nitrogen. Thiophene-based structures are popular donors because thiophene is a stronger electron donor than benzene, while being less aromatic which can lower the bandgap³⁷. In addition, thiophene has a smaller bond angle to reduce torsional strain with neighboring units. As noted, the relative strength of each component is important, and using a very strong donor can raise the HOMO too much at the expense of oxidative stability⁶⁷ or lowering the device's open circuit voltage⁷¹.

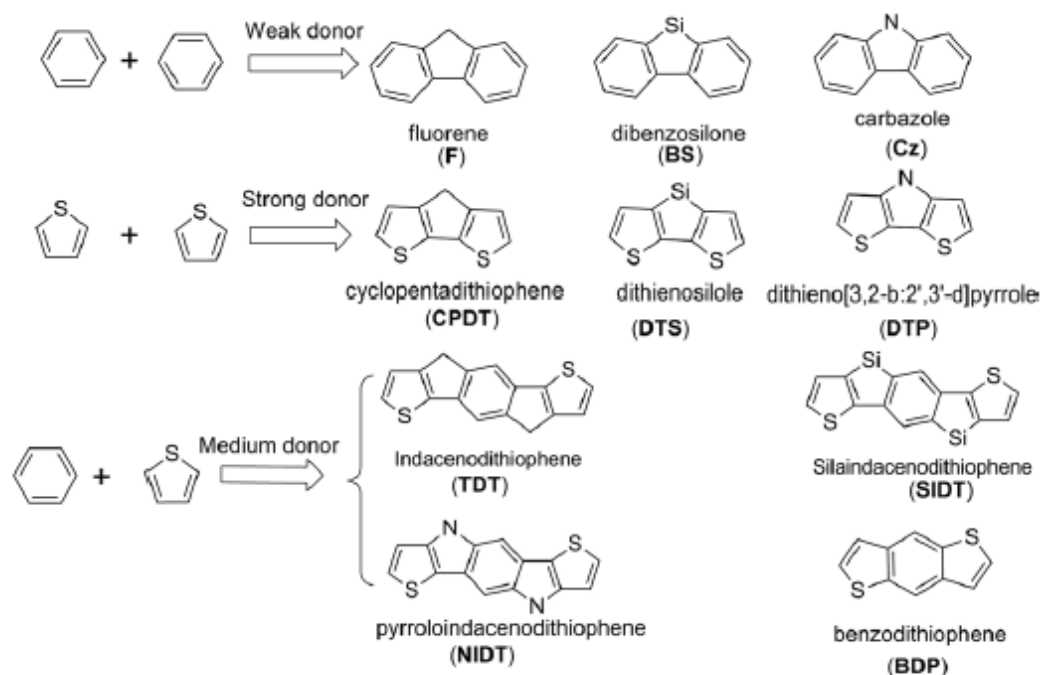


Figure 1.13. Representative donors used in OPVs.⁵⁴

The strength of an acceptor, shown in **Figure 1.14**, can be evaluated by comparing its ability to lower the LUMO of the polymer when each is polymerized with a common donor. Weak donors such as thiazolothiazole and benzobisthiazole contain electron-rich sulfur atoms, as does thienopyrroledione, yet the latter functions as a medium strength donor because the imide atop the molecule promotes the quinoid form. It is common to use sp^2 -hybridized nitrogens throughout the array of acceptors, and lactams increase the strength of isoindigo and diketopyrrolopyrrole as well as provide a site for alkylation. Other aryl or N- substituents such as acyl, trifluoromethyl, and fluorine can further contribute to the strength of the acceptors.

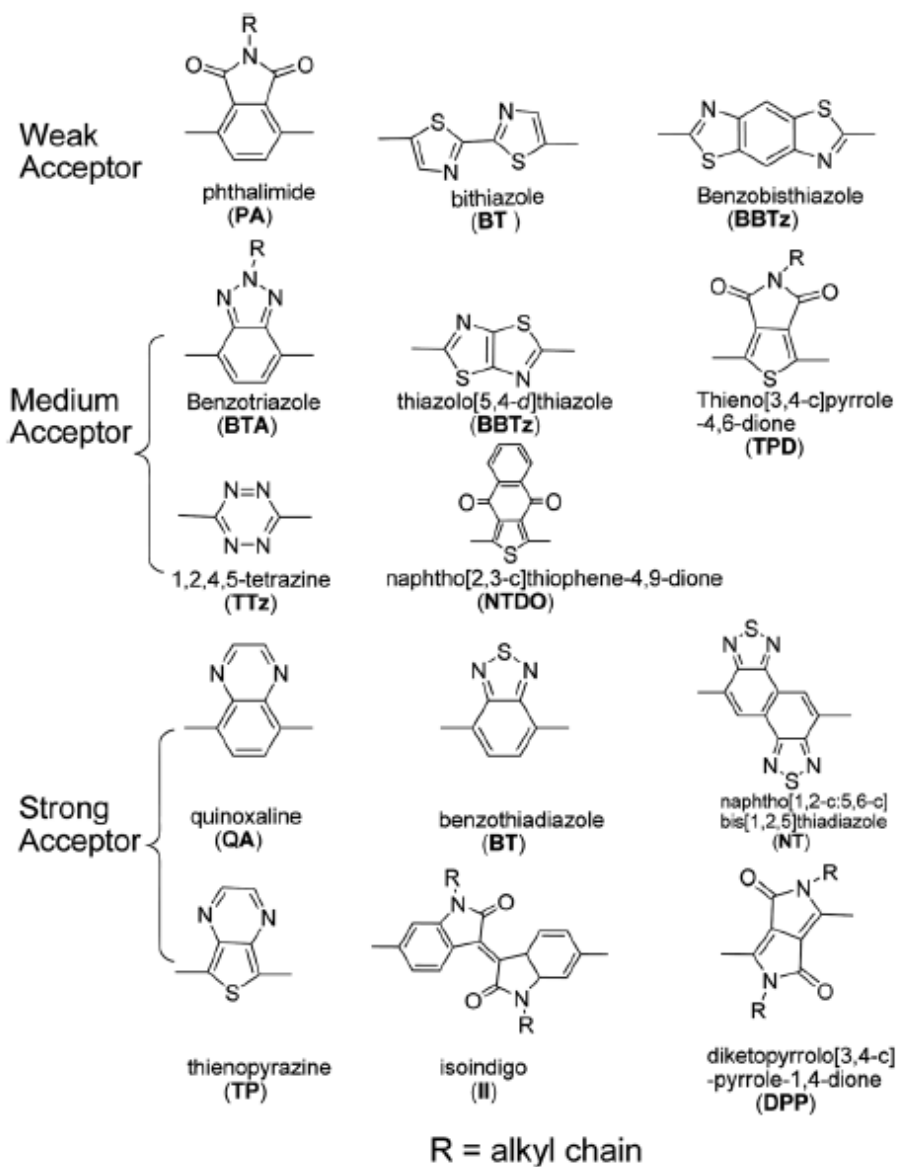


Figure 1.14. Representative acceptors used in OPVs.⁵⁴

1.5. Conclusion

In conclusion, knowledge of the operating principles of a bulk heterojunction organic solar cell along with basic strategies of how to tune the bandgap of conjugated polymers allows for the development of new materials for photovoltaic purposes. Some of the known monomers illustrated

in Section 1.4.5 are combined with newly developed units in the following chapters with the goal of creating narrow bandgap materials.

1.6. References

1. International Energy Outlook 2013. Administration, U. S. E. I., Ed. Washington, D.C., 2013.
2. (a) BP *BP Statistical Review of World Energy June 2015*; BP: 2015; (b) Shafiee, S.; Topal, E., When will fossil fuel reserves be diminished? *Energy Policy* **2009**, *37* (1), 181-189.
3. Roberts, B., Photovoltaic Solar Resource of the United States. NREL: 2013.
4. L.P., B. *New Energy Outlook 2015*; 2015.
5. Cardwell, D., Solar and Wind Energy Start to Win on Price vs. Conventional Fuels. *The New York Times* 2014.
6. Mulligan, C. J.; Wilson, M.; Bryant, G.; Vaughan, B.; Zhou, X.; Belcher, W. J.; Dastoor, P. C., A projection of commercial-scale organic photovoltaic module costs. *Solar Energy Materials and Solar Cells* **2014**, *120*, Part A (0), 9-17.
7. (a) Gaudiana, R.; Brabec, C., Organic materials: Fantastic plastic. *Nat Photon* **2008**, *2* (5), 287-289; (b) Forrest, S. R., The path to ubiquitous and low-cost organic electronic appliances on plastic. *Nature* **2004**, *428* (6986), 911-918.
8. (a) Krebs, F. C., Fabrication and processing of polymer solar cells: A review of printing and coating techniques. *Solar Energy Materials and Solar Cells* **2009**, *93* (4), 394-412; (b) Kopola, P.; Aernouts, T.; Sliz, R.; Guillerez, S.; Ylikunnari, M.; Cheyng, D.; Välimäki, M.; Tuomikoski, M.; Hast, J.; Jabbour, G.; Myllylä, R.; Maaninen, A., Gravure printed flexible organic photovoltaic modules. *Solar Energy Materials and Solar Cells* **2011**, *95* (5), 1344-1347; (c) Hoth, C. N.; Schilinsky, P.; Choulis, S. A.; Brabec, C. J., Printing Highly Efficient Organic Solar Cells. *Nano Letters* **2008**, *8* (9), 2806-2813; (d) Aernouts, T.; Aleksandrov, T.; Giroto, C.; Genoe, J.; Poortmans, J., Polymer based organic solar cells using ink-jet printed active layers. *Applied Physics Letters* **2008**, *92* (3), 033306; (e) Brabec, C. J.; Hauch, J. A.; Schilinsky, P.; Waldauf, C., Production Aspects of Organic Photovoltaics and Their Impact on the Commercialization of Devices. *MRS Bulletin* **2005**, *30* (01), 50-52.
9. (a) Kaltenbrunner, M.; White, M. S.; Głowacki, E. D.; Sekitani, T.; Someya, T.; Sariciftci, N. S.; Bauer, S., Ultrathin and lightweight organic solar cells with high flexibility. *Nat Commun* **2012**, *3*, 770; (b) Kylberg, W.; de Castro, F. A.; Chabrecek, P.; Sonderegger, U.; Chu, B. T.-T.; Nüesch, F.; Hany, R., Woven Electrodes for Flexible Organic Photovoltaic Cells. *Advanced Materials* **2011**, *23* (8), 1015-1019.

10. Zervos, H. D., Raghu; Ghaffarzadeh, Khasha *Organic Photo voltaics (OPV) 2013-2023: Technologies, Markets, Players*; IDTechEx: 2013.
11. (a) Darling, S. B.; You, F., The case for organic photovoltaics. *RSC Advances* **2013**, *3* (39), 17633-17648; (b) Yan, J.; Saunders, B. R., Third-generation solar cells: a review and comparison of polymer:fullerene, hybrid polymer and perovskite solar cells. *RSC Advances* **2014**, *4* (82), 43286-43314.
12. Osborn, M., Verified: Heliatek organic solar cell achieves 12% efficiency. *PVTech* 2013.
13. Shirakawa, H.; Louis, E. J.; MacDiarmid, A. G.; Chiang, C. K.; Heeger, A. J., Synthesis of electrically conducting organic polymers: halogen derivatives of polyacetylene,(CH) x. *Journal of the Chemical Society, Chemical Communications* **1977**, (16), 578-580.
14. Tang, C. W., Two-layer organic photovoltaic cell. *Applied Physics Letters* **1986**, *48* (2), 183-185.
15. Spanggaard, H.; Krebs, F. C., A brief history of the development of organic and polymeric photovoltaics. *Solar Energy Materials and Solar Cells* **2004**, *83* (2), 125-146.
16. Seeger, K., *Semiconductor Physics: An Introduction*. 5 ed.; Springer-Verlag: Berlin, 2013.
17. IUPAC, *Compendium of Chemical Terminology*. 2 ed.; Blackwell Scientific Publications: Oxford, 1997.
18. Klaerner, G.; Miller, R., Polyfluorene derivatives: effective conjugation lengths from well-defined oligomers. *Macromolecules* **1998**, *31* (6), 2007-2009.
19. Peierls, R. E., *Quantum theory of solids*. Oxford University Press: 1955.
20. Fincher Jr, C.; Chen, C.-E.; Heeger, A.; MacDiarmid, A.; Hastings, J., Structural determination of the symmetry-breaking parameter in trans-(CH) x. *Physical Review Letters* **1982**, *48* (2), 100.
21. Yannoni, C.; Clarke, T., Molecular geometry of cis-and trans-polyacetylene by nutation NMR spectroscopy. *Physical Review Letters* **1983**, *51* (13), 1191.
22. Longuet-Higgins, H.; Salem, L. In *The alternation of bond lengths in long conjugated chain molecules*, Proceedings of the Royal Society of London A: Mathematical, Physical and Engineering Sciences, The Royal Society: 1959; pp 172-185.
23. Sariciftci, N., Photoinduced electron transfer from a conducting polymer to buckminsterfullerene. *Science* **1992**, *258* (5087), 1474.

24. (a) Hoppe, H.; Sariciftci, N. S., Morphology of polymer/fullerene bulk heterojunction solar cells. *Journal of Materials Chemistry* **2006**, *16* (1), 45-61; (b) Chen, D.; Nakahara, A.; Wei, D.; Nordlund, D.; Russell, T. P., P3HT/PCBM bulk heterojunction organic photovoltaics: correlating efficiency and morphology. *Nano Letters* **2010**, *11* (2), 561-567.
25. Rim, S.-B.; Fink, R. F.; Schöneboom, J. C.; Erk, P.; Peumans, P., Effect of molecular packing on the exciton diffusion length in organic solar cells. *Applied Physics Letters* **2007**, *91* (17), 173504.
26. Li, G.; Yao, Y.; Yang, H.; Shrotriya, V.; Yang, G.; Yang, Y., "Solvent annealing" effect in polymer solar cells based on poly (3-hexylthiophene) and methanofullerenes. *Advanced Functional Materials* **2007**, *17* (10), 1636.
27. (a) Al-Ibrahim, M.; Ambacher, O.; Sensfuss, S.; Gobsch, G., Effects of solvent and annealing on the improved performance of solar cells based on poly (3-hexylthiophene): fullerene. *Applied Physics Letters* **2005**, *86* (20), 201120; (b) Ayzner, A. L.; Wanger, D. D.; Tassone, C. J.; Tolbert, S. H.; Schwartz, B. J., Room to improve conjugated polymer-based solar cells: understanding how thermal annealing affects the fullerene component of a bulk heterojunction photovoltaic device. *The Journal of Physical Chemistry C* **2008**, *112* (48), 18711-18716.
28. (a) Lee, J. K.; Ma, W. L.; Brabec, C. J.; Yuen, J.; Moon, J. S.; Kim, J. Y.; Lee, K.; Bazan, G. C.; Heeger, A. J., Processing Additives for Improved Efficiency from Bulk Heterojunction Solar Cells. *J Am Chem Soc* **2008**, *130* (11), 3619-3623; (b) Peet, J.; Kim, J. Y.; Coates, N. E.; Ma, W. L.; Moses, D.; Heeger, A. J.; Bazan, G. C., Efficiency enhancement in low-bandgap polymer solar cells by processing with alkane dithiols. *Nature materials* **2007**, *6* (7), 497-500; (c) Hoven, C. V.; Dang, X. D.; Coffin, R. C.; Peet, J.; Nguyen, T. Q.; Bazan, G. C., Improved performance of polymer bulk heterojunction solar cells through the reduction of phase separation via solvent additives. *Advanced Materials* **2010**, *22* (8), E63-E66.
29. MARK T. GREINER, L. C., and ZHENG-HONG LU ORGANIC PHOTOVOLTAICS: Transition metal oxides increase organic solar-cell power conversion. <http://www.laserfocusworld.com/articles/print/volume-48/issue-06/features/transition-metal-oxides-increase-organic-solar-cell-power-conversion.html> (accessed July 27, 2015).
30. Hwang, I.-W.; Moses, D.; Heeger, A. J., Photoinduced carrier generation in P3HT/PCBM bulk heterojunction materials. *The Journal of Physical Chemistry C* **2008**, *112* (11), 4350-4354.
31. Blom, P. W. M.; Mihailetschi, V. D.; Koster, L. J. A.; Markov, D. E., Device Physics of Polymer:Fullerene Bulk Heterojunction Solar Cells. *Advanced Materials* **2007**, *19* (12), 1551-1566.
32. Brédas, J.-L.; Norton, J. E.; Cornil, J.; Coropceanu, V., Molecular Understanding of Organic Solar Cells: The Challenges. *Accounts of Chemical Research* **2009**, *42* (11), 1691-1699.

33. Forster, T., 10th Spiers Memorial Lecture. Transfer mechanisms of electronic excitation. *Discussions of the Faraday Society* **1959**, 27 (0), 7-17.
34. Li, Y.; Guo, Q.; Li, Z.; Pei, J.; Tian, W., Solution processable D-A small molecules for bulk-heterojunction solar cells. *Energy & Environmental Science* **2010**, 3 (10), 1427-1436.
35. (a) Hummelen, J. C.; Knight, B. W.; LePeq, F.; Wudl, F.; Yao, J.; Wilkins, C. L., Preparation and Characterization of Fulleroid and Methanofullerene Derivatives. *The Journal of Organic Chemistry* **1995**, 60 (3), 532-538; (b) Cheung, D. L.; Troisi, A., Theoretical Study of the Organic Photovoltaic Electron Acceptor PCBM: Morphology, Electronic Structure, and Charge Localization†. *The Journal of Physical Chemistry C* **2010**, 114 (48), 20479-20488.
36. (a) D'Avino, G.; Mothy, S.; Muccioli, L.; Zannoni, C.; Wang, L.; Cornil, J.; Beljonne, D.; Castet, F., Energetics of Electron–Hole Separation at P3HT/PCBM Heterojunctions. *The Journal of Physical Chemistry C* **2013**, 117 (25), 12981-12990; (b) Arkhipov, V.; Emelianova, E.; Bäessler, H., Hot exciton dissociation in a conjugated polymer. *Physical review letters* **1999**, 82 (6), 1321.
37. Cheng, Y.-J.; Yang, S.-H.; Hsu, C.-S., Synthesis of Conjugated Polymers for Organic Solar Cell Applications. *Chem Rev* **2009**, 109 (11), 5868-5923.
38. contributors, W. Theory of solar cells
https://en.wikipedia.org/w/index.php?title=Theory_of_solar_cells&oldid=674835217
 Primary contributors: Revision history statistics (accessed 23 August 2015 21:06 UTC).
39. Scharber, M. C.; Mühlbacher, D.; Koppe, M.; Denk, P.; Waldauf, C.; Heeger, A. J.; Brabec, C. J., Design Rules for Donors in Bulk-Heterojunction Solar Cells—Towards 10 % Energy-Conversion Efficiency. *Advanced Materials* **2006**, 18 (6), 789-794.
40. Janssen, R. A.; Nelson, J., Factors limiting device efficiency in organic photovoltaics. *Advanced Materials* **2013**, 25 (13), 1847-1858.
41. De, S.; Pascher, T.; Maiti, M.; Jespersen, K. G.; Kesti, T.; Zhang, F.; Inganäs, O.; Yartsev, A.; Sundström, V., Geminate charge recombination in alternating polyfluorene copolymer/fullerene blends. *Journal of the American Chemical Society* **2007**, 129 (27), 8466-8472.
42. Koster, L. J. A.; Mihailetschi, V. D.; Blom, P. W. M., Bimolecular recombination in polymer/fullerene bulk heterojunction solar cells. *Applied Physics Letters* **2006**, 88 (5), 052104.
43. Qi, B.; Wang, J., Fill factor in organic solar cells. *Physical Chemistry Chemical Physics* **2013**, 15 (23), 8972-8982.
44. Kim, M.-S.; Kim, B.-G.; Kim, J., Effective Variables To Control the Fill Factor of Organic Photovoltaic Cells. *ACS Applied Materials & Interfaces* **2009**, 1 (6), 1264-1269.

45. Gupta, D.; Mukhopadhyay, S.; Narayan, K. S., Fill factor in organic solar cells. *Solar Energy Materials and Solar Cells* **2010**, *94* (8), 1309-1313.
46. Hung, L.; Tang, C.; Mason, M., Enhanced electron injection in organic electroluminescence devices using an Al/LiF electrode. *Applied Physics Letters* **1997**, *70* (2), 152-154.
47. (a) Xue, J.; Uchida, S.; Rand, B. P.; Forrest, S. R., 4.2% efficient organic photovoltaic cells with low series resistances. *Applied Physics Letters* **2004**, *84*, 3013; (b) Ishii, H.; Sugiyama, K.; Ito, E.; Seki, K., Energy level alignment and interfacial electronic structures at organic/metal and organic/organic interfaces. *Advanced Materials* **1999**, *11* (8), 605-625.
48. Servaites, J. D.; Yeganeh, S.; Marks, T. J.; Ratner, M. A., Efficiency enhancement in organic photovoltaic cells: consequences of optimizing series resistance. *Advanced Functional Materials* **2010**, *20* (1), 97.
49. Tress, W.; Petrich, A.; Hummert, M.; Hein, M.; Leo, K.; Riede, M., Imbalanced mobilities causing S-shaped IV curves in planar heterojunction organic solar cells. *Applied Physics Letters* **2011**, *98* (6), 063301.
50. Nunzi, J.-M., Organic photovoltaic materials and devices. *Comptes Rendus Physique* **2002**, *3* (4), 523-542.
51. Müllen, K.; Scherf, U., *Organic light emitting devices: synthesis, properties and applications*. John Wiley & Sons: 2006.
52. Katz, H. E., Recent advances in semiconductor performance and printing processes for organic transistor-based electronics. *Chemistry of Materials* **2004**, *16* (23), 4748-4756.
53. Roncali, J., Molecular Engineering of the Band Gap of π -Conjugated Systems: Facing Technological Applications. *Macromolecular Rapid Communications* **2007**, *28* (17), 1761-1775.
54. Zhang, Z.-G.; Wang, J., Structures and properties of conjugated Donor-Acceptor copolymers for solar cell applications. *Journal of Materials Chemistry* **2012**, *22* (10), 4178-4187.
55. Brédas, J. L., Relationship between band gap and bond length alternation in organic conjugated polymers. *Journal of Chemical Physics* **1985**, *82* (8), 3808.
56. Kim, Y.; Cook, S.; Tuladhar, S. M.; Choulis, S. A.; Nelson, J.; Durrant, J. R.; Bradley, D. D. C.; Giles, M.; McCulloch, I.; Ha, C.-S.; Ree, M., A strong regioregularity effect in self-organizing conjugated polymer films and high-efficiency polythiophene:fullerene solar cells. *Nat Mater* **2006**, *5* (3), 197-203.
57. (a) Hertel, D.; Scherf, U.; Bässler, H., Charge Carrier Mobility in a Ladder-Type Conjugated Polymer. *Advanced Materials* **1998**, *10* (14), 1119-1122; (b) Babel, A.; Jenekhe, S.

- A., High electron mobility in ladder polymer field-effect transistors. *Journal of the American Chemical Society* **2003**, *125* (45), 13656-7.
58. Amrutha, S. R.; Jayakannan, M., Probing the pi-stacking induced molecular aggregation in pi-conjugated polymers, oligomers, and their blends of p-phenylenevinylenes. *The journal of physical chemistry. B* **2008**, *112* (4), 1119-29.
59. Bjørnholm, T.; Greve, D. R.; Reitzel, N.; Hassenkam, T.; Kjaer, K.; Howes, P. B.; Larsen, N. B.; Bøgelund, J.; Jayaraman, M.; Ewbank, P. C., Self-assembly of regioregular, amphiphilic polythiophenes into highly ordered π -stacked conjugated polymer thin films and nanocircuits. *Journal of the American Chemical Society* **1998**, *120* (30), 7643-7644.
60. Hou, J.; Tan, Z. a.; Yan, Y.; He, Y.; Yang, C.; Li, Y., Synthesis and photovoltaic properties of two-dimensional conjugated polythiophenes with bi (thienylenevinylene) side chains. *Journal of the American Chemical Society* **2006**, *128* (14), 4911-4916.
61. Moroni, M.; Le Moigne, J.; Pham, T.; Bigot, J.-Y., Rigid rod conjugated polymers for nonlinear optics. 3. Intramolecular H bond effects on poly (phenyleneethynylene) chains. *Macromolecules* **1997**, *30* (7), 1964-1972.
62. (a) Gaylord, B. S.; Wang, S.; Heeger, A. J.; Bazan, G. C., Water-soluble conjugated oligomers: Effect of chain length and aggregation on photoluminescence-quenching efficiencies. *Journal of the American Chemical Society* **2001**, *123* (26), 6417-6418; (b) McQuade, D. T.; Pullen, A. E.; Swager, T. M., Conjugated polymer-based chemical sensors. *Chemical reviews* **2000**, *100* (7), 2537-2574.
63. Garnier, F.; Yassar, A.; Hajlaoui, R.; Horowitz, G.; Deloffre, F.; Servet, B.; Ries, S.; Alnot, P., Molecular engineering of organic semiconductors: design of self-assembly properties in conjugated thiophene oligomers. *Journal of the American Chemical Society* **1993**, *115* (19), 8716-8721.
64. Geraldine, L. C. P.; Moon-Ho, H.; Michael, S. S., Anomalous thickness-dependence of photocurrent explained for state-of-the-art planar nano-heterojunction organic solar cells. *Nanotechnology* **2012**, *23* (9), 095402.
65. Dang, M. T.; Hirsch, L.; Wantz, G., P3HT:PCBM, Best Seller in Polymer Photovoltaic Research. *Advanced Materials* **2011**, *23* (31), 3597-3602.
66. Solar Simulator Characterisation (200-2500nm). <http://www.bentham.co.uk/solsim.htm>.
67. de Leeuw, D., Stability of n-type doped conducting polymers and consequences for polymeric microelectronic devices. *Synthetic metals* **1997**, *87* (1), 53.
68. Bredas, J. L.; Beljonne, D.; Coropceanu, V.; Cornil, J., Charge-transfer and energy-transfer processes in pi-conjugated oligomers and polymers: a molecular picture. *Chem Rev* **2004**, *104* (11), 4971-5004.

69. Manceau, M.; Bundgaard, E.; Carlé, J. E.; Hagemann, O.; Helgesen, M.; Søndergaard, R.; Jørgensen, M.; Krebs, F. C., Photochemical stability of π -conjugated polymers for polymer solar cells: a rule of thumb. *Journal of Materials Chemistry* **2011**, *21* (12), 4132-4141.
70. Knupfer, M., Exciton binding energies in organic semiconductors. *Appl Phys A* **2003**, *77* (5), 623-626.
71. Zhou, H.; Yang, L.; Stoneking, S.; You, W., A Weak Donor–Strong Acceptor Strategy to Design Ideal Polymers for Organic Solar Cells. *ACS Applied Materials & Interfaces* **2010**, *2* (5), 1377-1383.
72. (a) Havinga, E. E.; ten Hoeve, W.; Wynberg, H., Alternate donor-acceptor small-band-gap semiconducting polymers; Polysquaraines and polycroconaines. *Synthetic metals* **1993**, *55* (1), 299-306; (b) van Mullekom, H. A. M.; Vekemans, J. A. J. M.; Havinga, E. E.; Meijer, E. W., Developments in the chemistry and band gap engineering of donor–acceptor substituted conjugated polymers. *Materials Science and Engineering: R: Reports* **2001**, *32* (1), 1-40.
73. (a) Tsuji, M.; Saeki, A.; Koizumi, Y.; Matsuyama, N.; Vijayakumar, C.; Seki, S., Benzobisthiazole as weak donor for improved photovoltaic performance: microwave conductivity technique assisted molecular engineering. *Advanced Functional Materials* **2014**, *24* (1), 28-36; (b) Bundgaard, E.; Krebs, F. C., Low band gap polymers for organic photovoltaics. *Solar Energy Materials and Solar Cells* **2007**, *91* (11), 954-985.

CHAPTER 2

SYNTHESIS OF ORTHOESTERS AND HETEROCYCLES FROM TRITHIOORTHOSTERS

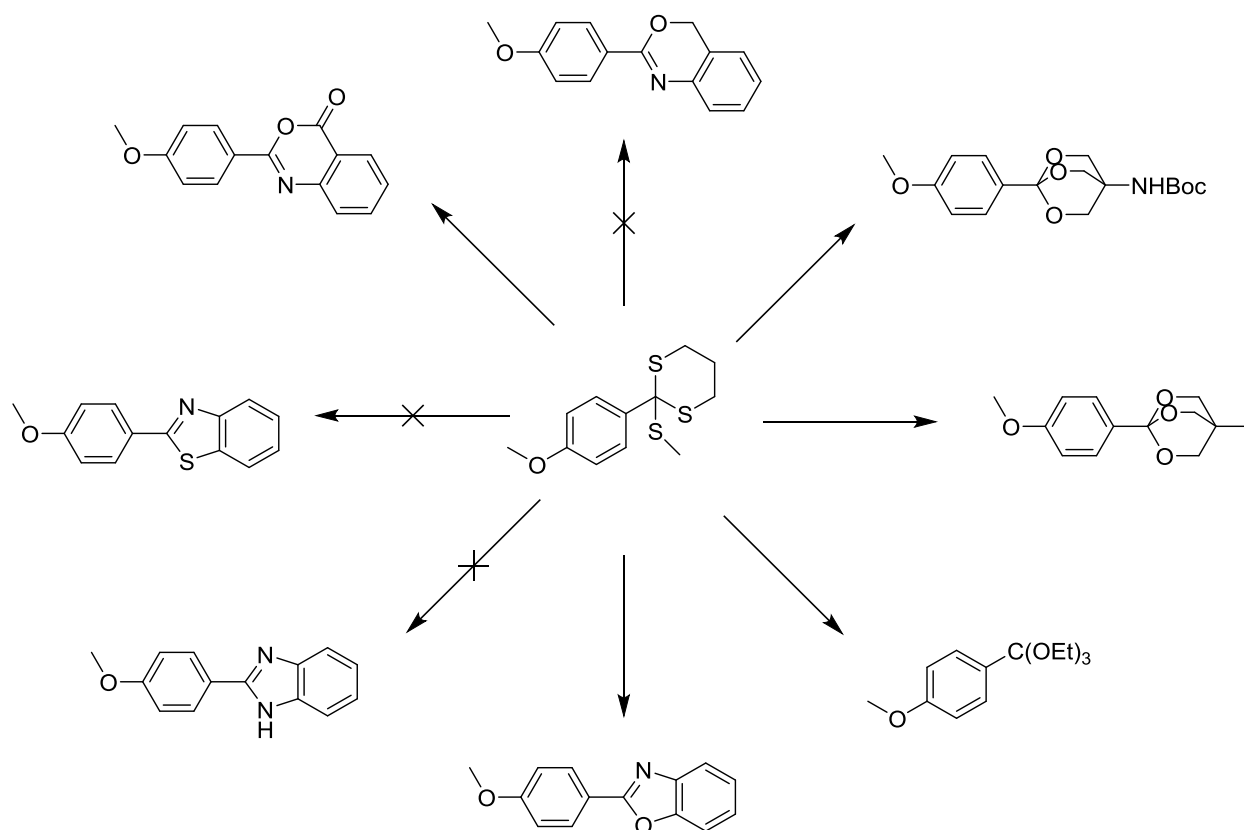


Figure 2.15. Transformations of 1,3-dithianes.

2.1. Introduction

Orthoesters are an obscure yet versatile functional group in organic chemistry. They serve many roles, as either a protecting group for esters and carboxylic acids¹ and sugars², a reactive intermediate for synthesis of heterocycles³, and are present in natural products⁴ (Figure 2.2). However, few methods are available to synthesize orthoesters, as shown in Scheme 2.1. The Pinner synthesis⁵ (A) is a common method which under acidic conditions transforms a nitrile into an

iminoester hydrochloride salt and then the orthoester. A long reaction time is typical and the yields can be low. The Tschitschibabin orthoester synthesis⁶ (B) involves formation of a

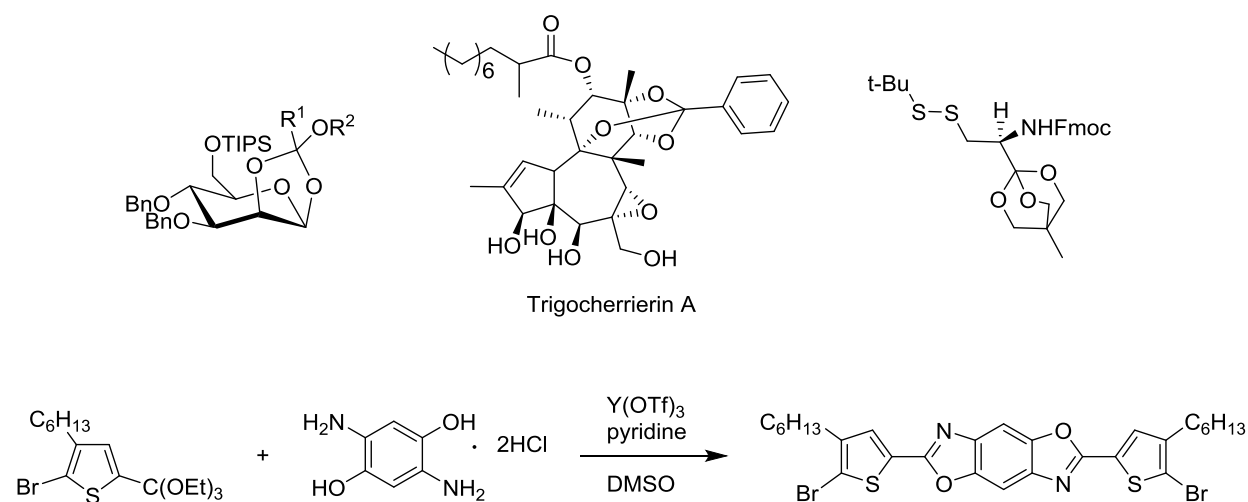
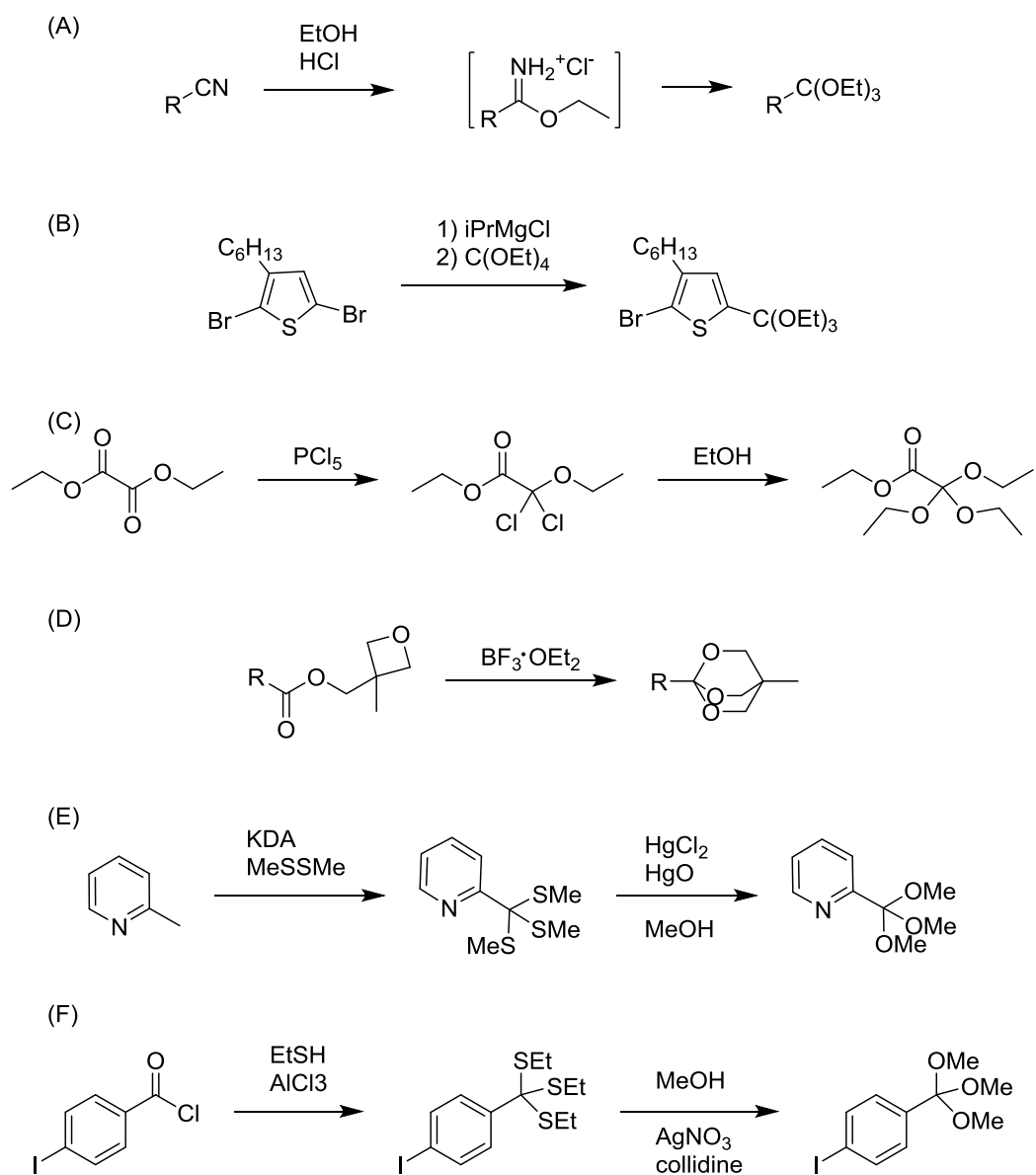
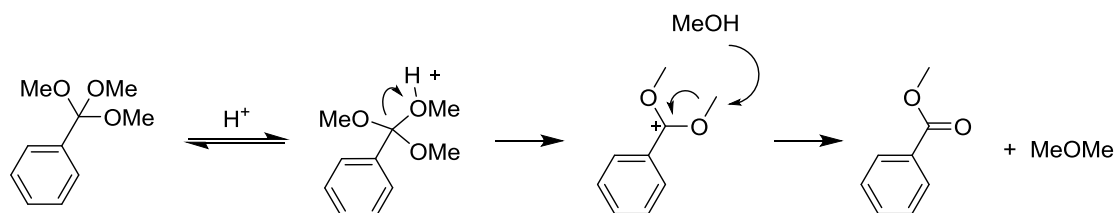


Figure 2.16. Orthoesters in organic chemistry.

Grignard reagent which is reacted with tetraethyl orthocarbonate, as demonstrated below with the formation of a thienyl orthoester^{3a}. The limitation of this reaction is that functional groups tolerant of Grignard reagents must be used. Chlorination of diethyl oxalate with PCl_5 followed by attack of ethanol yields an ester orthoester⁷ (C). Bicyclic orthoesters⁸ (D) are novel structures formed by acid-catalyzed rearrangements and this group offers the advantage of being a more robust protecting group than acyclic orthoesters. The last two reactions presented in Scheme 2.1 illustrate the transformation of trithioorthoesters into orthoesters. They differ in both the synthesis of the trithioorthoester and conditions to synthesize the orthoester. The formation of the trithioorthoester in (E) with KDA and MeSSMe is unique to the acidic nature of the methyl group of picoline, while the AlCl_3 catalyzed substitution (F) with an acid chloride could provide a more general method. The picoline orthoester is then synthesized using more traditional mercuric reagents⁹, commonly used to deprotect 1,3-dithianes. A variation is to use AgNO_3 under basic conditions so as to protect the orthoester from acid-catalyzed decomposition to an ester, as shown in Scheme 2.2.

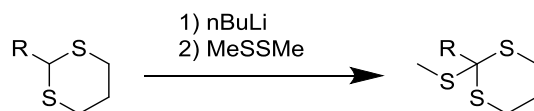


Scheme 2.1. Methods of synthesizing orthoesters.



Scheme 2.2. Mechanism of acid-catalyzed decomposition of orthoesters to esters.

Our research required the synthesis of novel orthoesters and we found the methods of trithioorthoesters to be appealing due to the mild conditions and functional group tolerance, but difficult to implement the trithioorthoesters due to the limited scope of the method based on picoline or the foul reaction conditions with ethanethiol. In searching for an alternative synthesis of the trithioorthoesters, we noted that the common carbonyl protecting group, 1,3-dithiane, already possessed two of the needed sulfur substituents and the third sulfur group could be installed by metallation of the reactive 2-position followed by the electrophile dimethyl disulfide (Scheme 2.3). Indeed, Ellison *et al*¹⁰ had previously studied this moiety and used the mercuric conditions with 95% ethanol to synthesize esters, which mostly likely formed through an orthoester intermediate that was not isolated.



Scheme 2.3. Synthesis of trithioorthoester.

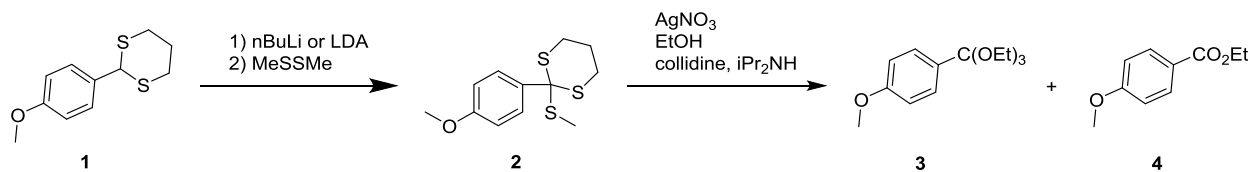
Drawing upon these advances we sought to develop a general methodology for the dithiane to orthoester conversion by making modifications to improve the efficiency of the reaction and purity of the product. Furthermore, we studied the versatility of the novel trithioorthoester intermediate to see what other nucleophiles were suitable for this reaction to develop mild route toward the synthesis of heterocycles.

2.1. Results & Discussion

2.1.1. Synthesis of orthoesters

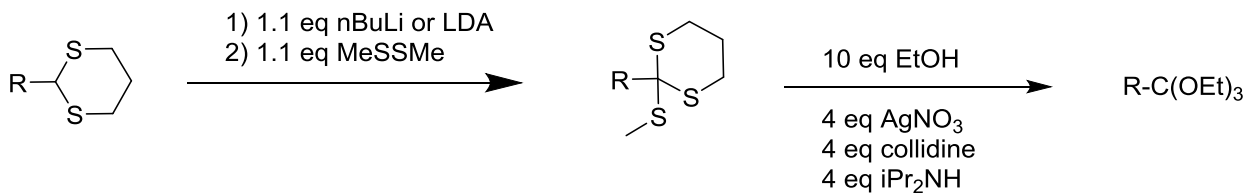
1,3-Dithianes were synthesized following literature conditions with 1,3-propanedithiol and either $\text{BF}_3 \cdot \text{OEt}_2$ or catalytic iodine, which gave equivalent yields, usually 80% yield or better.

Synthesis of the orthoester was optimized using the substrate 2-(4-methoxyphenyl)-1,3-dithiane (Scheme 2.4).



Scheme 2.4. Test reaction for synthesizing orthoester by oxidative solvolysis.

The dithiane was deprotonated with $n\text{-BuLi}$, followed by addition of the electrophile dimethyl disulfide, resulting in complete conversion to the trithioorthoester. For the next step of solvolysis, we employed the method of Ellison *et al*, wherein excess anhydrous ethanol was added, followed by collidine and a solution of AgNO_3 in acetonitrile. The product was successfully recovered after filtration of the silver salts and extraction of the organic layer, with the main impurities being a small amount of ester, the hydrolysis side-product, and excess collidine. The collidine could be removed by either distillation, reduced pressure, or washing the organic layer with aq. $\text{Cu}(\text{NO}_3)_2$. We found that the addition of a second base, triisopropylamine, suppressed the formation of the ester to increase the purity of the orthoester. Usually no additional purification was needed, but the orthoester could be vacuum distilled or passed through a neutral alumina column to avoid decomposition on silica gel, a more acidic medium. The conversion from dithiane to orthoester was completed in one pot with no isolation of the intermediate trithioorthoester. This helped to reduce transfer losses and exclude water from the reaction.

Table 2.1. Yields of orthoesters.

Orthoester	#	Yield	Orthoester	#	Yield
	4	0% ^a		11	30%
	5	0% ^a		12	92%
	3	88%		13	29%
	6	55%		14	48%
	7	90%		15	0% ^b
	8	78%		16	0% ^b
	9	84%		17	0% ^a
	10	79%			

^adecomposition, ^bstarting material recovered

Having fine-tuned the conditions of the reaction, we then studied the scope of reactivity by varying the substrates and a clear pattern of electronic effects emerged, as shown in Table 2.1.

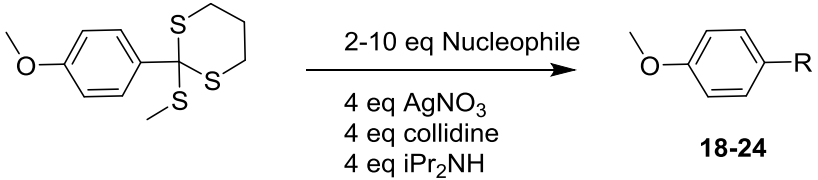
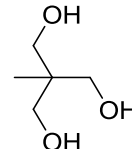
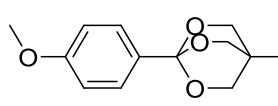
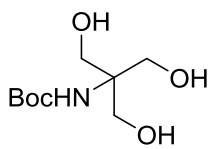
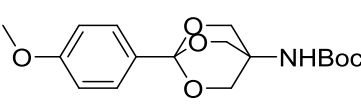
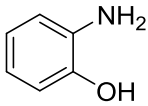
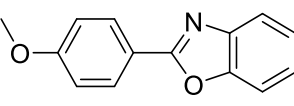
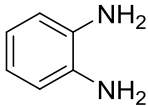
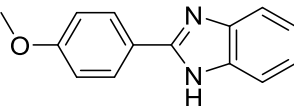
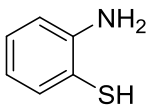
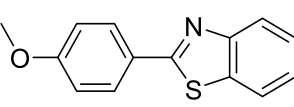
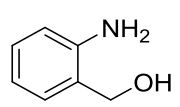
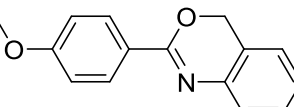
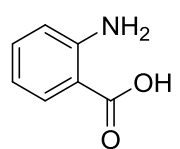
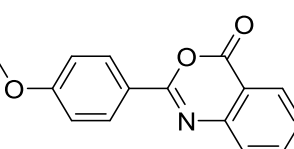
The reactions were performed in one pot and *n*-BuLi was used to deprotonate the dithiane with the exception of the brominated or esterified starting materials, in which case LDA was used. Electron-rich aromatic substrates performed the best, as in compounds **3**, **7**, **8**, **9**, **10**, and the thiophene orthoester **12**, all with yields near 80% or better. More strongly electron-donating alkoxy groups are preferred, compared to unsubstituted benzene and toluene which did not yield product (**4** and **5**) but instead a complex mixture was recovered. Meanwhile the naphthyl derivative, **11**, gave a low yield of 30%. A longer alkyl chain on the benzene ring did promote the reaction, resulting in 84% of compound **9**. A TBDMS-protected alcohol was tolerated in the reaction, yielding 55% of **6**. The 4-iodo-2,5-dimethoxyphenyl substrate contained a mixture of donating/withdrawing functionality and suffered a lower yield of 29%. In a related fashion, **15** and **16** with electron-withdrawing bromo- and ester substituents in the *para*-position returned cleanly the dithiane starting material. The dithianes in this case were most likely successfully deprotonated by LDA, a conventional reaction, yet the resulting anion was not nucleophilic enough to attack the disulfide even with heat or extended reaction time, because of the electronic effects imparted by these substituents. Placing the bromine at the *meta*-position illustrates the impact of this effect, as in this case product **14** was formed in 48%. Lastly, an alkyl substrate was tested and no product (**17**) was obtained, resembling the problems encountered with the phenyl and tolyl substrates. The preference for electron-rich substrates can be rationalized by considering the reaction mechanism wherein the silver abstracts the sulfur group, creating a cation that is stabilized by these aromatic substituents.

2.1.2. Synthesis of heterocycles

Having established the reactivity of various aromatic substrates for the formation of orthoesters, we then studied what nucleophiles besides ethanol could be used with our general method. Since orthoesters are often a synthetic intermediate of more complex products, we wondered if the trithioorthoester could perform in a similar way, thereby eliminating a synthetic step or providing new synthetic pathways to formation of heterocycles (Table 2.2). The two cyclic orthoesters were formed in a one-pot reaction as before. The following aniline-based nucleophiles were used in a two-step variation: synthesis and isolation of the trithioorthoester followed by the AgNO_3 reaction conditions. In this case 2 equivalents of the various nucleophiles were used instead of the larger excess used previously. The reason for these changes was to remove any possible interferences from the reaction by isolating the intermediate and then use a smaller amount of nucleophile, which in some scenarios could be a more valuable component.

Besides ethanol, other alcoholic nucleophiles could be implemented to form bicyclic orthoesters, either **18** or an *N*-Boc variation **19**. A compound such as **18** is appealing compared to the simple ethyl orthoester since it forms a solid that can be purified by recrystallization. The formation of benzazoles using these intermediates was studied. This class of heteroaromatic compounds differ only in the substitution of *N*, *O*, or *S* heteroatoms. Interestingly, only the benzoxazole, **20**, was formed in 69% yield. Under the reaction conditions with either *o*-phenylenediamine or 2-aminobenzenethiol the solution turned black and appeared to decompose, perhaps due to oxidation of the aromatic amine by the AgNO_3 . The benzoxazine (**23**) was not recovered whereas a benzoxazinone, (**24**), was successfully produced from anthranilic acid.

Table 2.2. Synthesis of heterocycles from trithioorthoesters.

			
Nucleophile	Product	#	Yield
		18	77%
		19	84%
		20	69%
		21	x
		22	x
		23	x
		24	65%

2.2. Conclusion

In conclusion, we have explored the conversion of trithioorthoesters into orthoesters and other heterocycles. A study of the reactivity of various substrates for orthoesters indicates that electron-rich aromatic units perform best in this role.

2.3. Acknowledgements

Synthesis of the dithiane starting materials and orthoesters was distributed between Dana Drochner and James Klimavicz. Additionally, J. Klimavicz synthesized the cyclic orthoesters while D. Drochner synthesized the heterocycles.

2.4. Experimental

Materials

Tetrahydrofuran was dried using an Innovative Technology, Inc. solvent purification system. Other reagents were obtained from commercial sources and used without further purification.

Characterization

Nuclear magnetic resonance (NMR) spectra were recorded on a Varian MR (400 MHz) or a Bruker Avance III (600 MHz). Spectra were internally referenced to the residual protonated solvent peak. Chemical shifts are given in ppm (δ) relative to the solvent.

Synthesis and characterization of compounds **3**¹¹, **8**¹¹, **9**¹², **10**¹¹, **12**¹¹, **18**¹¹, and **19**¹¹ have been reported elsewhere.

General one-pot synthesis of orthoesters. The 2-substituted-1,3-dithiane (2 mmol) was dissolved in an oven-dried flask kept under an argon atmosphere and cooled to -78 °C in a dry ice/acetone bath. 2.2 M n-Butyllithium in hexanes (1.1 mL, 2.4 mmol) was added dropwise and the solution

was stirred for 0.5-1 h, followed by the dropwise addition of MeSSMe (0.18 mL, 2.1 mmol). The solution was removed from the cold bath and allowed to warm to room temperature. Anhydrous ethanol (3 mL) was added to the solution, followed by collidine (1 mL, 8 mmol) and diisopropylamine (1.1 mL, 8 mmol). Silver nitrate (1.36 g, 8 mmol) was dissolved in dry acetonitrile and added dropwise to the reaction solution and a precipitate formed. The solution was stirred at room temperature for 1 h, then filtered and the filter cake was washed well with diethyl ether. The filtrate was washed with water, aq Cu(NO₃)₂, and brine. The organic layer was dried over sodium sulfate, filtered, and concentrated by rotary evaporation to yield the product.

tert-Butyldimethyl(4-(triethoxymethyl)phenoxy)silane (6). 55% yield.

1,4-Dimethoxy-2-(triethoxymethyl)benzene (7). 90% yield. ¹H NMR (400 MHz, Chloroform-d) δ 7.35 (t, *J* = 1.8 Hz, 1H), 6.84 (d, *J* = 1.8 Hz, 2H), 3.80 (s, 3H), 3.79 (s, 3H), 3.35 (q, *J* = 7.1 Hz, 6H), 1.16 (t, *J* = 7.1 Hz, 9H). ¹³C NMR (101 MHz, cdcl₃) δ 15.14, 32.52, 55.77, 56.56, 57.53, 112.85, 113.99, 117.22, 126.84, 151.93.

General synthesis of heterocycles. 2-(4-Methoxyphenyl)-1,3-dithiane (0.45 g, 2 mmol) was dissolved in an oven-dried flask kept under an argon atmosphere and cooled to -78 °C in a dry ice/acetone bath. 2.2 M n-Butyllithium in hexanes (1.1 mL, 2.4 mmol) was added dropwise and the solution was stirred for 0.5-1 h, followed by the dropwise addition of MeSSMe (0.18 mL, 2.1 mmol). The solution was removed from the cold bath and allowed to warm to room temperature. Water was added and the product was extracted with diethyl ether. The organic layer was washed with brine, dried over sodium sulfate, filtered, and concentrated by rotary evaporation. The trithioorthoester was dissolved in 20 mL THF, followed by the addition of collidine (1 mL, 8 mmol) and diisopropylamine (1.1 mL, 8 mmol). Silver nitrate (1.36 g, 8 mmol) was dissolved in

dry acetonitrile and added dropwise to the reaction solution and a precipitate formed. The solution was stirred at room temperature for 1 h, then filtered and the filter cake was washed well with diethyl ether. The filtrate was washed with water, aq $\text{Cu}(\text{NO}_3)_2$, and brine. The organic layer was dried over sodium sulfate, filtered, and concentrated by rotary evaporation to yield the crude product.

2-(4-Methoxyphenyl)benzo[d]oxazole (20). 69% yield. ^1H NMR (600 MHz, Chloroform-d) δ 8.23 (d, $J = 8.9$ Hz, 2H), 7.78 – 7.73 (m, 1H), 7.59 – 7.53 (m, 1H), 7.36 – 7.31 (m, 2H), 7.08 – 7.01 (m, 2H), 3.90 (s, 3H).

2-(4-methoxyphenyl)-4H-benzo[d][1,3]oxazin-4-one (24). 65% yield. ^1H NMR (400 MHz, Chloroform-d) δ 8.27 (d, $J = 8.8$ Hz, 2H), 8.22 (dd, $J = 7.9, 1.5$ Hz, 1H), 7.81 (td, $J = 7.7, 1.5$ Hz, 1H), 7.65 (d, $J = 8.1$ Hz, 1H), 7.48 (t, $J = 7.6$ Hz, 1H), 7.01 (d, $J = 8.9$ Hz, 2H), 3.90 (s, 3H). ^{13}C NMR (101 MHz, cdCl_3) δ 55.66, 114.29, 116.85, 122.67, 127.05, 127.85, 128.70, 130.42, 136.64, 147.47, 157.27, 159.93, 163.42.

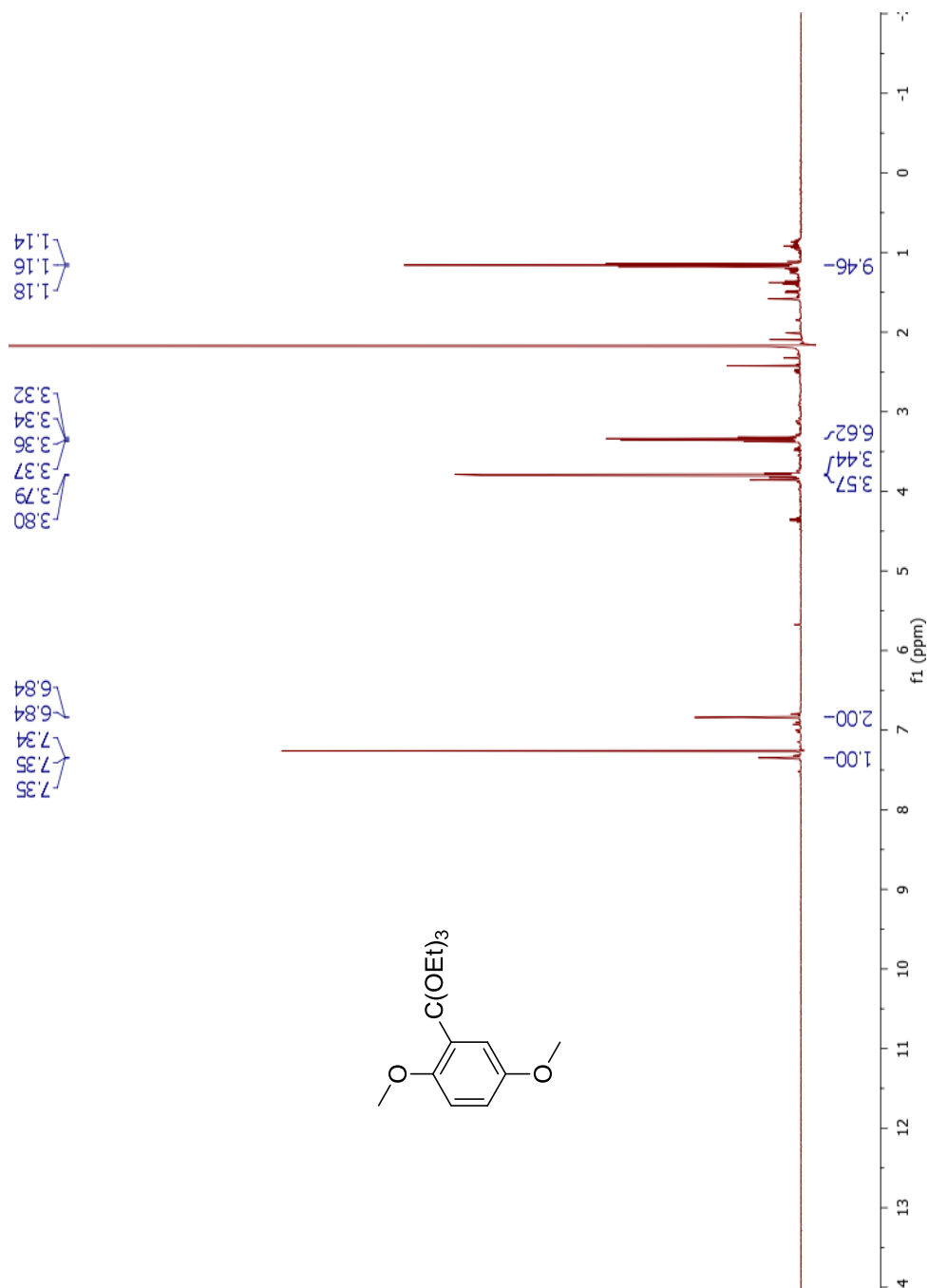


Figure 2.17. ^1H NMR of 1,4-Dimethoxy-2-(triethoxymethyl)benzene (7).

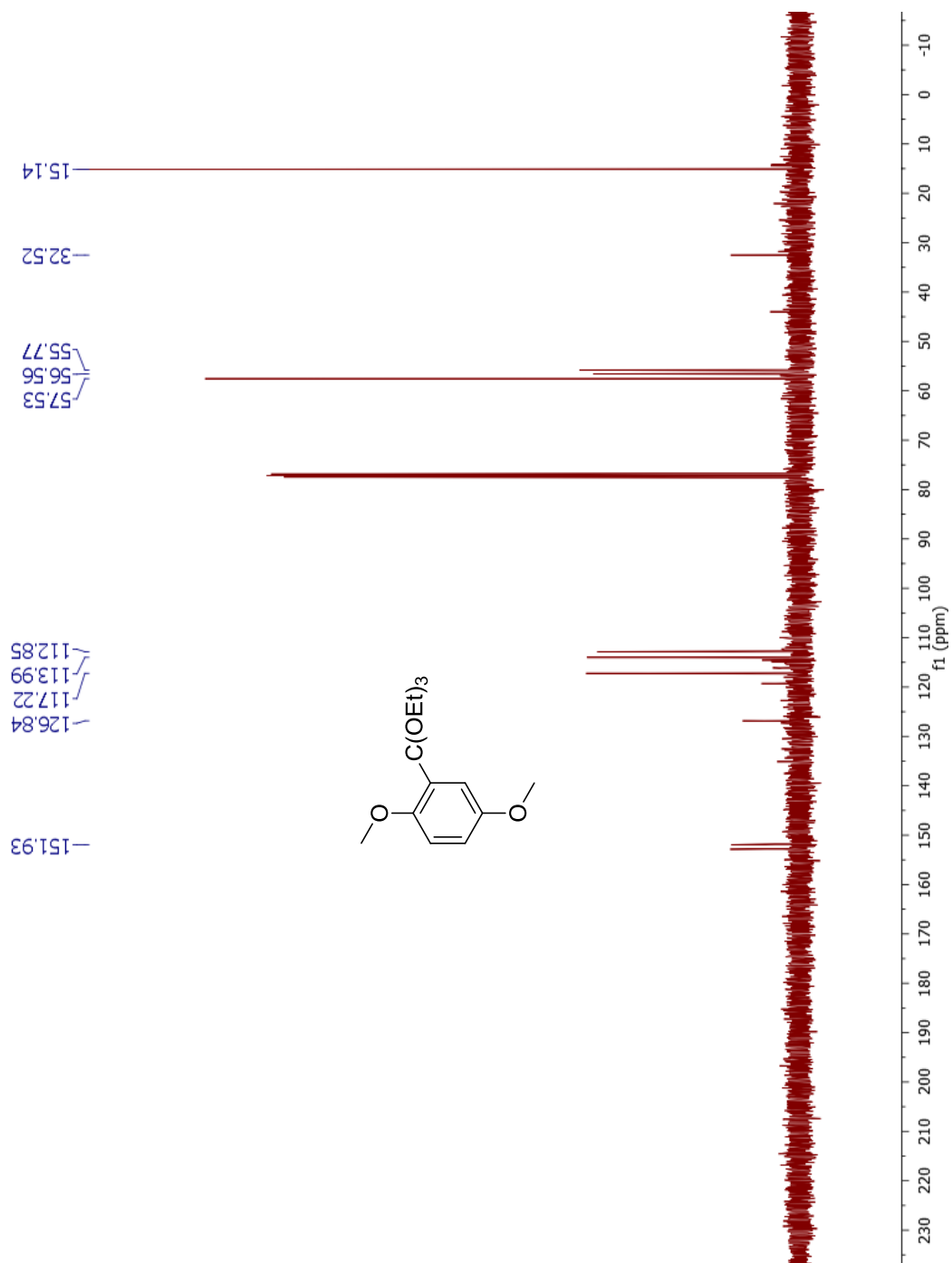


Figure 2.18. ^{13}C NMR of 1,4-Dimethoxy-2-(triethoxymethyl)benzene (7).

2.5. References

- Huang, Z.; Derksen, D. J.; Vederas, J. C., Preparation and use of cysteine orthoesters for solid-supported synthesis of peptides. *Organic letters* **2010**, *12* (10), 2282-2285.
- (a) Bochkov, A. F.; Betaneli, V. I.; Kochetkov, N. K., Orthoesters of sugars. *Russ Chem Bull* **1974**, *23* (6), 1299-1304; (b) Liu, X.; Wada, R.; Boonyarattanakalin, S.; Castagner, B.; Seeberger, P. H., Automated synthesis of lipomannan backbone [small alpha](1-6) oligomannoside viaglycosyl phosphates: glycosyl tricyclic orthoesters revisited. *Chemical Communications* **2008**, (30), 3510-3512.
- (a) Mike, J. F.; Intemann, J. J.; Cai, M.; Xiao, T.; Shinar, R.; Shinar, J.; Jeffries-EL, M., Efficient synthesis of benzobisazole terpolymers containing thiophene and fluorene. *Polymer Chemistry* **2011**, *2* (10), 2299-2305; (b) Mike, J. F.; Inteman, J. J.; Ellern, A.; Jeffries-El, M., Facile synthesis of 2, 6-disubstituted benzobisthiazoles: Functional monomers for the design of organic semiconductors. *The Journal of Organic Chemistry* **2009**, *75* (2), 495-497; (c) Mike, J. F.; Makowski, A. J.; Jeffries-El, M., An Efficient Synthesis of 2,6-Disubstituted Benzobisoxazoles: New Building Blocks for Organic Semiconductors. *Organic Letters* **2008**, *10* (21), 4915-4918; (d) Bastug, G.; Eviolitte, C.; Markó, I. E., Functionalized Orthoesters as Powerful Building Blocks for the Efficient Preparation of Heteroaromatic Bicycles. *Organic Letters* **2012**, *14* (13), 3502-3505.
- (a) Wender, P. A.; Buschmann, N.; Cardin, N. B.; Jones, L. R.; Kan, C.; Kee, J.-M.; Kowalski, J. A.; Longcore, K. E., Gateway synthesis of daphnane congeners and their protein kinase C affinities and cell-growth activities. *Nat Chem* **2011**, *3* (8), 615-619; (b) Bourjot, M.; Leyssen, P.; Neyts, J.; Dumontet, V.; Litaudon, M., Trigocherrierin A, a Potent Inhibitor of Chikungunya Virus Replication. *Molecules* **2014**, *19* (3), 3617.
- (a) Pinner, A.; Klein, F., Umwandlung der nitrile in imide. *Berichte der deutschen chemischen Gesellschaft* **1877**, *10* (2), 1889-1897; (b) McElvain, S.; Nelson, J. W., the Preparation of Orthoesters. *Journal of the American Chemical Society* **1942**, *64* (8), 1825-1827.
- Tachitschibabin, A. E., Neue Synthesen mit Hilfe der magnesiumorganischen Verbindungen. *Berichte der deutschen chemischen Gesellschaft* **1905**, *38* (1), 561-566.
- Jones, R. G., The condensation of ethyl triethoxyacetate and some active methylene compounds. *J. Am. Chem. Soc.* **1951**, *73* (Copyright (C) 2015 American Chemical Society (ACS). All Rights Reserved.), 5168-9.
- (a) Corey, E. J.; Raju, N., A new general synthetic route to bridged carboxylic ortho esters. *Tetrahedron letters* **1983**, *24* (50), 5571-5574; (b) Giner, J.-L., DMOBO: An Improvement on the OBO Orthoester Protecting Group. *Organic letters* **2005**, *7* (3), 499-501.
- Corey, E.; Erickson, B. W., Oxidative hydrolysis of 1, 3-dithiane derivatives to carbonyl compounds using N-halosuccinimide reagents. *The Journal of organic chemistry* **1971**, *36* (23), 3553-3560.

10. Ellison, R. A.; Woessner, W. D.; Williams, C. C., New synthetic methods from dithianes. Convenient oxidation of aldehydes to acids and esters. *The Journal of organic chemistry* **1972**, 37 (17), 2757-2759.
11. Klimavicz, J. S. Syntheses of donor-acceptor benzo(bis)oxazole small molecules. Iowa State University, Ames, Iowa, 2013.
12. Tlach, B. C.; Tomlinson, A. L.; Ryno, A. G.; Knoble, D. D.; Drochner, D. L.; Krager, K. J.; Jeffries-El, M., Influence of Conjugation Axis on the Optical and Electronic Properties of Aryl-Substituted Benzobisoxazoles. *The Journal of Organic Chemistry* **2013**, 78 (13), 6570-6581.

CHAPTER 3

TOWARD THE SYNTHESIS OF 2,6-ASYMMETRIC BENZOBISOXAZOLES

3.1. Introduction to benzobisoxazoles

The donor-acceptor approach to synthesizing conjugated polymers, wherein electron-rich and deficient monomers are copolymerized¹, has proven to be an effective technique toward producing low bandgap polymers for optoelectronic applications such as organic photovoltaics². In our group we have widely studied benzobisazoles, a class of heterocycles which includes *trans*-benzobisoxazole (*trans*-BBO), *cis*-benzobisoxazole (*cis*-BBO), and *trans*-benzobisthiazole (*trans*-BBTZ) (Fig. 1).

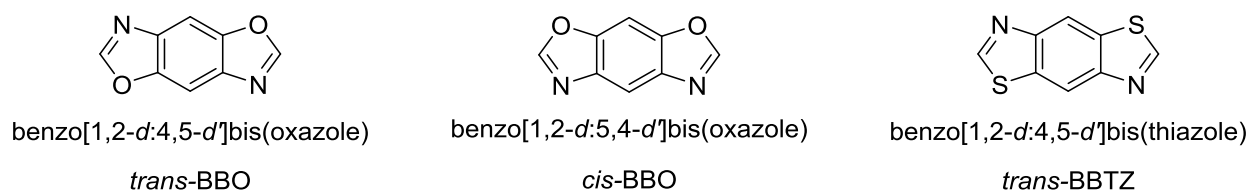


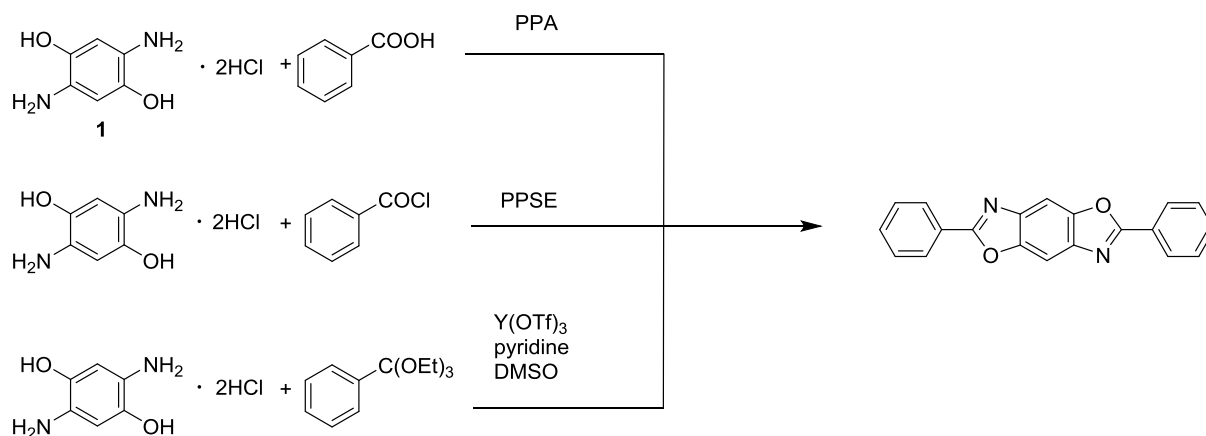
Figure 3.1. Structures of benzobisazoles.

Benzobisazoles are an appealing family for the development of materials for organoelectronic purposes due to the extended, planar pi system, high charge carrier mobilities³ and thermal stability⁴. While traditionally synthesized in harsh conditions like condensations with polyphosphoric acid (PPA)⁵, our group's advances in benzobisazole synthesis via orthoester condensation⁶ expanded the scope of reactivity by increasing solubility and functional group tolerance under the mild reaction conditions. Our research, among others, has demonstrated that

benzobisazoles are relatively weak acceptors⁷, in comparison to other well-known acceptors, producing wide bandgap materials. This is beneficial for the synthesis of materials for use in organic light emitting diodes⁸, but for photovoltaic applications that require narrow bandgap materials, new BBO-containing materials are needed. Other groups have studied the use of benzobisthiazole as a donor molecule⁹ and have observed good efficiencies⁹⁻¹⁰. In this new approach, we sought to explore the use of benzobisoxazoles as a “pi spacer¹¹,” a relatively weaker electron-donating/withdrawing unit used to extend conjugation and improve the molar absorptivity of the molecule. Typically, vinylene, ethynyl, benzene, thiophene, or furan are used as pi spacers in the synthesis of conjugated polymers and small molecules. Similarly, the large pi system and weak electron-donating and withdrawing properties of BBO suggest that it could be used for this purpose as an alternative role to either a donor or acceptor. The use of BBOs as a pi spacer requires the synthesis of new 2,6-asymmetric BBOs (ABBOs), a greater synthetic challenge compared to the usual symmetric structures.

3.1.1. Synthesis of benzobisoxazoles and benzoxazoles

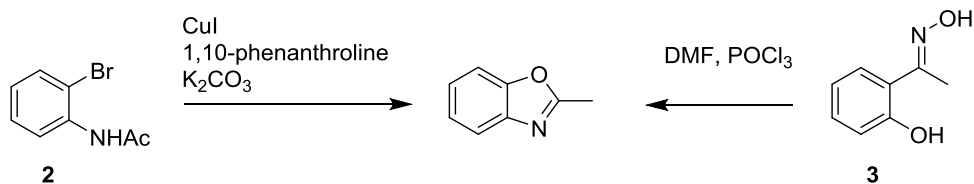
We began by reviewing current methods of synthesizing BBOs and benzoxazoles to gain insight on how to approach the new synthesis. An overview of the synthetic methods herein focuses on the *trans*-BBO isomer, as the research discussed later focuses on synthesis of the



Scheme 3.1. Synthesis of *trans*-BBO.

A-trans-BBO. Traditional methods for the synthesis of the BBO involve condensation of diaminohydroquinone (DAHQ) hydrochloride salt (**1**) and reaction conditions can range from harsh to mild. The use of polyphosphoric acid (PPA) to couple DAHQ and a carboxylic acid is a high temperature and strongly acidic method and, as a result, the BBOs produced can have limited solubility and functionality tolerated in these reaction conditions. Using polyphosphoric silyl ether (PPSE)¹² and an acid chloride with DAHQ can tolerate some functionality such as alkyl chains, though yields of this reaction average 50%. A milder and higher yielding method was developed by our group⁶, inspired by known methods of benzoxazole synthesis from orthoesters. After optimization, it was found that BBOs with many functional groups could be synthesized at low temperature with catalytic amounts of Y(OTf)_3 or Yb(OTf)_3 , which functions as a Lewis acid.

While benzoxazoles can be synthesized similarly to BBOs some additional methods are shown in Scheme 3.2. The C-O bond can be formed by copper catalyzed cyclization of an *ortho*-bromoacetanilide¹³ (**2**). A benzoxazole can be formed from an *ortho*-hydroxy aryl oxime (**3**) via a Beckmann rearrangement¹⁴ which is catalyzed by the Vilsmeier reagent, formed *in situ* from POCl_3 and DMF.

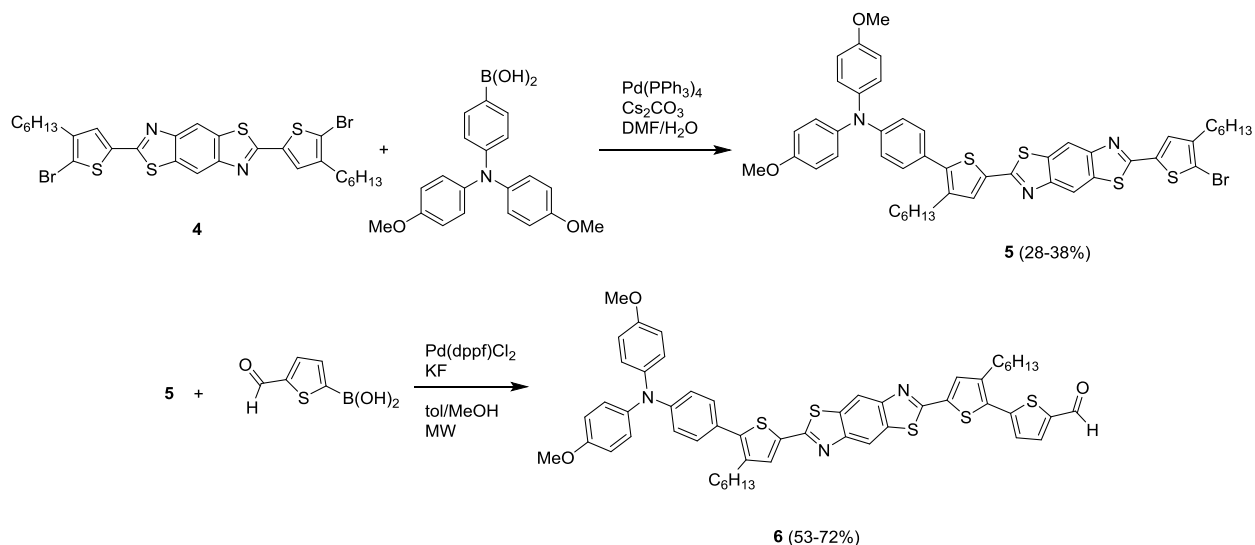


Scheme 3.2. Synthesis of 2-methylbenzoxazole.

3.1.2. Asymmetric BBOs

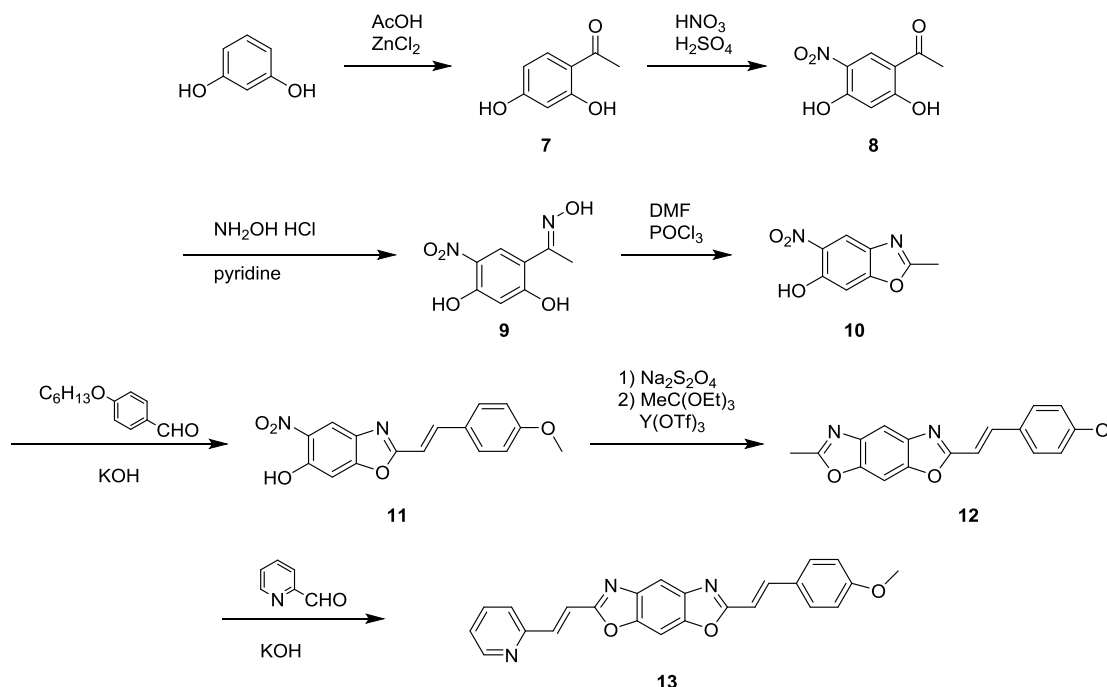
3.1.2.1. Via cross-coupling reactions

There have been very few syntheses of asymmetric benzobisazoles. In one case, a BBTZ was synthesized with alkylthiophenes at the 2,6-positions (Scheme 3.3). Bromination of the flanking thiophenes (**4**) allowed for stepwise coupling of different aromatic units to either side by a Suzuki reaction in low yields due to the mixture of substituted products and starting material that can be recovered from this non-regioselective approach¹⁵.



Scheme 3.3. Synthesis of asymmetric BBTZ via Suzuki cross-coupling.

3.1.2.2. Via Beckmann rearrangement



Scheme 3.4. Synthesis of vinylene A-*cis*-BBO via Beckmann rearrangement and Knoevenagel condensation.

Previous research in our group made progress toward the synthesis of A-*trans*-BBOs and resulted in a new synthesis of an A-*cis*-BBO. The key was synthesizing the benzene core with different precursor functional groups which could be individually transformed to produce the A-*cis*-BBO as shown in Scheme 3.4. J. Klimavicz produced the A-*cis*-BBO starting from resorcinol, which was acylated and nitrated to make 2,4-dihydroxy-5-nitroacetophenone, **8**. The carbonyl group was transformed into an oxime under basic conditions, and finally the Beckmann rearrangement with POCl₃/DMF was used to create the benzoxazole, **10**. To demonstrate proof of concept, **10** and p-anisaldehyde were condensed in a Knoevenagel-like reaction to join the two aromatic groups by a vinylene linkage. Reduction of the nitro group and orthoester condensation on the other side completed the A-*cis*-BBO (**12**). Finally, another Knoevenagel-type condensation with 2-pyridine carboxaldehyde resulted in the other vinylene linkage.

3.2. Synthesis of asymmetric trans-BBOs

With a known method of synthesizing *A-cis*-BBOs, we turned our attention to the synthesis of *A-trans*-BBOs, an isomer which is more commonly used and has a better quinoid structure, a resonance form which is important to consider when designing conjugated polymers, as shown in Figure 3.2.

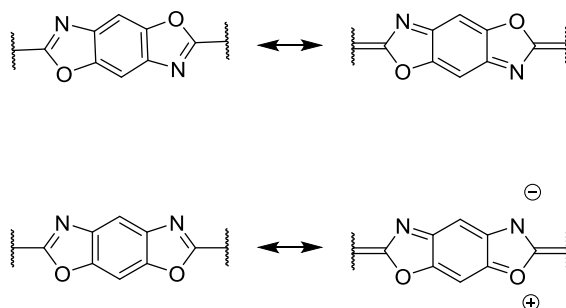
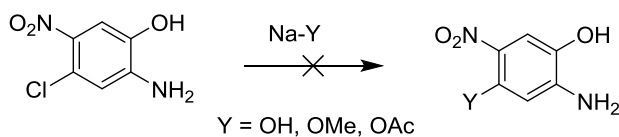


Figure 3.2. Aromatic and quinoid resonance forms of *trans*-BBO and *cis*-BBO

3.2.1. Via nucleophilic aromatic substitution

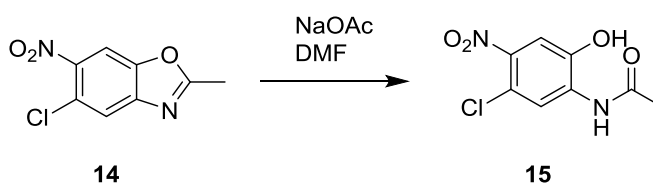


Scheme 1.5. Attempted nucleophilic aromatic substitution.

2-Amino-4-chloro-5-nitrophenol was commercially available and appeared to be an ideal starting material, since 3 of the 4 needed aromatic substituents were in place. It was envisioned that the remaining chloro group could be replaced with an oxygen substituent via nucleophilic aromatic substitution, which should be a favorable reaction since the chloro group was ortho to a nitro group to facilitate the reaction. The simplest first reaction was direct substitution of the chloro group of 2-amino-4-chloro-5-nitrophenol with the nucleophiles sodium hydroxide, methoxide or

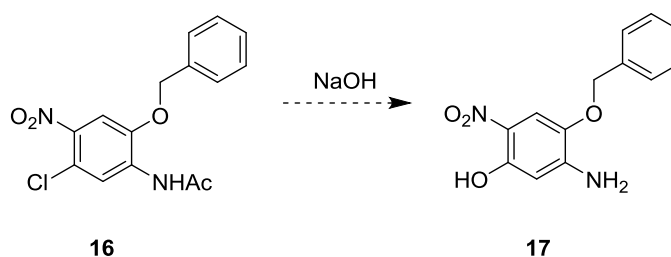
acetate (Scheme 3.5). In all cases, starting material was returned, perhaps because the base only deprotonated the alcohol group and deactivated the aromatic ring from reacting.

Next, it was thought that if the benzoxazole was formed first, then the substitution might proceed, so 6-chloro-2-methyl-5-nitrobenzoxazole (**14**) was synthesized. This was used as the substrate with sodium acetate as the nucleophile. Unfortunately, the product's NMR indicated that the benzoxazole was ring opened, which is known to occur in basic conditions¹⁶. This proved that a benzoxazole was unstable to this type of reaction and other nucleophiles were not tested.



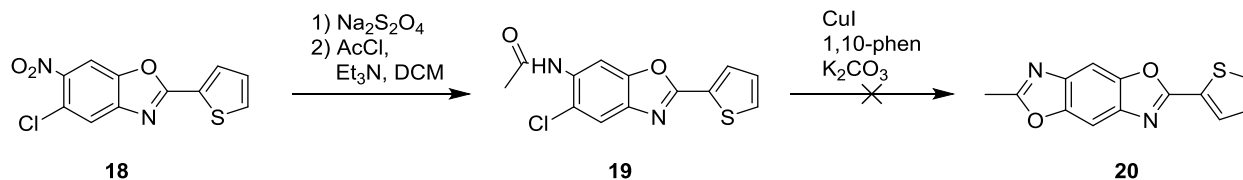
Scheme 3.6. Attempted nucleophilic aromatic substitution of a benzoxazole resulted in ring opening.

To overcome this complication, it was determined that a base-stable protecting group should be employed. *N*-acylation of 2-amino-4-chloro-5-nitrophenol followed by benzylation of the alcohol afforded **16** containing the base-tolerant benzyl group. Nucleophilic aromatic substitutions can be attempted on this compound, providing a path toward an *A-trans*-BBO as illustrated in Scheme 3.7.



Scheme 3.7. Nucleophilic aromatic substitution in the presence of a benzyl group.

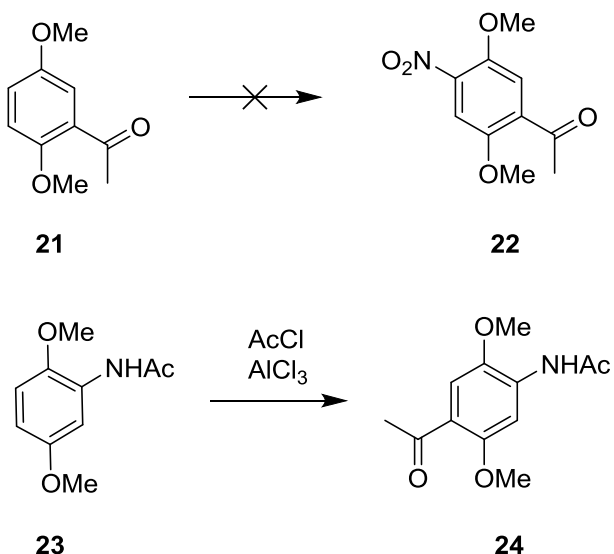
3.2.2. Via copper catalyzed cyclization



Scheme 3.8. Attempted copper-catalyzed benzoxazole formation

It was known that ortho-haloacetanilides with copper could be transformed to benzoxazoles so compound **19** was synthesized. The copper-catalyzed reaction was attempted with copper (I) iodide, 1,10-phenanthroline and potassium carbonate according to similar literature procedures (Scheme 3.8), yet no product was formed. While it might be possible that a bromo- instead of a chloro- substituent could facilitate the reaction, experience with test reactions with similar compounds showed that this reaction performed best when there was no other electron-withdrawing group on the benzene ring. Therefore it was clear that the reaction would not occur with the benzoxazole already on the ring.

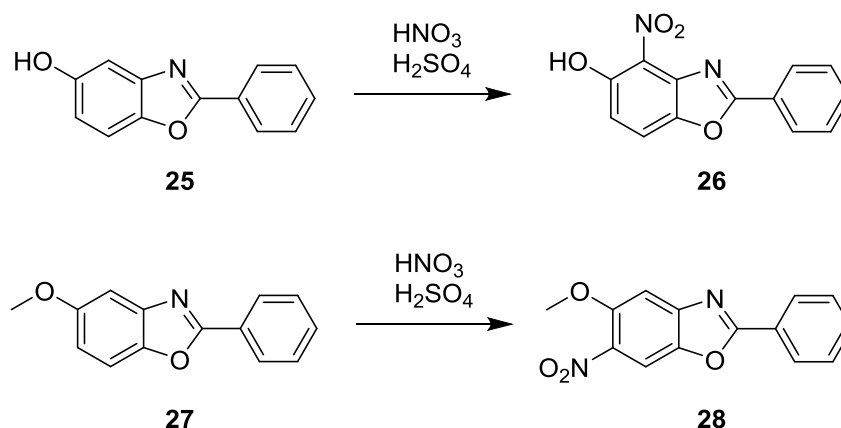
3.2.3. Via Beckmann rearrangement



Scheme 3.9. Routes toward substituted acetophenones for A-*trans*-BBO via Beckmann rearrangement.

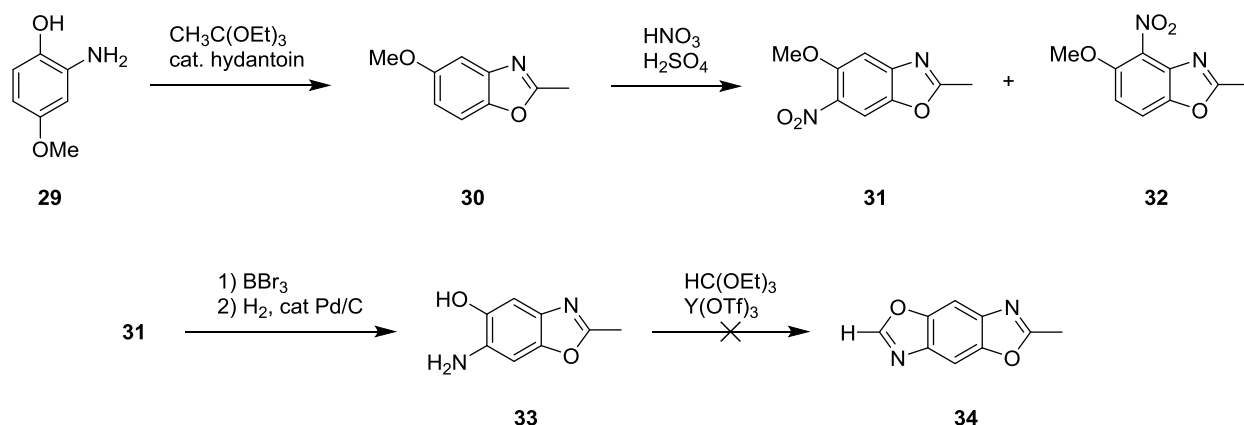
It was investigated if the Klimavicz method of *A-cis*-BBOs would work for *A-trans*-BBOs. First the ketone and nitro groups needed to be installed *para*- to each other as shown in Scheme 3.9. Based on the directing effect of the ketone, it was known that nitration of 2,5-dimethoxyacetophenone would not produce the correct isomer, **22**. However, Friedel-Crafts acylation of 2,5-dimethoxyacetanilide would create a structure (**24**) that could be used similarly to the Klimavicz synthesis. Unfortunately, an optimized synthesis of the ketone could not be obtained, either with AlCl_3 or SnCl_4 , and the reactant appeared to decompose instead.

3.2.4. Via nitration of methoxybenzoxazole



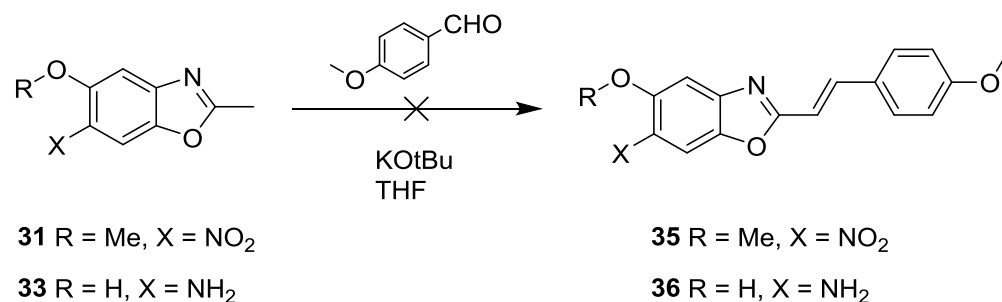
Scheme 3.10. Nitration of 6-hydroxy- or 6-methoxybenzoxazole results in different substitution patterns.

Previous research by the Jeffries-EL group demonstrated an interesting reaction pattern of benzoxazoles (Scheme 3.10). A 2-phenyl-5-hydroxybenzoxazole could be nitrated at the 4-position (**26**), whereas nitration of the 5-methoxy derivative resulted in substitution at the 6-position (**28**). Therefore, a 6-methoxybenzoxazole (**28**) was synthesized to further investigate the possibility of using this as a core for ABBOs.



Scheme 3.11. Synthesis of *A-trans*-BBO via a 5-amino-6-hydroxybenzoxazole.

The 5-methoxy-2-methylbenzoxazole was synthesized from an aminophenol by an orthoester condensation as in Scheme 3.11. Compound **30** was nitrated, resulting in a 3:2 mixture of substitution products **31** and **32** from which the desired isomer (**31**) could be isolated by recrystallization from ethyl acetate. Demethylation with boron tribromide and then catalytic hydrogenation yielded **33**. Lastly, the ring on the opposite side needed to be closed, and it was decided to attempt this with our usual orthoester/ $\text{Y}(\text{OTf})_3$ conditions. Unfortunately, the starting material decomposed under these conditions. This approach remains a promising path toward the *A-trans*-BBO and other methods of ring closing the final hydroxyamine could be tested, such as acylation and dehydration.

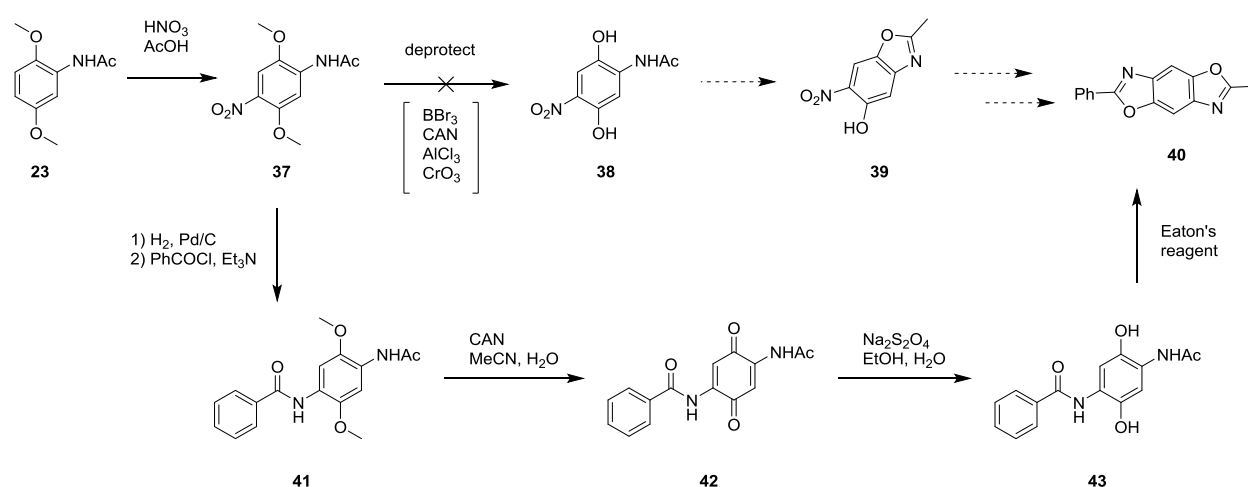


Scheme 3.12. Attempted Knoevenagel condensations of 6-methoxybenzoxazoles

It was investigated if the order of reactions could be altered to yield the vinylene benzoxazole, wherein a Knoevenagel-like condensation occurred before ring closing the second oxazole ring

(Scheme 3.11). The nitro- (**29**) and aminobenzoxazoles (**31**) were each tested with the condensation of p-anisaldehyde under modified Knoevenagel condensation conditions of KOtBu in THF, as well as the usual method of KOH/DMF¹⁷. While the cis-BBO derivative (**11**) had previously survived the condensation reaction, both (**35**) and (**36**) were not recovered and instead the starting materials appeared to decompose. It was also attempted to deoxygenate the solvents by bubbling argon and conducting the reaction under an argon atmosphere, yet to no avail.

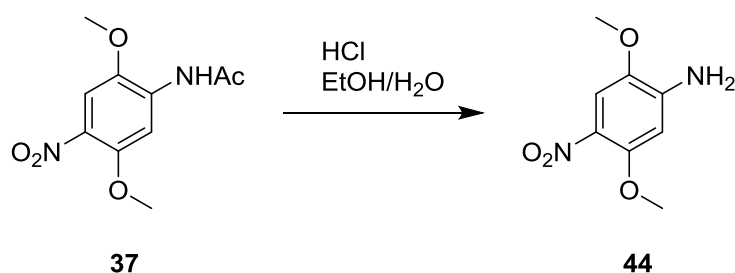
3.2.5. Via acid-catalyzed dehydration/cyclization



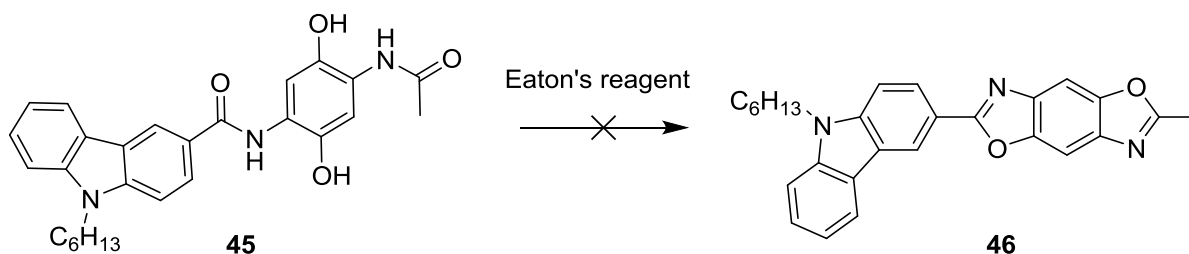
Scheme 3.13. Pathways toward an *A-trans*-BBO via protected hydroquinones.

Another strategy toward the synthesis of ABBOs is by substitution of protected hydroquinones (Scheme 3.13). Nitration of 2,5-dimethoxyacetanilide occurs at the 4-position in high yield, thus installing all oxygen and nitrogen substituents needed for the ABBO core. In his research, J. Klimavicz sought to demethylate this compound and then ring-close to form the first oxazole ring (**39**). Many deprotection conditions were tried, such as boron tribromide, ceric ammonium nitrate, aluminum chloride, and chromium trioxide, yet unfortunately all methods resulted in decomposition or returned starting material. Other alcohol protecting groups were also evaluated in this fashion, but did not lead to success.

This strategy seemed promising and I hypothesized that the presence of the nitro group was deactivating the reaction. The order of reactions was rearranged to continue with the synthesis so the deprotection was needed later. First, the nitro group was transformed into a phenyl amide (**41**) and then the demethylation successfully occurred with ceric ammonium nitrate to form the quinone (**42**) followed by reduction to the hydroquinone (**43**) by sodium dithionite. Lastly, the BBO **40** was formed by acid-catalyzed dehydration by heating in Eaton's reagent, a milder alternative to PPA. Precipitation into water yielded the ABBO in 73% yield.

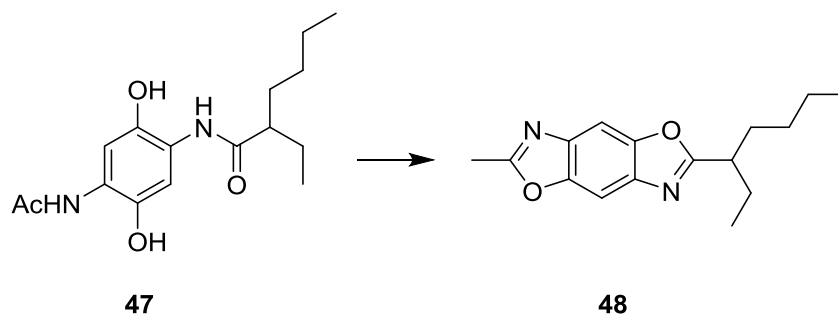


Scheme 3.14. Synthesis of the core starting material for A-*trans*-BBO.



Scheme 3.15. Dehydration with Eaton's reagent resulted in decomposition.

To create a general method, 2,5-dimethoxy-4-nitroaniline (**44**) was synthesized as the core starting material by hydrolysis of *N*-(2,5-dimethoxy-4-nitrophenyl)acetamide (Scheme 3.14). A more complex diamidohydroquinone featuring carbazole and methyl substituents (**45**) was synthesized to expand the scope of the ABBO synthesis. As shown in Scheme 3.15, the substituted



Scheme 3.16. A compound with asymmetric alkyl chains was used to test dehydration/cyclization conditions.

hydroquinone was heated with Eaton's reagent and precipitation into water resulted in black, decomposed material. It was evident that Eaton's reagent was too harsh to complete the reaction in the presence of additional functional groups and another reagent needed to be used.

To test conditions for the final ring closure, a molecule with asymmetric alkyl substituents on the amides (**47**, Scheme 3.16) was synthesized with the intent that the longer alkyl chain would aid with solubility. This molecule also decomposed with Eaton's reagent. In my experience, acetic anhydride was an efficient dehydrating reagent for the similar formation of benzoxazoles but in this case resulted, surprisingly, in a very low yield of 2,6-dimethyl-*trans*-BBO. Triphenyl phosphine with carbon tetrachloride was reported to be a mild dehydrating agent but the reaction never achieved completion by TLC so this method was abandoned. Refluxing toluene with catalytic *p*TSA also did not make product after extended reaction times. The problem with these conditions was the insolubility of the starting material in hot toluene, thus a more polar solvent was needed. The starting material was soluble in hot POCl₃/CHCl₃ or POCl₃/DMF but the reaction again was not complete after heating for multiple days, perhaps due to equilibration of the starting material and product mixture.

3.3. Conclusion

Several methods were attempted to synthesize an *A-trans*-BBO. It was found that the Beckmann rearrangement used to synthesize an *A-cis*-BBO could not be used for an *A-trans*-BBO due to the inability to synthesize the ketone starting material and copper-catalyzed benzoxazole formation did not complete the ring formation. Selection of the benzyl protecting group could provide a pathway for nucleophilic aromatic substitution to succeed. Other methods have made progress toward the synthesis of *A-trans*-BBOs. Another approach involved the synthesis of a 5-amino-6-hydroxybenzoxazole and new conditions to achieve the final ring closure to complete the BBO can be explored. An alternative synthesis included dehydration of asymmetrically substituted 2,5-diacetanilidehydroquinones with Eaton's reagent, although this method does not tolerate functionality. New methods of dehydration that accommodate additional functionality and solubility issues need to be developed in order to achieve a general synthetic method for producing a library of 2,6-asymmetric *trans*-BBOs.

3.4. Acknowledgements

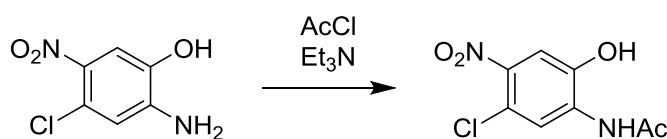
All experiments were performed by the author unless stated otherwise. All text was written by the author.

3.5. Experimental

4-methoxy-2-nitrophenol¹⁸, 2,5-dimethoxyacetanilide¹⁹, and *N*-hexylcarbazole-3-carboxylic acid²⁰ were synthesized according to literature procedures. All other materials were purchased from commercial sources and used without further purification. Nuclear magnetic resonance (NMR) spectra were recorded on a Varian MR (400 MHz) or a Bruker Avance III (600 MHz).

Spectra were internally referenced to the residual protonated solvent peak. Chemical shifts are given in ppm (δ) relative to the solvent.

6-chloro-2-methyl-5-nitrobenzo[d]oxazole (14). 2-amino-4-chloro-5-nitrophenol (1.50 g, 8 mmol), triethyl orthoacetate (2.2 mL, 12 mmol) and yttrium triflate (24 mg, 0.05 mmol) were mixed in 5 mL DMSO and heated to 70 °C for 2 h. The mixture was cooled and poured into water. The pale yellow solid was filtered, washed well with water and dried to yield the product (1.58 g, 93%) $^1\text{H NMR}$ (600 MHz, Chloroform- d) δ 8.06 (s, 1H), 7.80 (s, 1H), 2.71 (s, 2H).

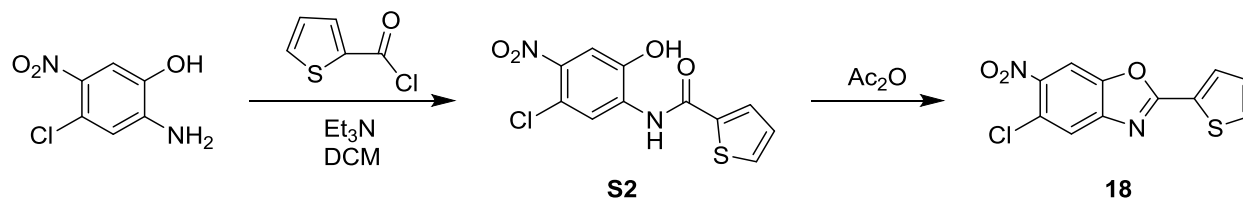


S1

***N*-(5-chloro-2-hydroxy-4-nitrophenyl)acetamide (S1).** 2-amino-4-chloro-5-nitrophenol (0.83 g, 4.4 mmol) and triethylamine (0.9 mL, 6.6 mmol) were mixed in 15mL DCM. Acetyl chloride (0.3mL, 4.8mmol) was added dropwise. A yellow precipitate soon formed and dilute HCl was added. The solid was filtered and recrystallized with EtOH (0.61 g, 60%). $^1\text{H NMR}$ (400 MHz, Chloroform- d) δ 7.94 (s, 0H), 6.84 (s, 0H), 4.33 (s, 3H), 2.37 (s, 1H).

***N*-(2-(benzyloxy)-5-chloro-4-nitrophenyl)acetamide (16).** *N*-(5-chloro-2-hydroxy-4-nitrophenyl)acetamide (S1) (1.13 g, 4.9 mmol), potassium carbonate (1 g, 7.4 mmol), and benzyl chloride (0.7 mL, 5.9 mmol) were mixed in 5 mL DMF and heated to 50 °C overnight and then cooled to room temperature. The organic layer was extracted with chloroform and then washed with 1 M NaOH, water and brine. The organic layer was dried with sodium sulfate, filtered, and concentrated by rotary evaporation. The crude product was recrystallized from EtOH, filtered, and

dried to yield the product (1.16 g, 74%). ¹H NMR (400 MHz, Chloroform-d) δ 8.71 (s, 1H), 7.86 (s, 1H), 7.62 (s, 1H), 7.47 – 7.39 (m, 5H), 5.18 (s, 2H), 2.21 (s, 3H).



***N*-(5-chloro-2-hydroxy-4-nitrophenyl)thiophene-2-carboxamide (S2).** 2-amino-4-chloro-5-nitrophenol (1.89 g, 10 mmol) and triethylamine (2 mL, 15 mmol) were mixed in 30 mL DCM and thiophene-2-carbonyl chloride (1.61 g, 11 mmol) was added dropwise. A yellow solid formed which was filtered and rinsed with water and chloroform, then dried (2.72 g, 91%).

5-chloro-6-nitro-2-(thiophen-2-yl)benzo[d]oxazole (18). *N*-(5-chloro-2-hydroxy-4-nitrophenyl)thiophene-2-carboxamide (S2) (2.38 g, 8 mmol) was refluxed in 20 mL acetic anhydride with one drop of concentrated sulfuric acid. The solution was cooled and poured into ice water and allowed to sit while a solid formed. The solid was filtered and recrystallized from MeOH/H₂O (1.70 g, 84%). ¹H NMR (400 MHz, Chloroform-d) δ 8.13 (s, 1H), 8.05 (d, J = 8.7 Hz, 0H), 7.95 (dd, J = 3.9, 1.2 Hz, 1H), 7.75 (dd, J = 5.1, 1.2 Hz, 1H), 7.52 (s, 1H), 7.21 (dd, J = 5.0, 3.9 Hz, 1H).

2-amino-4-methoxyphenol (29). 4-Methoxy-2-nitrophenol (6.49 g, 38.3 mmol) was suspended in methanol and the solution was degassed by bubbling argon. 0.80 g of 10% Pd/C was added and then hydrogen was bubbled through the solution overnight and it turned from yellow to colorless. The solution was flushed with argon and filtered through a Büchner funnel to remove the Pd/C. The solvent of the filtrate was removed by rotary evaporation to afford the product

(5.12 g, 36.7 mmol) as a brown solid in 96% yield. $^1\text{H NMR}$ (400 MHz, DMSO- d_6) δ 8.44 (s, 1H), 6.50 (s, 0H), 6.19 (s, 1H), 5.95 (dd, $J = 8.5, 2.9$ Hz, 1H), 4.53 (s, 2H), 3.58 (s, 3H).

5-methoxy-2-methylbenzo[d]oxazole (30). 2-amino-4-methoxyphenol (2.05 g, 14.7 mmol), 1,3-Dibromo-5,5-dimethylhydantoin (20 mg, 0.07 mmol) and 10 mL triethyl orthoacetate were mixed together and heated to 60 °C for 0.5 h. The mixture was concentrated by vacuum distillation. The residue was passed through a silica gel column with 1:1 hexanes:ethyl acetate and isolated by rotary evaporation. The solid was recrystallized with cold hexanes and filtered to yield the product (2.12 g, 82%) as pinkish crystals. $^1\text{H NMR}$ (400 MHz, cdcl_3) δ 7.46 (dd, $J = 8.9, 2.4$ Hz, 1H), 7.00 (dd, $J = 8.9, 2.5$ Hz, 1H). $^1\text{H NMR}$ (400 MHz, cdcl_3) δ 7.46 (dd, $J = 8.9, 2.4$ Hz, 1H), 7.00 (dd, $J = 8.9, 2.5$ Hz, 1H), 3.96 (s, 3H), 2.73 (s, 3H).

5-methoxy-2-methyl-6-nitrobenzo[d]oxazole (31). 5-methoxy-2-methylbenzo[d]oxazole (1.30 g, 8 mmol) was dissolved in a flask with 5 mL concentrated sulfuric acid, which was chilled in an ice bath. 15.8 M nitric acid (0.57 mL, 9 mmol) was added to the solution dropwise. The solution was stirred for 0.5 h and then poured into ice water. The solid was filtered and rinsed well with water. The solid was recrystallized with ethyl acetate and the solid product was isolated by filtration (0.76 g, 3.6 mmol) in 46%. $^1\text{H NMR}$ (400 MHz, Chloroform- d) δ 8.03 (s, 1H), 7.30 (s, 1H), 4.00 (s, 3H), 2.68 (s, 3H).

2-Methyl-6-nitrobenzo[d]oxazol-5-ol (33). 5-Methoxy-2-methyl-6-nitrobenzo[d]oxazole (0.2 g, 1 mmol) was mixed with 5 mL dichloromethane in a round bottom flask. The flask was flushed with argon and cooled to -78 °C. Boron tribromide was added dropwise and the solution turned from cloudy white to clear bright orange. The flask was allowed to warm to room temperature and then the solution was added dropwise to cold water. The solution was extracted with

dichloromethane, and then the organic layer was washed with brine. The organic layer was dried with magnesium sulfate and then filtered and rotovapped to yield 0.15 g (0.8 mmol, 80%). ^1H NMR (400 MHz, Chloroform- d) δ 10.69 (s, 1H), 8.24 (s, 1H), 7.35 (s, 1H), 2.69 (s, 3H).

***N*-(2,5-dimethoxy-4-nitrophenyl)acetamide (37).** *N*-(2,5-dimethoxyphenyl)acetamide (0.82 g, 4.2 mmol) was dissolved in 10 mL AcOH. 70% nitric acid (0.3 mL, 5 mmol) was added dropwise and the solution was stirred for 15 min and then poured into ice water. The resulting bright yellow solid was filtered and washed well with water and dried to yield the product (0.83 g, 82%).

***N*-(4-acetamido-2,5-dimethoxyphenyl)benzamide (41).** Benzoyl chloride was added dropwise at 0 °C to a solution of *N*-(4-amino-2,5-dimethoxyphenyl)acetamide (1.03 g, 4.9 mmol) and triethylamine (1.4 mL, 10 mmol) in 10 mL dichloromethane. The reaction was stirred at room temperature for one hour. Water was added and the organic layer was extracted with a separatory funnel. The organic layer was washed with 1 M HCl, aq. NaHCO_3 , and brine and then dried with Mg_2SO_4 and rotovapped. The crude product was purified by recrystallization with MeOH/ H_2O . 0.78 g, 51%. ^1H NMR (600 MHz, Chloroform- d) δ 8.55 (s, 1H), 8.34 (s, 1H), 8.21 (s, 1H), 7.89 (d, $J = 7.4$ Hz, 2H), 7.78 (s, 1H), 7.55 (t, $J = 7.3$ Hz, 1H), 7.50 (t, $J = 7.5$ Hz, 2H), 3.92 (d, $J = 1.8$ Hz, 7H), 2.21 (s, 3H).

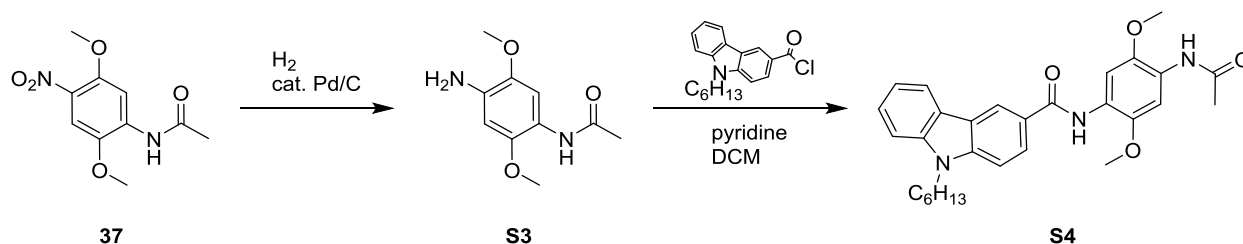
***N*-(4-acetamido-2,5-dihydroxyphenyl)benzamide (43).** *N*-(4-acetamido-2,5-dimethoxyphenyl)benzamide (0.71 g, 2.3 mmol) was dissolved in 30 mL MeCN. Ceric ammonium nitrate (3.78 g, 6.9 mmol) was dissolved in water and this was added to the MeCN solution. The solution was refluxed for 20 min and then water was added and the mixture was cooled in an ice bath. An orange solid was filtered and rinsed with water and used for the next

step without further purification. ^1H NMR (600 MHz, Chloroform- d) δ 9.14 (s, 1H), 8.33 (s, 1H), 7.90 (d, J = 8.1 Hz, 2H), 7.70 (s, 1H), 7.62 (t, J = 7.5 Hz, 1H), 7.59 (d, J = 1.9 Hz, 1H), 7.54 (t, J = 6.7 Hz, 1H), 2.27 (s, 3H).

The orange solid was refluxed in a 1:1 v/v solution of H_2O and EtOH. Sodium dithionite (1.06 g, 6.9 mmol) was added in portions and the solution turned colorless. The solution was cooled and poured onto ice and then filtered to yield 0.64 g of *N*-(4-acetamido-2,5-dihydroxyphenyl)benzamide (96% overall yield). ^1H NMR (600 MHz, DMSO- d_6) δ 9.34 (s, 1H), 9.24 (s, 1H), 9.17 (d, J = 7.6 Hz, 2H), 7.94 (d, 2H), 7.59 (t, 1H), 7.53 (t, J = 7.5 Hz, 2H), 7.47 (s, 1H), 7.36 (s, 1H), 2.09 (s, 3H).

2-methyl-6-phenylbenzo[1,2- d :4,5- d']bis(oxazole) (40). *N*-(4-acetamido-2,5-dihydroxyphenyl)benzamide (0.64 g, 2.2 mmol) was mixed with 3 mL of Eaton's reagent (10% P_2O_5 w/w in methanesulfonic acid) and heated to 90 °C for 3 h. The solution was cooled and poured into ice water and a white solid formed, which was filtered and rinsed with water to yield 0.4 g (1.6 mmol, 73%) of product. ^1H NMR (600 MHz, Chloroform- d) δ 8.29 – 8.23 (m, 2H), 7.82 (d, J = 2.1 Hz, 2H), 7.56 – 7.51 (m, 3H), 2.69 (s, 3H). ^{13}C NMR (151 MHz, CDCl_3) δ 14.94, 100.65, 100.83, 127.09, 127.76, 129.14, 131.87, 139.66, 139.92, 148.33, 148.77, 164.25, 165.46.

2,5-dimethoxy-4-nitroaniline (44). *N*-(4-amino-2,5-dimethoxyphenyl)acetamide (4.63 g, 19.3 mmol) was refluxed in a 1:1 v/v solution of EtOH/1M HCl for 3 h. The solution was cooled and a brown solid formed. The crystals were filtered to yield 3.62 g (18.2 mmol, 1.95%) without need for further purification. ^1H NMR (600 MHz, Chloroform- d) δ 7.56 (d, J = 4.3 Hz, 1H), 6.59 – 6.15 (m, 2H), 4.58 (s, 4H), 3.89 (s, 2H), 3.86 (s, 3H).



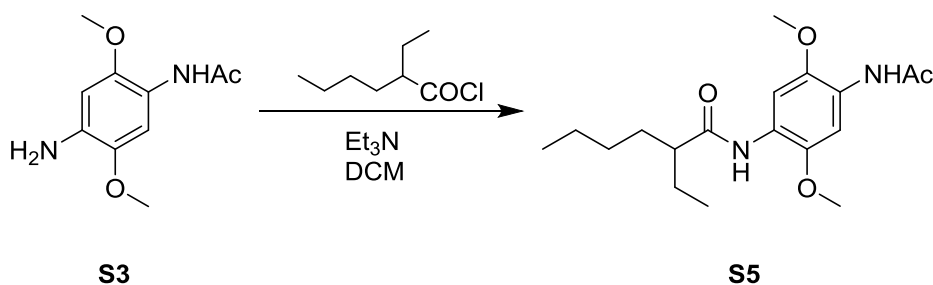
***N*-(4-amino-2,5-dimethoxyphenyl)acetamide (S3).** A suspension of 0.97 g (4.0 mmol) *N*-(2,5-dimethoxy-4-nitrophenyl)acetamide in methanol was degassed by bubbling argon. 0.2 g of 10% Pd/C was added and then hydrogen was bubbled through the solution overnight, which eventually turned from a yellow suspension to a colorless solution. The solution was purged with argon, and then the mixture was filtered with a Büchner funnel to remove the Pd/C. The filtrate was concentrated by rotary evaporation to yield 0.78 g of solid product, 93% yield.

***N*-(4-acetamido-2,5-dimethoxyphenyl)-9-hexyl-9H-carbazole-3-carboxamide (S4).** *N*-hexylcarbazole-3-carboxylic acid (0.69 g, 2.3 mmol) was mixed in dichloromethane and thionyl chloride (0.2 mL, 2.8 mmol) was added dropwise at room temperature. The solution was refluxed for 1 h then cooled to room temperature. The excess thionyl chloride was removed by distillation. In another round bottom flask was mixed *N*-(4-amino-2,5-dimethoxyphenyl)acetamide (0.48 g, 2.3 mmol) and pyridine (0.28 mL, 3.5 mmol) in dichloromethane. The acid chloride was dissolved in some dichloromethane and added dropwise to the pyridine solution at room temperature. The solution was refluxed 1 h and then cooled. The product was extracted, washed with dil HCl, water, brine, and dried over magnesium sulfate. The organic layer was filtered and concentrated by rotary evaporation. The crude product was recrystallized from EtOH to yield the product (0.83 g, 72%)

^1H NMR (400 MHz, Chloroform- d) δ 8.69 (s, 1H), 8.42 (s, 1H), 8.23 (s, 1H), 8.18 (d, $J = 7.7$ Hz, 1H), 8.00 (dd, $J = 8.6, 1.8$ Hz, 1H), 7.79 (s, 1H), 7.53 (t, $J = 7.6$ Hz, 1H), 7.46 (t, $J = 8.2$ Hz, 1H),

7.30 (t, $J = 7.5$ Hz, 1H), 4.34 (t, $J = 7.3$ Hz, 1H), 3.96 (s, 2H), 3.95 (s, 2H), 2.22 (s, 2H), 1.93 – 1.81 (m, 1H), 1.40 (t, $J = 7.9$ Hz, 1H), 1.31 – 1.23 (m, 1H), 0.87 (t, $J = 6.8$ Hz, 3H).

***N*-(4-acetamido-2,5-dihydroxyphenyl)-9-hexyl-9H-carbazole-3-carboxamide (45).** *N*-(4-acetamido-2,5-dimethoxyphenyl)-9-hexyl-9H-carbazole-3-carboxamide (**S4**) (0.60 g, 1.2 mmol) was dissolved in 10 mL dichloromethane, flushed with argon and cooled to -78 °C. Boron tribromide (0.46 mL, 4.8 mmol) was added dropwise to the solution which was then allowed to warm to room temperature. The solution was added to water and the precipitate was filtered and purified by recrystallization with ethanol (0.47 g, 85%). $^1\text{H NMR}$ (400 MHz, DMSO- d_6) δ 9.47 (s, 1H), 9.28 (s, 1H), 9.22 (s, 2H), 8.84 (d, $J = 1.8$ Hz, 1H), 8.26 (d, $J = 7.8$ Hz, 1H), 8.07 (dd, $J = 8.7$, 1.8 Hz, 1H), 7.72 (d, $J = 8.7$ Hz, 1H), 7.67 (d, $J = 8.2$ Hz, 1H), 7.54 – 7.49 (m, 1H), 7.48 (s, 1H), 7.39 (s, 1H), 7.27 (t, $J = 7.6$ Hz, 1H), 4.45 (t, $J = 7.0$ Hz, 2H), 2.10 (s, 3H), 1.79 (t, $J = 7.2$ Hz, 2H), 1.31 – 1.13 (m, 8H), 0.80 (t, $J = 6.9$ Hz, 3H).



***N*-(4-acetamido-2,5-dimethoxyphenyl)-2-ethylhexanamide (S5).** *N*-(4-amino-2,5-dimethoxyphenyl)acetamide (**S1**) (0.78 g, 3.7 mmol) and triethylamine (1 mL, 7 mmol) were mixed in dichloromethane to which 2-ethylhexanoyl chloride was added dropwise at room temperature and stirred for 0.5 h. 1M HCl was added and the organic layer was extracted with DCM and washed with water, 1 M NaOH and brine. The organic layer was dried over sodium sulfate, filtered, and concentrated by rotary evaporation to yield the product with no need for

further purification (1.27 g, quant. yield). ^1H NMR (400 MHz, Chloroform- d) δ 8.52 (s, 1H), 7.97 (s, 1H), 7.57 (s, 1H), 3.98 (s, 3H), 3.94 (s, 3H), 2.16-2.24 (m, 2H), 1.77 – 1.58 (m, 4H), 1.42-1.26 (m, 6H), 1.01 – 0.92 (m, 3H), 0.94 – 0.85 (m, 3H).

N-(4-acetamido-2,5-dihydroxyphenyl)-2-ethylhexanamide (47). *N*-(4-acetamido-2,5-dimethoxyphenyl)-2-ethylhexanamide (**S5**) (1.24 g, 3.7 mmol) was dissolved in 10 mL dichloromethane, placed under an argon atmosphere, and cooled to $-78\text{ }^\circ\text{C}$. Boron tribromide (1.45 mL, 15 mmol) was added dropwise and the solution was allowed to warm to room temperature and then was added to water. The solid was filtered and recrystallized from methanol and filtered to yield the product (0.70 g, 61%). ^1H NMR (600 MHz, DMSO- d_6) δ 9.13 (s, 2H), 9.07 (s, 1H), 7.36 (s, 1H), 7.26 (s, 1H), 2.45 – 2.37 (m, 1H), 2.06 (s, 3H), 1.58 – 1.46 (m, 2H), 1.45 – 1.33 (m, 2H), 1.32 – 1.17 (m, 4H), 0.93 – 0.76 (m, 6H).

3.6. References

1. (a) Havinga, E. E.; ten Hoeve, W.; Wynberg, H., Alternate donor-acceptor small-band-gap semiconducting polymers; Polysquaraines and polycroconaines. *Synthetic metals* **1993**, *55* (1), 299-306; (b) van Mullekom, H. A. M.; Vekemans, J. A. J. M.; Havinga, E. E.; Meijer, E. W., Developments in the chemistry and band gap engineering of donor-acceptor substituted conjugated polymers. *Materials Science and Engineering: R: Reports* **2001**, *32* (1), 1-40.
2. (a) Coakley, K. M.; McGehee, M. D., Conjugated polymer photovoltaic cells. *Chemistry of Materials* **2004**, *16* (23), 4533-4542; (b) Bredas, J.-L.; Durrant, J. R., Organic Photovoltaics. *Accounts of Chemical Research* **2009**, *42* (11), 1689-1690.
3. Subramaniam, S.; Kim, F. S.; Ren, G.; Li, H.; Jenekhe, S. A., High Mobility Thiazole-Diketopyrrolopyrrole Copolymer Semiconductors for High Performance Field-Effect Transistors and Photovoltaic Devices. *Macromolecules* **2012**, *45* (22), 9029-9037.
4. Tamargo-Martínez, K.; Villar-Rodil, S.; Paredes, J. I.; Martínez-Alonso, A.; Tascón, J. M. D., Studies on the Thermal Degradation of Poly (p-phenylene benzobisoxazole). *Chemistry of Materials* **2003**, *15* (21), 4052-4059.
5. Wolfe, J. F.; Arnold, F., Rigid-rod polymers. 1. Synthesis and thermal properties of para-aromatic polymers with 2, 6-benzobisoxazole units in the main chain. *Macromolecules* **1981**, *14* (4), 909-915.

6. Mike, J. F.; Makowski, A. J.; Jeffries-El, M., An Efficient Synthesis of 2,6-Disubstituted Benzobisoxazoles: New Building Blocks for Organic Semiconductors. *Organic Letters* **2008**, *10* (21), 4915-4918.
7. Bhuwarka, A.; Mike, J. F.; He, M.; Intemann, J. J.; Nelson, T.; Ewan, M. D.; Roggers, R. A.; Lin, Z.; Jeffries-El, M., Quaterthiophene–Benzobisazole Copolymers for Photovoltaic Cells: Effect of Heteroatom Placement and Substitution on the Optical and Electronic Properties. *Macromolecules* **2011**, *44* (24), 9611-9617.
8. Intemann, J. J.; Mike, J. F.; Cai, M.; Bose, S.; Xiao, T.; Mauldin, T. C.; Roggers, R. A.; Shinar, J.; Shinar, R.; Jeffries-El, M., Synthesis and Characterization of Poly(9,9-dialkylfluorenevinylene benzobisoxazoles): New Solution-Processable Electron-Accepting Conjugated Polymers. *Macromolecules* **2011**, *44* (2), 248-255.
9. Tsuji, M.; Saeki, A.; Koizumi, Y.; Matsuyama, N.; Vijayakumar, C.; Seki, S., Benzobisthiazole as weak donor for improved photovoltaic performance: microwave conductivity technique assisted molecular engineering. *Advanced Functional Materials* **2014**, *24* (1), 28-36.
10. Gopal, A.; Saeki, A.; Ide, M.; Seki, S., Fluorination of Benzothiadiazole–Benzobisthiazole Copolymer Leads to Additive-Free Processing with Meliorated Solar Cell Performance. *ACS Sustainable Chemistry & Engineering* **2014**, *2* (11), 2613-2622.
11. (a) Gao, P.; Tsao, H. N.; Yi, C.; Grätzel, M.; Nazeeruddin, M. K., Extended π -Bridge in Organic Dye-Sensitized Solar Cells: the Longer, the Better? *Advanced Energy Materials* **2014**, *4* (7); (b) Cai, N.; Li, R.; Wang, Y.; Zhang, M.; Wang, P., Organic dye-sensitized solar cells with a cobalt redox couple: influences of [small pi]-linker rigidification and dye-bath solvent selection. *Energy & Environmental Science* **2013**, *6* (1), 139-147.
12. (a) Osman, A.; Mohamed, S., HETEROCYCLIC-COMPOUNDS. 4. SYNTHESIS OF 2, 6-DIALKYL BENZOBISOXAZOLES. *INDIAN JOURNAL OF CHEMISTRY* **1973**, *11* (9), 868-870; (b) Imai, Y.; Itoya, K.; Kakimoto, M. a., Synthesis of aromatic polybenzoxazoles by silylation method and their thermal and mechanical properties. *Macromolecular Chemistry and Physics* **2000**, *201* (17), 2251-2256.
13. Evindar, G.; Batey, R. A., Parallel Synthesis of a Library of Benzoxazoles and Benzothiazoles Using Ligand-Accelerated Copper-Catalyzed Cyclizations of ortho-Halobenzanilides. *The Journal of Organic Chemistry* **2006**, *71* (5), 1802-1808.
14. Fujita, S.; Koyama, K.; Inagaki, Y., The Beckmann Rearrangement by Means of Phosphoryl Chloride/N, N-Dimethylacetamide; A Novel and Convenient Method for Preparing Benzoxazoles. *Synthesis* **1982**, *1982* (01), 68-69.
15. Dessì, A.; Barozzino Consiglio, G.; Calamante, M.; Reginato, G.; Mordini, A.; Peruzzini, M.; Taddei, M.; Sinicropi, A.; Parisi, M. L.; Fabrizi de Biani, F.; Basosi, R.; Mori, R.; Spatola, M.; Bruzzi, M.; Zani, L., Organic Chromophores Based on a Fused Bis-Thiazole Core and Their Application in Dye-Sensitized Solar Cells. *European Journal of Organic Chemistry* **2013**, *2013* (10), 1916-1928.

16. Sawada, Y.; Yanai, T.; Nakagawa, H.; Tsukamoto, Y.; Yokoi, S.; Yanagi, M.; Toya, T.; Sugizaki, H.; Kato, Y.; Shirakura, H.; Watanabe, T.; Yajima, Y.; Kodama, S.; Masui, A., Synthesis and insecticidal activity of benzoheterocyclic analogues of N'-benzoyl-N-(tert-butyl)benzohydrazide. Part 1. Design of benzoheterocyclic analogues. *Pest Manage. Sci.* **2003**, *59* (Copyright (C) 2015 American Chemical Society (ACS). All Rights Reserved.), 25-35.
17. Klimavicz, J. S.; Mike, J. F.; Bhuwarka, A.; Tomlinson, A. L.; Jeffries-EL, M., Synthesis of benzobisoxazole-based D- π -A- π -D organic chromophores with variable optical and electronic properties. *Pure and Applied Chemistry* **2012**, *84* (4), 991-1004.
18. Imoto, M.; Matsui, Y.; Takeda, M.; Tamaki, A.; Taniguchi, H.; Mizuno, K.; Ikeda, H., A Probable Hydrogen-Bonded Meisenheimer Complex: An Unusually High S_NAr Reactivity of Nitroaniline Derivatives with Hydroxide Ion in Aqueous Media. *J. Org. Chem.* **2011**, *76* (Copyright (C) 2015 American Chemical Society (ACS). All Rights Reserved.), 6356-6361.
19. Nawrat, C. C.; Lewis, W.; Moody, C. J., Synthesis of Amino-1,4-benzoquinones and Their Use in Diels-Alder Approaches to the Aminonaphthoquinone Antibiotics. *J. Org. Chem.* **2011**, *76* (Copyright (C) 2015 American Chemical Society (ACS). All Rights Reserved.), 7872-7881.
20. Liang, Y. K.; Ruan, B. F.; Tian, Y. P., Synthesis, crystal structure and in vitro antitumor activity of a novel organotin(IV) complex with 9-hexyl-9H-carbazole-3-carboxylic acid. *Russ. J. Coord. Chem.* **2012**, *38* (Copyright (C) 2015 American Chemical Society (ACS). All Rights Reserved.), 396-401.

CHAPTER 4

TUNING THE BANDGAP OF BENZOBISOXAZOLE SEMICONDUCTING MATERIALS BY 2,6-SUBSTITUTION

4.1. Introduction

Research in the field of organic electronics continuously seeks to develop new structures to obtain improved performance from devices such as solar cells¹, transistors^{1c, 2}, and light emitting diodes³. The class of benzobisazoles, including benzobisoxazole (BBO) and benzobisthiazole have been studied for such purposes⁴ since these rigid, polycyclic heteroaromatic systems have good charge transport and thermal stability⁵ and can be synthesized under mild conditions⁶. To synthesize a narrow bandgap material for an organic photovoltaic function, a popular strategy is to copolymerize electron-donating monomers with electron accepting comonomers. In this regard, benzobisazoles have proven to be weak acceptors⁷, resulting in high lowest unoccupied molecular orbitals (LUMOs) and therefore bandgaps wider than the 1.5-1.7 eV generally desired for optimal OPV performance⁸. Herein we investigate a new strategy toward the goal of developing BBO as a stronger acceptor.

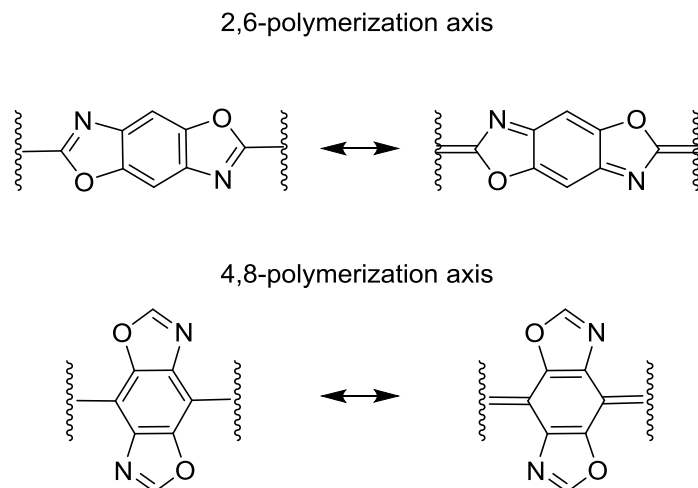


Figure 4.19. Aromatic and quinoid resonance forms of BBO through alternate conjugation axes.

To improve the electroluminescent properties of BBO-containing polymers for OLEDs, J. Intemann, et al.⁹, polymerized BBO through the 4,8-axis instead of the more commonly studied 2,6-axis and this greatly increased the brightness and luminous efficiencies of the host-guest OLEDs. Noting that the new configuration can stabilize its quinoid structure (Figure 4.1) in conjugated polymers which results in a narrower bandgap¹⁰, we saw the potential to use the BBO in this way for photovoltaic applications. Figure 4.202 shows the energy levels resulting from substitution of BBOs and other acceptor units among a common dithienosilole donor, along with those of P3HT and PCBM included for reference. Switching the polymerization axis from the 2,6- to the 4,8- slightly lowered the bandgap, though not as much as that achieved when stronger acceptor units of diketopyrrolopyrrole or benzothiadiazole were used.

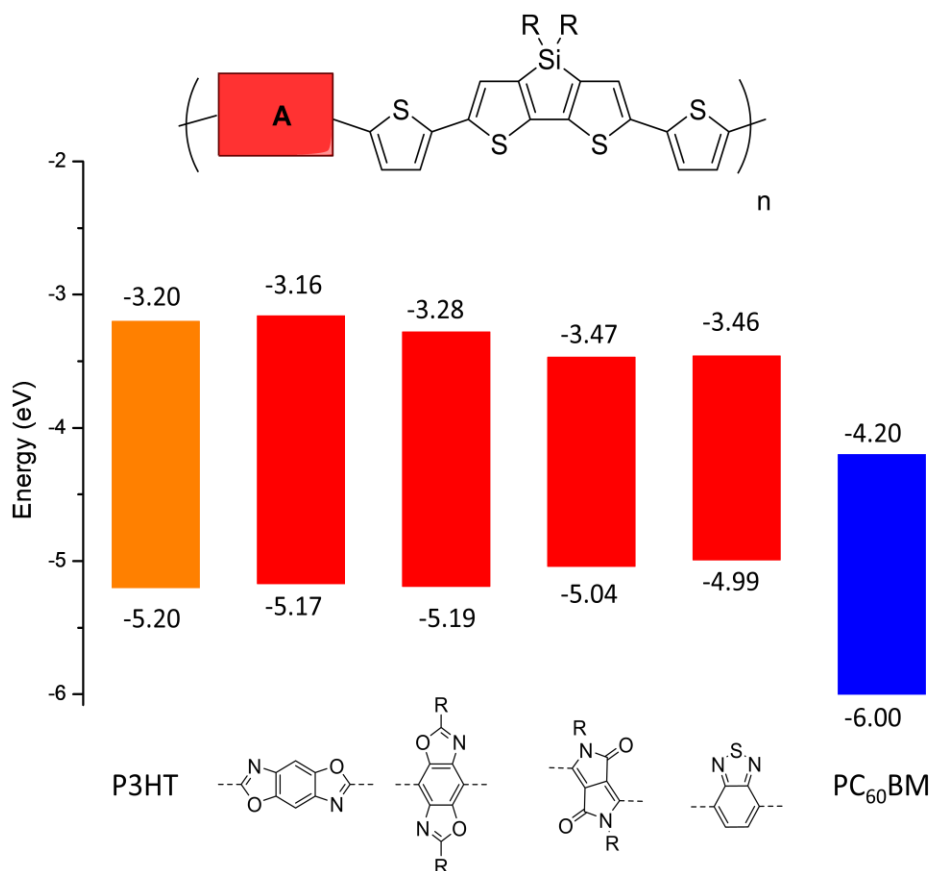


Figure 4.20. Comparison of acceptor monomers and their effect on energy levels of the polymer.

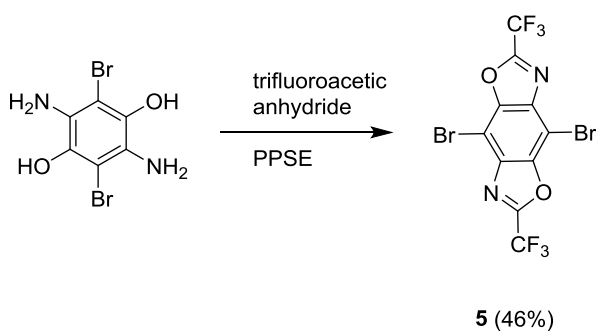
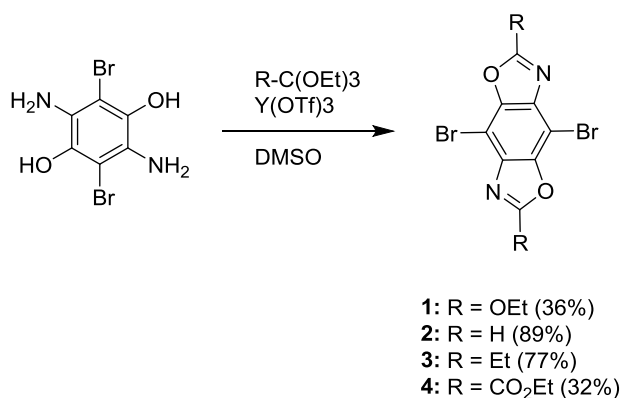
By studying BBO-based cruciform materials, the research of B. Tlach¹¹, et al, demonstrated that the highest occupied molecular orbital (HOMO) of the BBO molecule can be controlled by substitution of the 4,8-axis and, likewise, the LUMO can be tuned independently by substitution of the 2,6-axis. With this in mind, we envisioned that polymerization through the 4,8-axis with additional substitution at the 2,6-axis will further tune the material's properties. We predicted that incorporation of a stronger electron-withdrawing substituent would (1) alter the electron density distribution (2) promote the quinoid form and (3) lower the LUMO, factors which should all contribute to lowering the bandgap. Herein, the properties of small molecules with 2,6-variations were studied and then a polymer was synthesized to demonstrate the utility of the new monomer, 2,6-bis(trifluoromethyl)BBO.

4.2. Results & Discussion

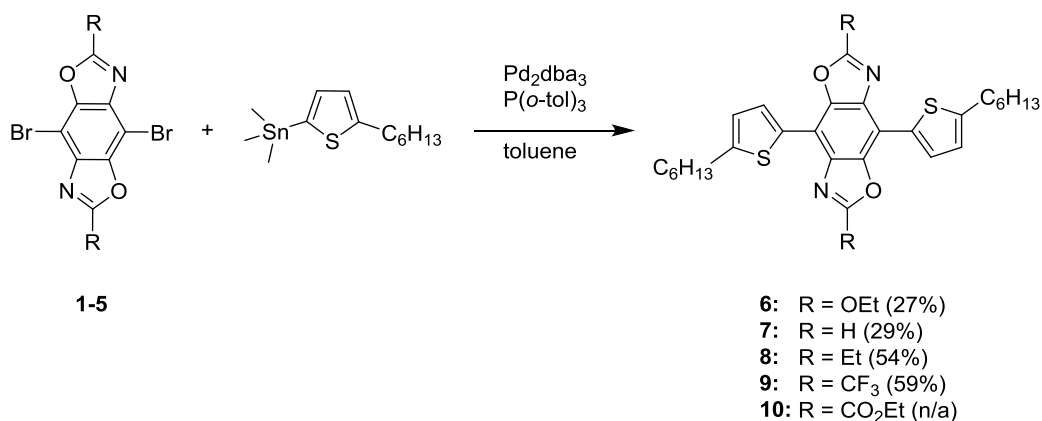
4.2.1. Small molecules

4.2.1.1. Synthesis

4,8-DibromoBBOs with varying 2,6-substitutions were synthesized in two ways starting with 2,6-diamino-3,5-dibromohydroquinone, as shown in Scheme 4.1. Lewis acid-catalyzed orthoester condensations^{6b} were used to produce the 2,6-unsubstituted-4,8-dibromo BBO as well as 2,6-di(ethoxy), ethyl carboxylate, and ethyl BBOs. Following a modified literature procedure¹², 2,6-bis(trifluoromethyl)BBO was synthesized with trifluoroacetic anhydride in PPSE in 46% yield and the product was soluble in chloroform and toluene. Synthesis of other 2,6-disubstituted BBOs was attempted but did not yield product, such as a 2,6-bis(*N,N*-dimethylamino)BBO from the condensation of *N,N*-dimethylcarbamoyl chloride with the PPSE reaction conditions. Different methods of synthesizing a 2,6-dicarbaldehydeBBO were examined, such as oxidation of an alcohol, methyl oxidation with SeO₂, and periodate-mediated alkene cleavage, yet either no reaction occurred or the materials decomposed.



Scheme 4.5. Synthesis of 2,6-substituted-4,8-dibromoBBOs



Scheme 4.6. Synthesis of BBO small molecules.

To study the structure-property effects of these variations, donor-acceptor-donor type small molecules were synthesized with the BBOs as the acceptor and 5-hexylthiophene donors by a Stille cross-coupling of (5-hexylthiophen-2-yl)trimethylstannane and the dibromo BBOs **1-5** (Scheme

4.2). **9** and **8** small molecules produced yields of 59% and 54%, respectively. **6** and **7** gave considerably lower yields of 27% and 29%, respectively, and the ester derivative **10** gave a low mass recovery plus a mixture of products to result in no recoverable product. The reactions to produce **6,7,**and **10** may have suffered from decomposition, as the reaction mixture turned black whereas the reactions to form **8** and **9** did not under the same conditions. Nevertheless, purification of the small molecules was accomplished by column chromatography followed by recrystallization. During the synthesis of **10**, it may be possible that the palladium complexed with the ester carbonyl and imine nitrogen of the benzobisoxazole unit which could lead to incomplete reaction, undesired side reactions, or decomposition. Compounds **6-9** were carried forward for characterization.

4.2.1.2. DFT calculations

DFT calculations are underway to understand the effects of these 2,6-substitutions on the electronic properties of the small molecule.

4.2.1.3. Optical properties

The normalized chloroform solution and film UV-vis spectra for compounds **6-9** are shown in Figure 4.3 and Figure 4.4, respectively, and summarized in Table 4.1. Overall, the spectra display a large amount of fine structure due to the rigidity of this planar conjugated system. In chloroform solution, **6** shows the most vibronic detail and **9** shows lesser detail with a broader λ_{max} peak. The absorption maximum ranges from 341 nm for **6** to 409 nm for **9**. In the solid state, **6** and **9** have small red-shifting of the λ_{max} by 3 and 4 nm, respectively. **7** and **8** are both blue-shifted, going from 392 nm to 379 nm for **8** and 381 to 359 nm for **7**. All peaks are broadened overall but largely retain the same peak formations, except the formerly broad peak at the λ_{max} of **9** now has distinct peaks in that region. The bandgaps were calculated from the onset of absorption in the solid state.

Table 4.1. Optical and electronic properties for **6-9**.

Compound	λ_{\max} solution (nm)	λ_{\max} film (nm)	Abs _{onset} (nm)	$\epsilon \times 10^4$ ($M^{-1}cm^{-1}$)	E_g^{opt} (eV) ^a	E_{onset}^{ox} (V) ^b	HOMO ^c (eV)	LUMO ^d (eV)
6	341	344	468	1.49	2.65	0.80	-5.41	-2.76
7	381	359	456	3.78	2.72	0.80	-5.41	-2.69
8	392	379	453	4.73	2.74	0.94	-5.55	-2.81
9	409	417	496	4.41	2.5	0.93	-5.54	-3.04

^a Estimated from the optical absorption edge. ^b Onset of potentials (vs Fc). ^c HOMO = $-(E_{onset}^{ox} + 4.8)$ (eV). ^d LUMO = HOMO - E_g^{opt}

4.1.1.1. Electrochemical properties

The electrochemical properties of the small molecules were studied by cyclic voltammetry performed in dichloromethane solution nBu_4PF_6 electrolyte with an Ag/Ag⁺ reference electrode, as shown in Figure 4.3 and summarized in Table 4.1. All small molecules displayed quasi-reversible oxidation peaks, the onset of which was used to calculate the ionization potential which represents the highest occupied molecular orbital (HOMO) of the molecule. Despite their apparent electronic differences based on the substitution of trifluoromethyl and ethyl groups, both compounds **8** and **9** had similar HOMOs of -5.55 and -5.54 eV, respectively, and **6** and **7**

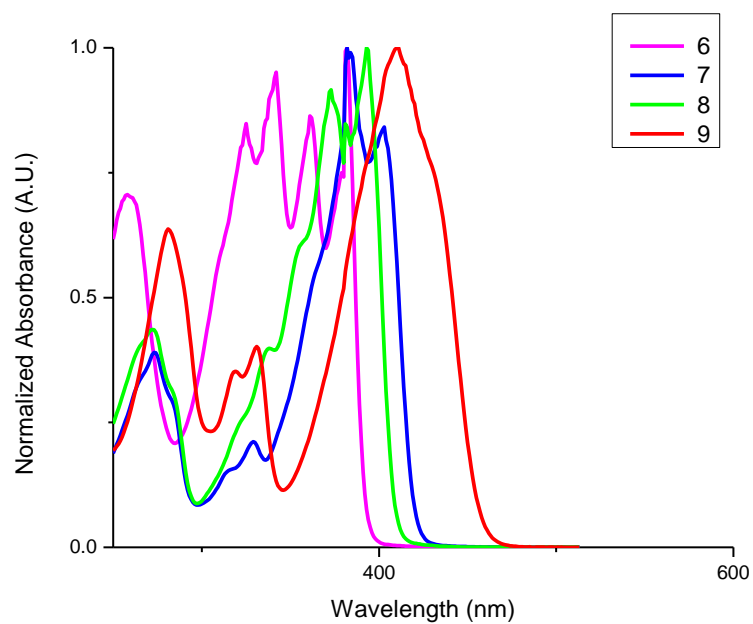


Figure 4.21. Small molecule solution UV-vis.

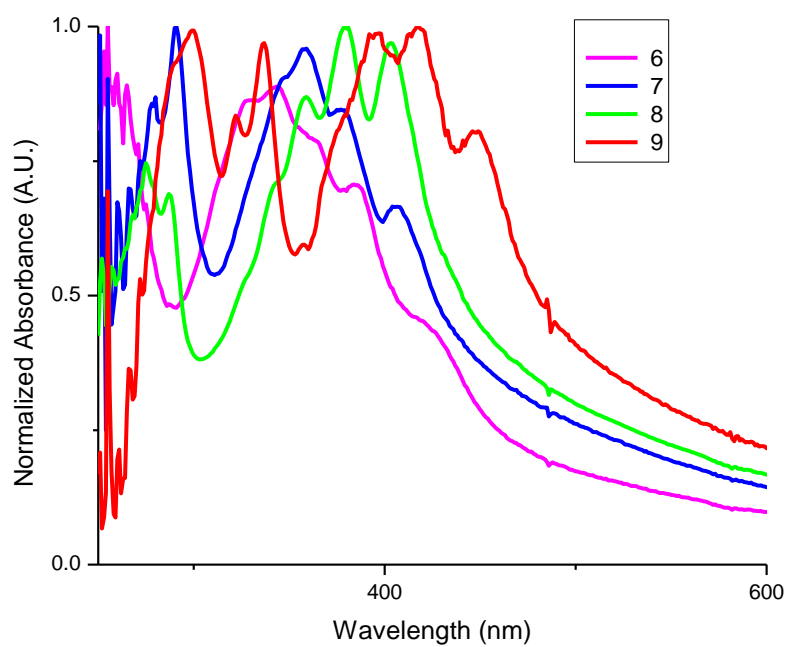


Figure 4.22. Small molecule film UV-vis.

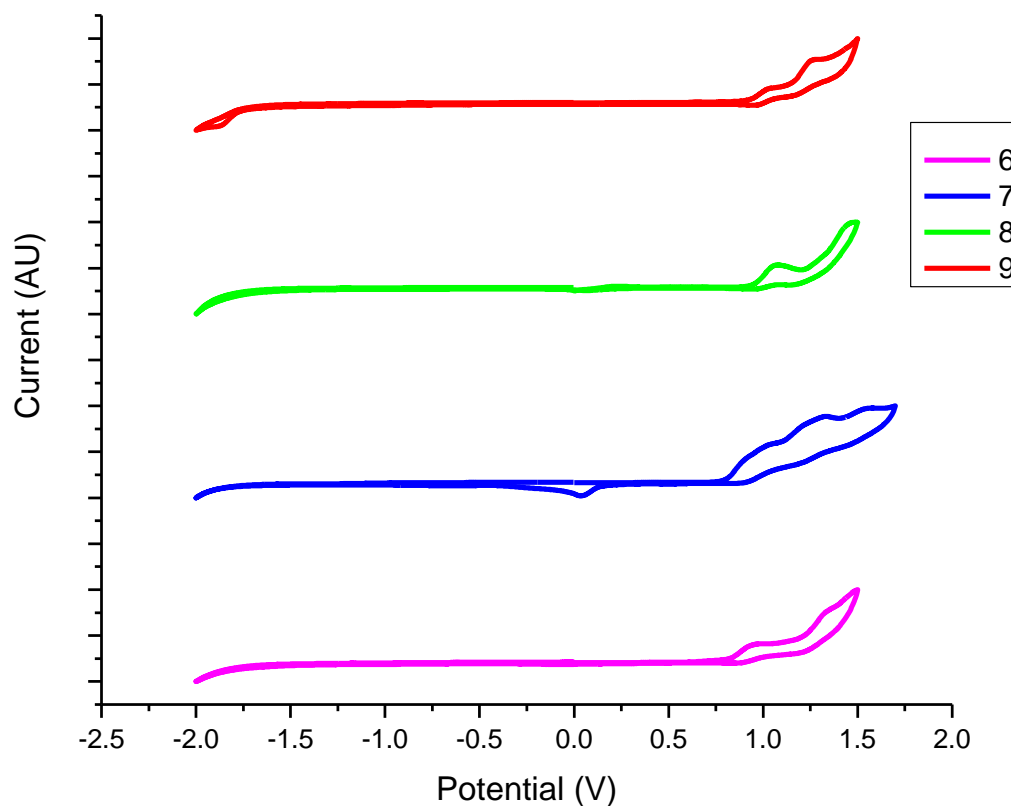


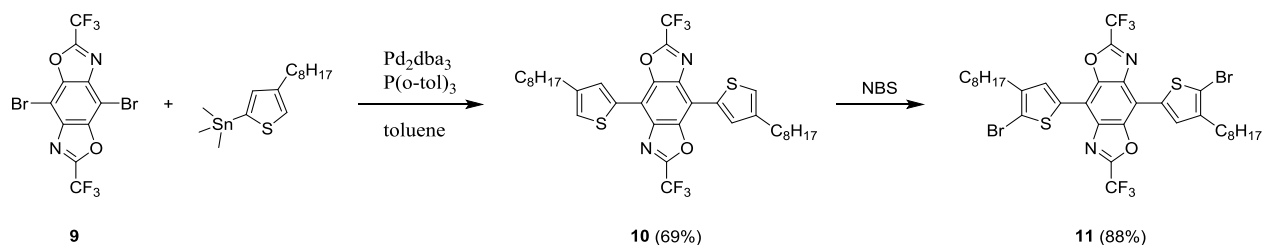
Figure 4.3. Cyclic voltammetry of small molecules **6-9**.

had the same HOMO of -5.41 eV. This indicates that the electronic effects of 2,6-substitution of the BBO does not create a trend in the position of the HOMO level, which is consistent with the results of Tlach, et al. All compounds did not display reversible reduction behavior when measured up to -2 V. Therefore the LUMO was calculated as $LUMO = HOMO - E_g^{opt}$. Due to the lower bandgap, **9** had the lowest LUMO of -3.04 eV.

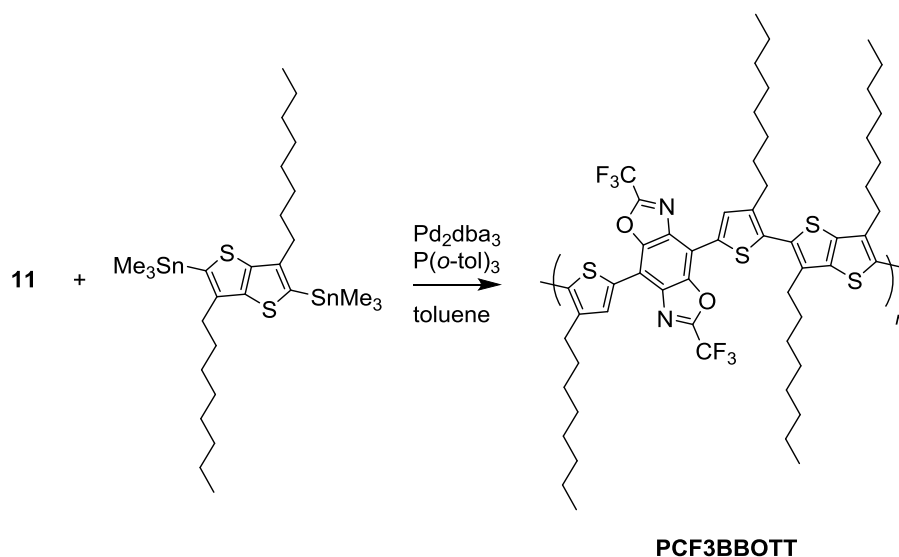
4.1.2. Polymer

4.1.2.1. Synthesis

Having demonstrated that the trifluoromethyl BBO, **9**, was the most effective at lowering the bandgap of the small molecules, a donor-acceptor copolymer was synthesized with this new monomer. The polymer was designed to incorporate solubilizing alkyl chains while maintaining crystallinity, planarity, and increasing conjugation length. First, flanking octylthiophene units were coupled to **9** with the alkyl chains oriented away from the BBO unit to reduce steric interactions (Scheme 4.3). The product **10** was then brominated to form the pi-acceptor-pi monomer (**11**) which was copolymerized with (3,6-dioctylthieno[3,2-b]thiophene-2,5-diyl)bis(trimethylstannane) via a Stille reaction to yield **PCF3BBOTT**, as shown in Scheme 4.4.



Scheme 4.7. Synthesis of monomer **11**.



Scheme 4.8. Synthesis of PCF3BBOTT.

4.1.2.2. Physical properties

PCF3BBOTT was purified by Soxhlet extraction and collected after precipitation into methanol, with a final recovery of 79% from the chloroform fraction. The polymer had a MW of 10.6 kDa and PDI of 1.7 and was soluble in common organic solvents, as summarized in Table 4.2. The polymer had a high decomposition temperature of 387 °C, as shown in the TGA in Figure 4.4.

Table 4.3. Physical properties of polymer.

Polymer	Yield	M_w		DP ^b	T_d (°C) ^c
		(kDa) ^a	PDI		
PCF3BBOTT	79%	10.6	1.70	10	387

^aDetermined by GPC in THF using polystyrene standards. ^bDegree polymerization calculated from the molecular weight. ^c5% weight loss temperature by TGA in air.

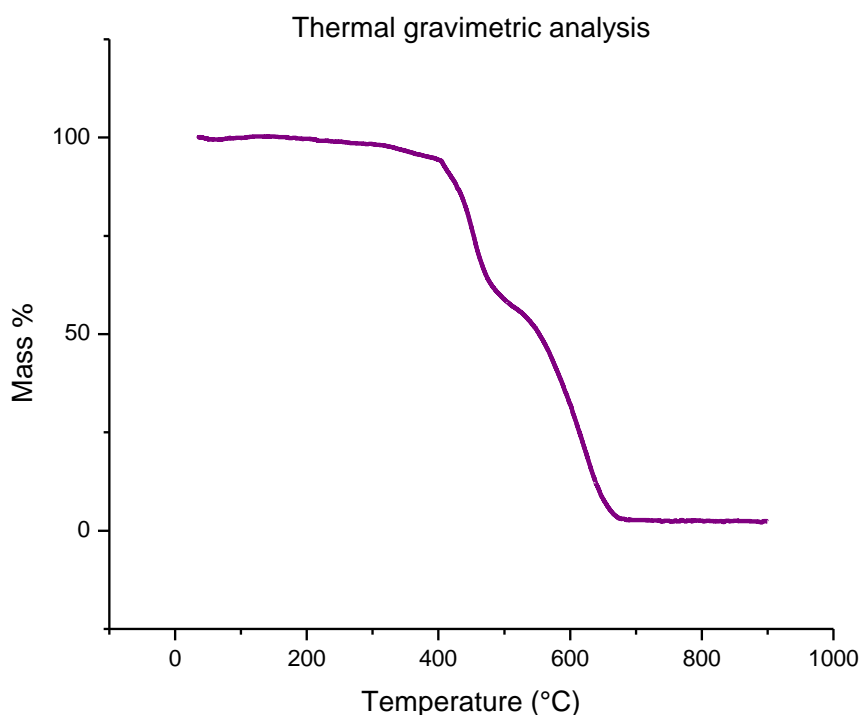


Figure 4.4. TGA of polymer

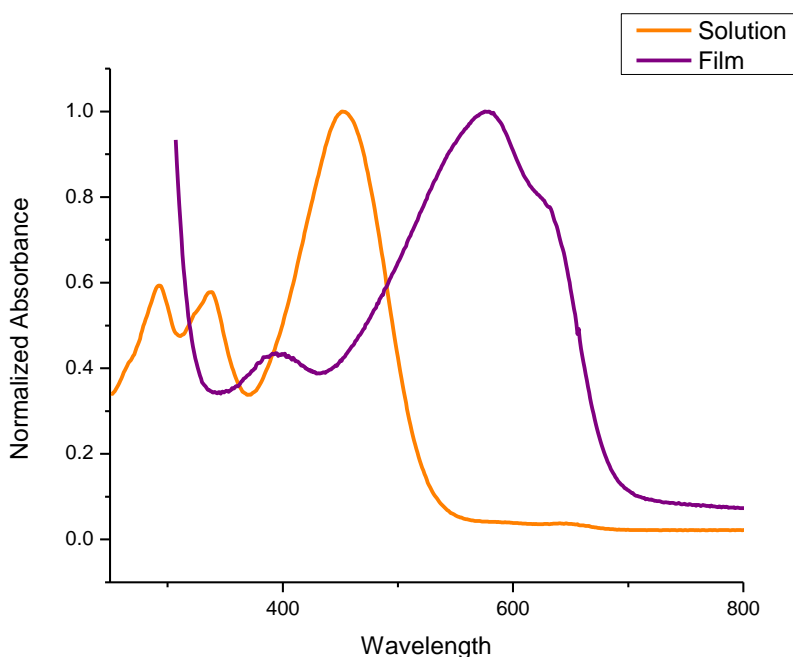
4.1.2.3. Optical

The physical properties of the polymer are summarized in Table 4.3. According to the UV-vis spectra, Figure 4.5, the polymer displays $\pi \rightarrow \pi^*$ transitions up to 400nm and an intramolecular charge transfer band with a λ_{\max} of 452 nm. This peak is greatly red-shifted by 127 nm in the solid state, to a λ_{\max} of 579 nm, due to the planarity of the aromatic backbone and strategic placement of side chains to promote crystallinity. The broad solid state absorption nearly matches the solar spectrum output, in which the most photons are emitted between 500 to 700 nm. Films of **PCF3BBOTT** spin coated from the chloroform solution exhibit a low energy shoulder. The bandgap, calculated from the onset of absorption, was determined to be 1.82 eV and is one of the lowest bandgaps of BBO polymers to date.

Table 4.4. Optoelectronic properties of polymer.

Compound	$\lambda_{\max}^{\text{soln}}$ (nm)	$\lambda_{\max}^{\text{film}}$ (nm)	λ_{onset} (nm)	E_g^{opt} (eV) ^a	$E_{\text{onset}}^{\text{ox}}$ (V)	LUMO (ev)	HOMO (ev)
PCF3BBOTT	452	579	682	1.82	0.82	-3.68	-5.53

^aEstimated from the optical absorption edge. ^bLUMO = HOMO - E_g^{opt} . ^cHOMO = -4.8- ($E_{\text{onset}}^{\text{ox}}$) (eV).

**Figure 4.5.** UV-vis spectroscopy of **PCF3BBOTT**

4.1.2.4. Electrochemical

Cyclic voltammetry was used to study the redox behavior of the polymer. Chlorobenzene solutions of polymer were drop-cast onto electrodes and data was obtained with a $\text{Bu}_4\text{NPF}_6/\text{acetonitrile}$ electrolyte solution, an Ag/Ag^+ reference electrode and Fc/Fc^+ was used as a reference value. The output voltammogram, as shown in Fig. 4.6, displays quasireversible

oxidation. The onset of oxidation was 0.82V from which the HOMO was calculated to be -5.53 eV according to the equation $\text{HOMO} = -(4.8 + (E_{\text{onset}}^{\text{ox}}))$ (eV). There was no reversible reduction character to the voltammogram so the LUMO was estimated by subtracting the optical bandgap from the HOMO, resulting in a value of -3.68 eV, which is the lowest reported

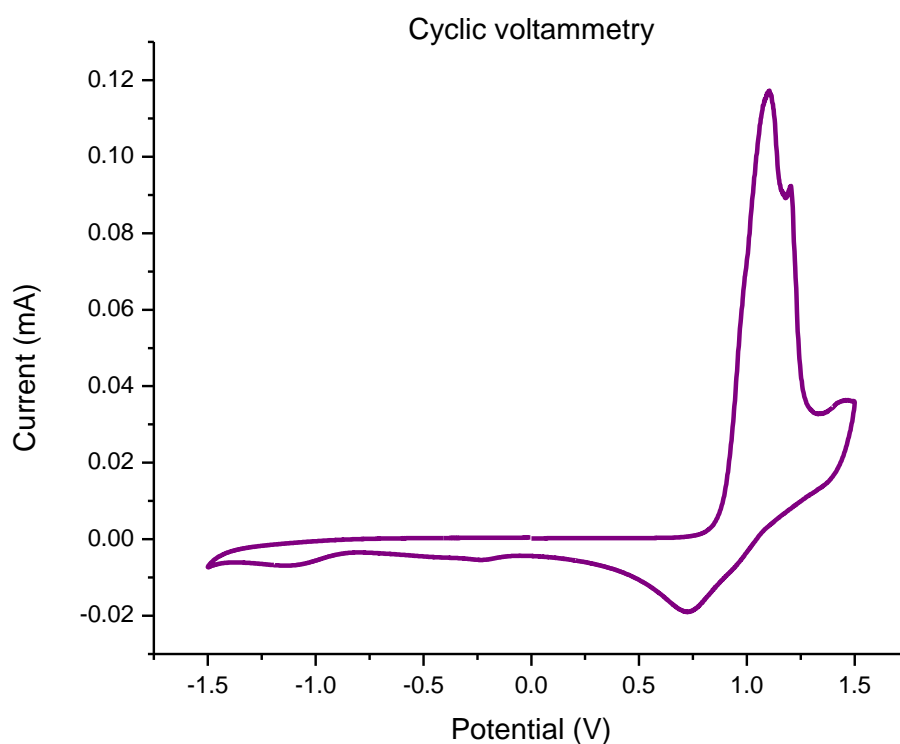


Figure 4.6. Cyclic voltammetry of **PCF3BBOTT**.

value of a BBO-based polymer to date. The BBO monomer could have influenced the low HOMO, an effect which has been observed in polymers with fluorinated acceptors¹³. Incorporation of fluorine atoms into conjugated polymers has become popular lately and resulted in high efficiencies, while the trifluoromethyl group has not been studied in detail. A comparison of

fluoro- vs. trifluoromethyl groups should be conducted in the future to ascertain the impact of these groups upon device performance.

4.1.3. Device data

Fabrication of OPV devices is currently in progress.

4.3. Conclusion

In conclusion we used small molecules to study the optoelectronic effects of varied substitution at the 2,6-positions of BBOs and determined that the electron-withdrawing trifluoromethyl group did indeed reduce the LUMO and bandgap. The 2,6-bis(trifluoromethyl)BBO monomer (**11**) was then polymerized with thienothiophene to synthesize a donor-acceptor copolymer (**PCF3BBOTT**) which exhibited good optical properties and a relatively low bandgap. Future studies will synthesize a series of conjugated polymers with variations of trifluoromethyl and fluoro substituents on the acceptor to investigate how these substituents affect the optoelectronic properties and device performance.

4.4. Acknowledgements

Synthetic contributions include that of Dawn Knoble for 4,8-dibromo-2,6-diethylbenzo[1,2-d:4,5-d']bis(oxazole), Jeremy Intemann for trimethyl(4-octylthiophen-2-yl)stannane, and Brandon Kobilka for (3,6-dioctylthieno[3,2-b]thiophene-2,5-diyl)bis(trimethylstannane); whereas all other synthesis and characterization was performed by the author of this dissertation. Benjamin Hale conducted the TGA and DSC analysis. All text was written by the author.

4.5. Experimental

Materials

4,8-Dibromobenzo[1,2-d:4,5-d']bis(oxazole) (**2**)¹⁴, 4,8-dibromo-2,6-diethylbenzo[1,2-d:4,5-d']bis(oxazole) (**3**)¹⁴, diethyl 4,8-dibromobenzo[1,2-d:4,5-d']bis(oxazole)-2,6-dicarboxylate (**4**)¹⁴, (5-hexylthiophen-2-yl)trimethylstannane¹⁵, trimethyl(4-octylthiophen-2-yl)stannane¹⁶, and (3,6-dioctylthieno[3,2-b]thiophene-2,5-diyl)bis(trimethylstannane)¹⁷ were synthesized according to literature procedures. Toluene was dried using an Innovative Technology, Inc. solvent purification system. Other reagents were obtained from commercial sources and used without further purification.

Characterization

Nuclear magnetic resonance (NMR) spectra were recorded on a Varian MR (400 MHz) or a Bruker Avance III (600 MHz). Spectra were internally referenced to the residual protonated solvent peak. Chemical shifts are given in ppm (δ) relative to the solvent. Absorption spectra were obtained on a photodiode-array Agilent 8453 UV-visible spectrophotometer using sample solutions in CHCl_3 or thin films made by spin-coating 25 x 25 x 1 mm glass slides using solutions of polymer (1-3 mg/mL) in CHCl_3 /chlorobenzene at a spin rate of 1200 rpm on a Headway Research, Inc. PWM32 spin-coater. Cyclic voltammetry was performed using an e-DAQ e-corder 410 potentiostat with a scanning rate of 50 mV/s. Ag/Ag^+ was used as the reference electrode and a platinum wire as the auxiliary electrode. The reported values are referenced to Fc/Fc^+ (-4.8 eV vs. vacuum). Polymer solutions in chlorobenzene (1-2 mg/mL) were drop-cast onto a platinum electrode. Polymer analysis was performed in deoxygenated solutions of 0.1 M tetrabutylammonium hexafluorophosphate electrolyte in CH_3CN under an argon atmosphere. Small molecule analysis were performed by dissolving 1mg/mL of small molecule sample in 0.1 M tetrabutylammonium hexafluorophosphate in DCM and deoxygenated with argon. Gel permeation chromatography (GPC) measurements were performed on a Shimadzu Prominence

UFLC instrument calibrated relative to polystyrene standards and equipped with RI and UV-Vis detectors. Measurements were conducted at 50 °C using CHCl₃ as the eluent with a flow rate of 1.0 mL/min. Thermal gravimetric analysis (TGA) and differential scanning calorimetry (DSC) measurements were performed with a Netzsch STA449 F1 instrument. TGA were conducted at a heating rate of 20 °C/min under ambient atmosphere. DSC was performed using a heat/cool/heat method at 15 °C/min under nitrogen.

Synthesis

4,8-dibromo-2,6-diethoxybenzo[1,2-d:4,5-d']bis(oxazole) (1). Tetraethylorthocarbonate (3.3 mL, 15.6 mmol), yttrium triflate (140 mg, 0.26 mmol) and 2,5-diamino-3,6-dibromohydroquinone (1.57 g, 5.2 mmol) were added to 20 mL of degassed DMSO and heated to 60 °C for 2 h. The solution was cooled and poured into ice water. The resulting solids were filtered and recrystallized from methanol to yield the product as a beige solid (0.77 g, 36%). mp: 208-213 °C. ¹H NMR (600 MHz, Chloroform-d) δ 4.70 (q, *J* = 7.1 Hz, 1H), 1.53 (t, *J* = 7.1 Hz, 2H). ¹³C NMR (151 MHz, CDCl₃) δ 14.47, 69.43, 89.91, 136.59, 143.57, 163.02. HRMS (ESI): [M+H]⁺ Calcd for C₁₂H₁₀N₂O₄Br₂, 549.2604; found, 549.2603.

4,8-dibromo-2,6-bis(trifluoromethyl)benzo[1,2-d:4,5-d']bis(oxazole) (5). To a solution of degassed PPSE in chlorobenzene was added trifluoroacetic anhydride (2.8 mL, 20 mmol) and 2,5-diamino-3,6-dibromohydroquinone (1.50 g, 5 mmol). The solution was heated overnight at 90 °C overnight. The solution was cooled and methanol was added and the resulting precipitate was filtered. The solid was recrystallized from methanol/water, filtered, and dried to yield the product (1.05 g, 46%) mp: >260 °C. ¹³C NMR (151 MHz, Chloroform-d) δ 154.02 (q, *J* = 45.2 Hz), 147.58, 139.28, 117.10 (t, *J* = 273.1 Hz), 95.74. HRMS (ESI): [M+H]⁺ Calcd for C₁₀Br₂N₂O₂F₆, 452.8303; found, 452.8318.

General procedure for small molecule synthesis

5mL degassed toluene was added to a 3-neck round bottom flask with a reflux condenser. The 2,6-substituted-4,8-dibromobenzobisoxazole (1 eq) and (5-hexylthiophen-2-yl)trimethylstannane (2.2 eq) were added to the flask followed by Pd₂(dba)₃ (0.02 eq), and P(*o*-tol)₃ (0.08 eq). The solution was further degassed by bubbling argon for another 10 min and then kept under an argon atmosphere and heated to 110 °C for 24 h. The solution was cooled and concentrated by rotary evaporation. The crude product was purified by column chromatography.

2,6-diethoxy-4,8-bis(5-hexylthiophen-2-yl)benzo[1,2-d:4,5-d']bis(oxazole) (6). mp: 85-92 °C.

¹H NMR (400 MHz, Chloroform-d) δ 8.03 (d, *J* = 3.7 Hz, 1H), 6.87 (d, *J* = 3.6 Hz, 2H), 4.75 (d, *J* = 7.1 Hz, 2H), 3.01 – 2.84 (m, 3H), 1.77 (s, 1H), 1.58 (d, *J* = 7.0 Hz, 3H), 1.41 (s, 3H), 1.36 – 1.29 (m, 5H), 0.93 – 0.85 (m, 3H). HRMS (ESI): [M+H]⁺ Calcd for C₃₂H₄₀N₂O₄S₂, 581.2502; found, 581.2501.

4,8-bis(5-hexylthiophen-2-yl)benzo[1,2-d:4,5-d']bis(oxazole) (7). mp: 175-180 °C. ¹H NMR

(600 MHz, Chloroform-d) δ 8.33 (s, 1H), 8.13 (d, *J* = 3.7 Hz, 1H), 6.93 (d, *J* = 3.8 Hz, 1H), 2.92 (t, *J* = 7.7 Hz, 2H), 1.78 (p, *J* = 7.7 Hz, 2H), 1.49 – 1.39 (m, 2H), 1.38 – 1.31 (m, 4H), 0.95 – 0.84 (m, 3H). HRMS (ESI): [M+H]⁺ Calcd for C₂₈H₃₂N₂O₂S₂, 493.1978; found, 493.1983.

2,6-diethyl-4,8-bis(5-hexylthiophen-2-yl)benzo[1,2-d:4,5-d']bis(oxazole) (8). mp: 98-100 °C.

¹³C NMR (151 MHz, CDCl₃) δ 11.35, 14.25, 22.76, 22.81, 29.02, 30.36, 31.77, 31.86, 107.75, 124.75, 128.76, 131.86, 135.36, 144.45, 148.13, 168.31. HRMS (ESI): [M+H]⁺ Calcd for C₃₂H₄₀N₂O₂S₂, 549.2604; found, 549.2603.

4,8-bis(5-hexylthiophen-2-yl)-2,6-bis(trifluoromethyl)benzo[1,2-d:4,5-d']bis(oxazole) (9).

mp: 167-168 °C. ¹H NMR (600 MHz, Chloroform-d) δ 8.15 (d, *J* = 3.7 Hz, 1H), 6.96 (d, *J* = 3.8

Hz, 1H), 2.93 (t, J = 7.6 Hz, 2H), 1.78 (p, J = 7.7 Hz, 2H), 1.49 – 1.38 (m, 2H), 1.41 – 1.27 (m, 4H), 0.91 (t, J = 6.6 Hz, 3H). ^{13}C NMR (151 MHz, CDCl_3) δ 14.18, 22.74, 29.00, 30.42, 31.73, 31.75, 77.37, 110.85, 115.85, 117.65, 125.40, 129.38, 130.69, 135.56, 144.79, 150.84. HRMS (ESI): $[\text{M}+\text{H}]^+$ Calcd for $\text{C}_{30}\text{H}_{29}\text{F}_6\text{N}_2\text{O}_2\text{S}_2$, 628.1647; found, 628.1646.

4,8-bis(4-octylthiophen-2-yl)-2,6-bis(trifluoromethyl)benzo[1,2-d:4,5-d']bis(oxazole) (10).

4,8-dibromo-2,6-bis(trifluoromethyl)benzo[1,2-d:4,5-d']bis(oxazole) (272 mg, 0.6 mmol) and trimethyl(4-octylthiophen-2-yl)stannane (482 mg, 1.3 mmol) were added to a flask, equipped with a reflux condenser, containing 4 mL of degassed toluene, followed by the addition of $\text{Pd}_2(\text{dba})_3$ (11 mg, 0.012 mmol) and $\text{P}(o\text{-tol})_3$ (15 mg, 0.048 mmol). The solution was degassed for another 10 min by bubbling argon and then kept under an argon atmosphere and heated to 110 °C for 24 h. The solution was cooled and then passed through a silica gel plug with chloroform. The solution was concentrated by rotary evaporation. The bright yellow solid was suspended in cold hexanes and then filtered to isolate the product (285 mg, 69%). mp: 175-177 °C. ^1H NMR (600 MHz, Chloroform- d) δ 8.16 (d, J = 1.4 Hz, 1H), 7.23 (d, J = 1.2 Hz, 1H), 2.74 (t, J = 7.7 Hz, 2H), 1.72 (t, J = 7.5 Hz, 2H), 1.47 – 1.38 (m, 2H), 1.38 – 1.33 (m, 2H), 1.33 – 1.24 (m, 6H), 0.88 (t, J = 6.9 Hz, 3H). HRMS (APCI): $[\text{M}+\text{H}]^+$ Calcd for $\text{C}_{34}\text{H}_{38}\text{F}_6\text{N}_2\text{O}_2\text{S}_2$, 685.2352; found, 685.2359.

4,8-bis(5-bromo-4-octylthiophen-2-yl)-2,6-bis(trifluoromethyl)benzo[1,2-d:4,5-

d']bis(oxazole) (11). 4,8-dibromo-2,6-bis(trifluoromethyl)benzo[1,2-d:4,5-d']bis(oxazole) (210 mg, 0.3 mmol) was added to 10 mL chloroform followed by NBS (125 mg, 0.7 mmol) all in one portion. The solution was heated to reflux for 3 h and then cooled. The bright yellow solid was filtered to obtain the product (222 mg, 88%). mp: 187-189 °C. HRMS (APCI): $[\text{M}+\text{H}]^+$ Calcd for $\text{C}_{34}\text{H}_{36}\text{Br}_2\text{F}_6\text{N}_2\text{O}_2\text{S}_2$, 841.0562; found, 841.0584.

Poly(4-(5-(5-methyl-3,6-dioctylthieno[3,2-b]thiophen-2-yl)-4-octylthiophen-2-yl)-8-(5-methyl-4-octylthiophen-2-yl)-2,6-bis(trifluoromethyl)benzo[1,2-d:4,5-d']bis(oxazole))

(PCF3BBOTT). A 3-neck round bottom flask was equipped with a reflux condenser and placed under an argon atmosphere. To this was added 4mL degassed dry toluene, 4,8-bis(5-bromo-4-octylthiophen-2-yl)-2,6-bis(trifluoromethyl)benzo[1,2-d:4,5-d']bis(oxazole) (**11**) (126 mg, 0.15 mmol), (3,6-dioctylthieno[3,2-b]thiophene-2,5-diyl)bis(trimethylstannane) (103 mg, 0.15 mmol), Pd₂dba₃ (2.7 mg, 0.003 mmol), and P(*o*-tol)₃ (3.6 mg, 0.012 mmol). The solution was heated to 110 °C for 4 d. One drop of trimethylphenyltin was added and this was heated for 2 h, followed by 0.1 mL of iodobenzene which was heated overnight. The solution was cooled and precipitated into methanol. The solid was filtered through a Soxhlet thimble and purified by Soxhlet extraction with methanol, hexanes, and chloroform. The chloroform fraction was concentrated by rotary evaporation to approximately 10 mL and then this was passed through a silica gel plug with chloroform eluent. The eluent was concentrated by rotary evaporation to approximately 10mL and then precipitated into methanol and isolated by filtration with a Büchner funnel. The dark purple solid was dried overnight in a vacuum oven (124 mg, 79% yield). ¹H NMR (600 MHz, Chloroform-d) δ 8.26 (s, 1H), 2.83 (s, 2H), 2.76 (s, 2H), 1.81 (s, 2H), 1.72 (s, 2H), 1.38 (s, 2H), 1.28 (d, J = 19.3 Hz, 24H), 0.85 (d, J = 23.2 Hz, 6H). GPC (CHCl₃): M_n = 6244, M_w = 10643, PDI = 1.70.

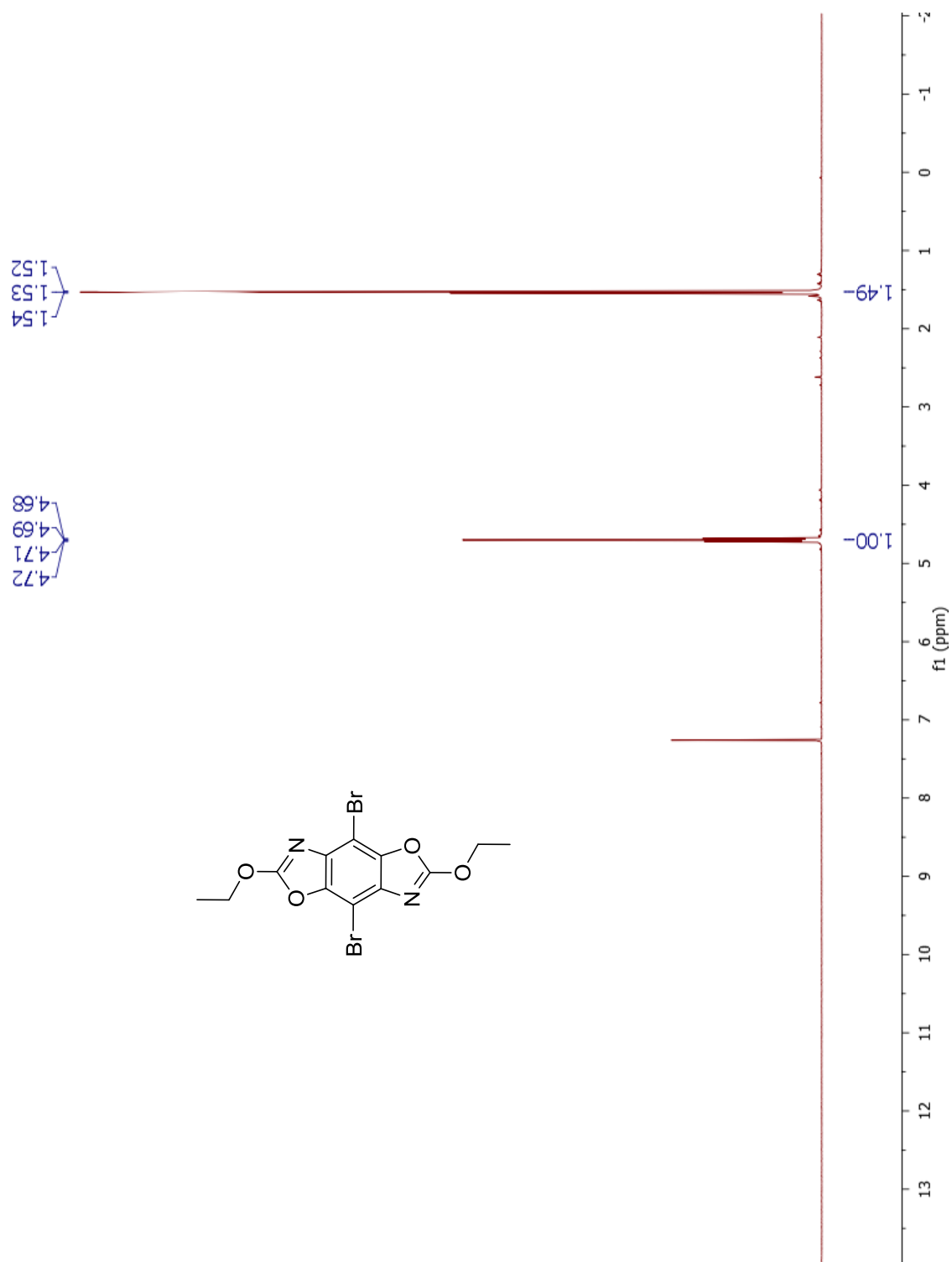


Figure 4.7. ^1H NMR of of 4,8-dibromo-2,6-diethoxybenzo[1,2-d:4,5-d']bis(oxazole) (1)

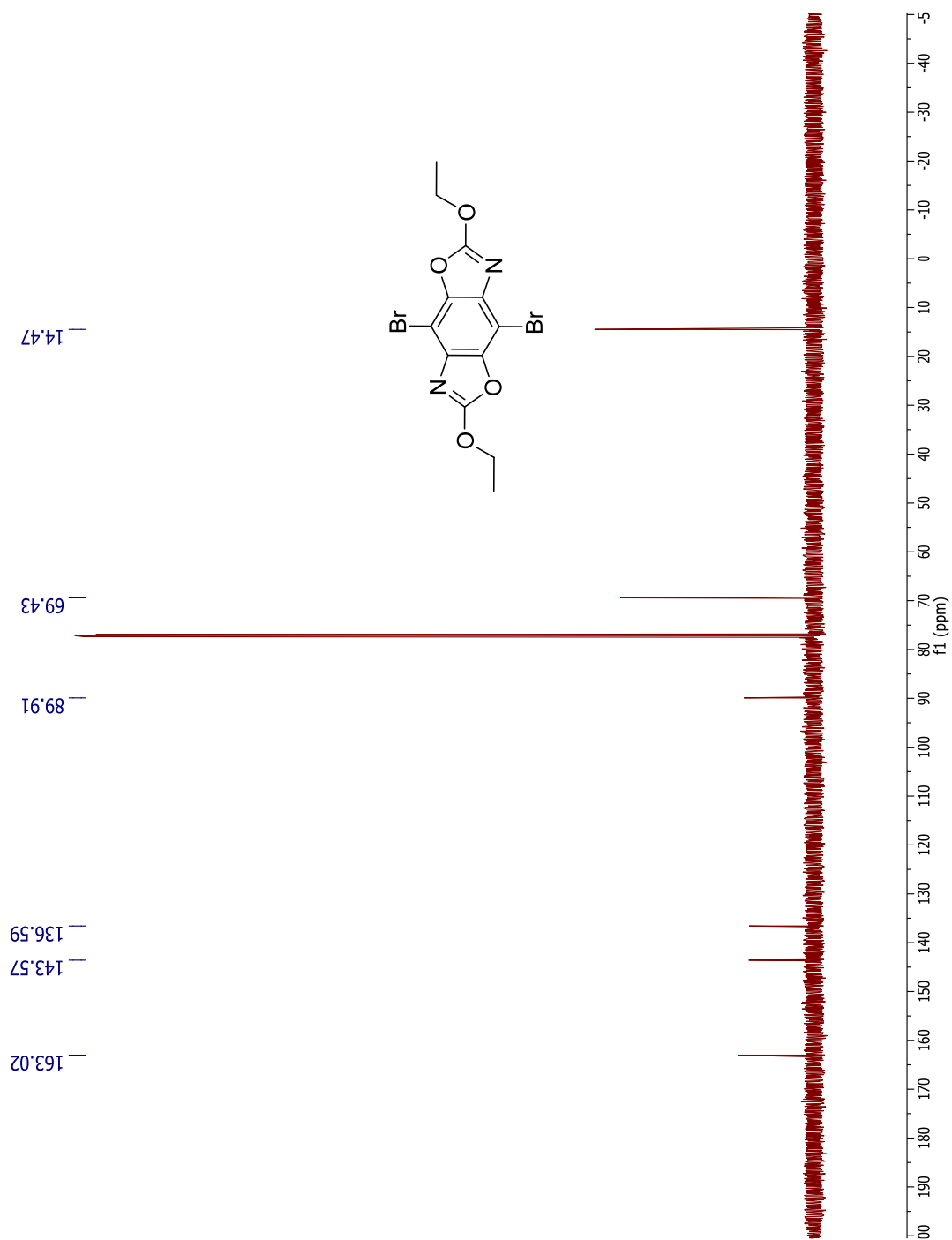


Figure 4.8. ^{13}C NMR of of 4,8-dibromo-2,6-diethoxybenzo[1,2-d:4,5-d']bis(oxazole) (**1**)

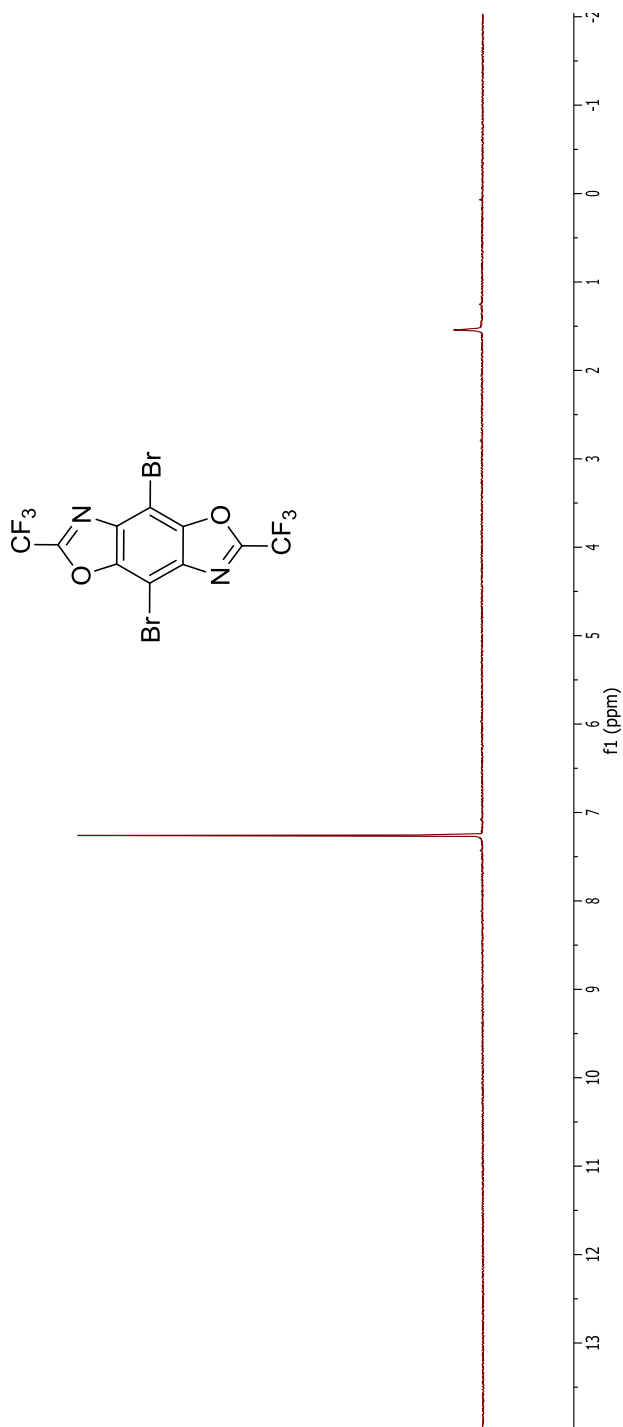


Figure 4.9. ¹H NMR of 4,8-dibromo-2,6-bis(trifluoromethyl)benzo[1,2-d:4,5-d']bis(oxazole) (5).

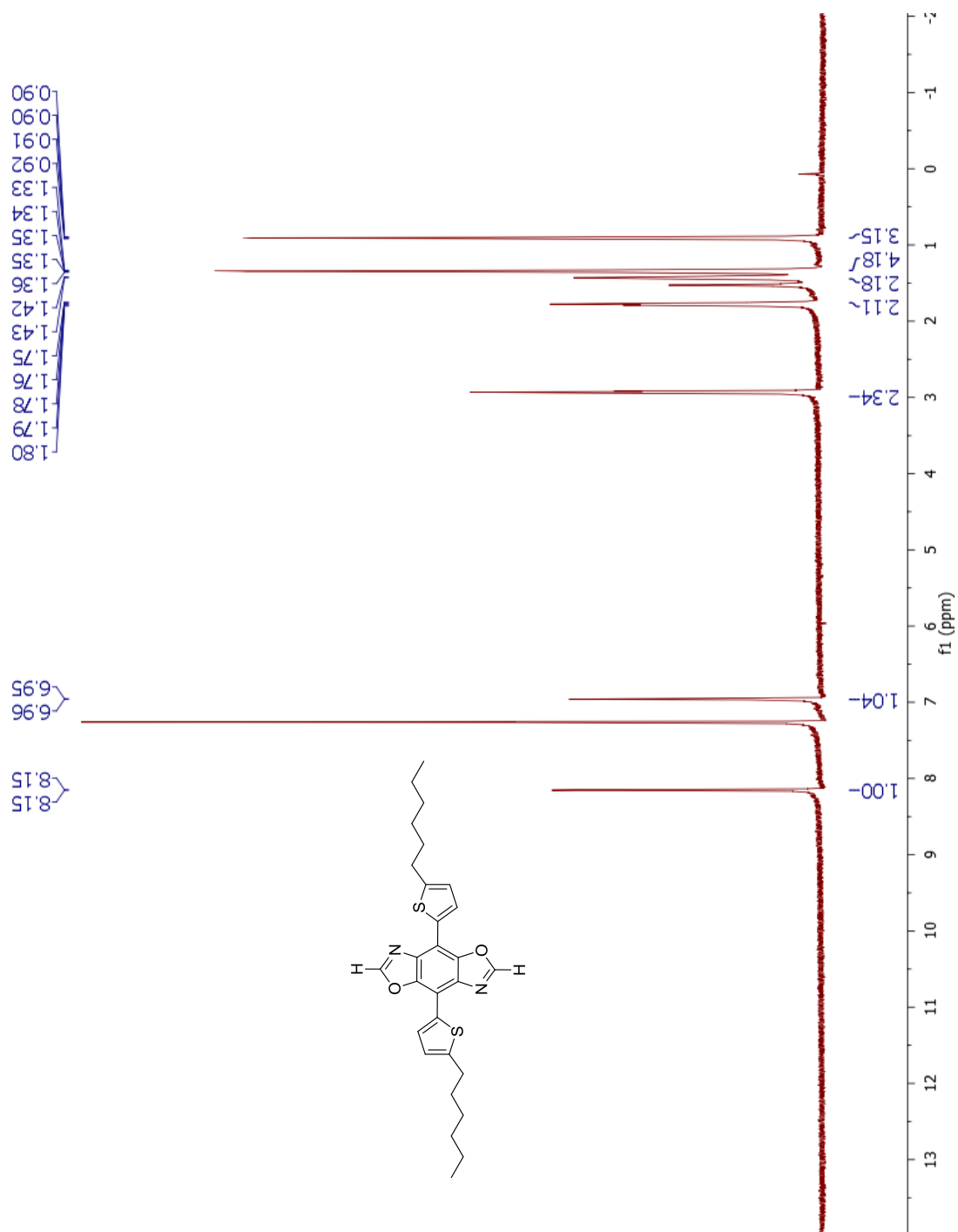


Figure 4.10. ^1H NMR of 4,8-bis(5-hexylthiophen-2-yl)benzo[1,2-d:4,5-d']bis(oxazole) (7)

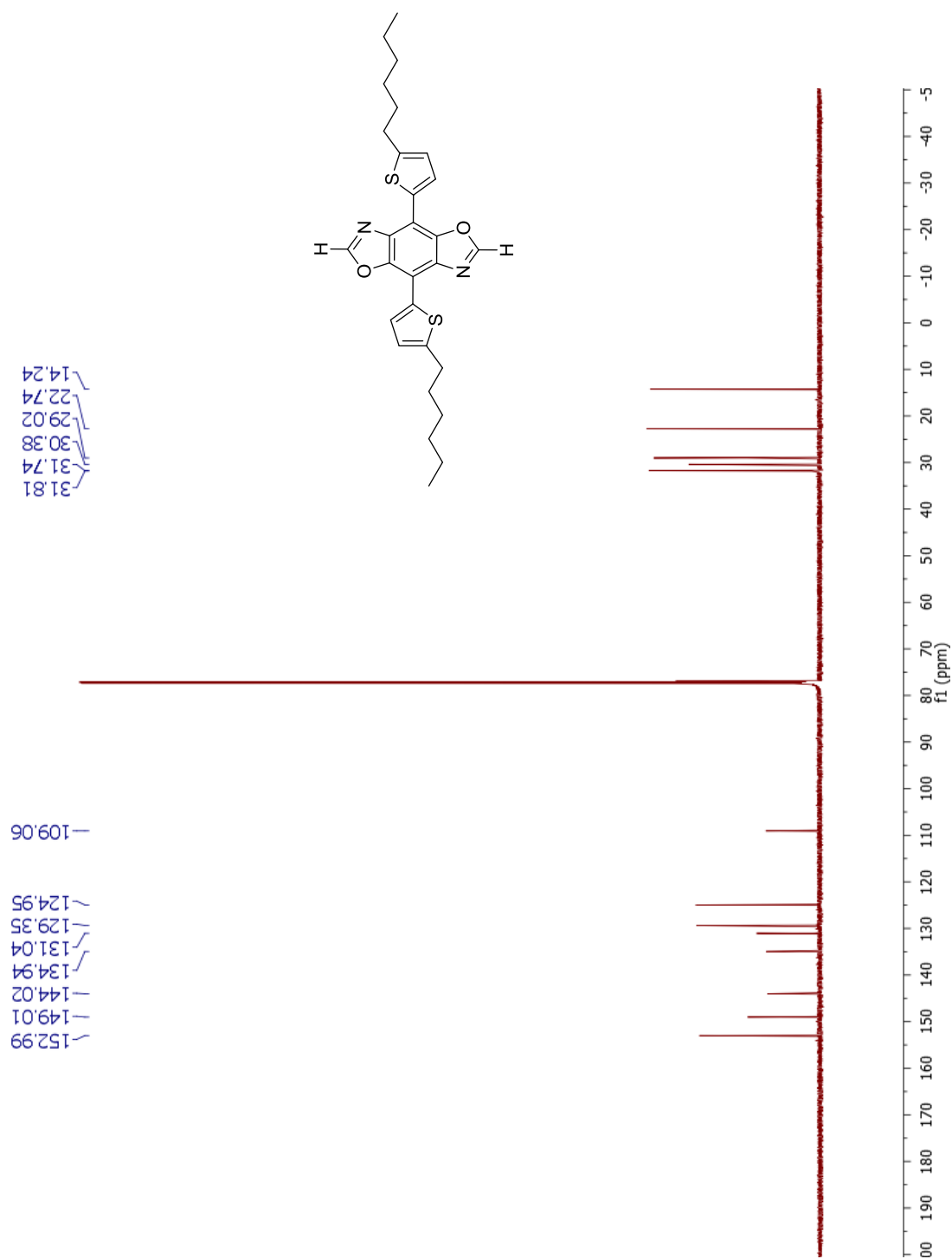


Figure 4.11. ^{13}C NMR of 4,8-bis(5-hexylthiophen-2-yl)benzo[1,2-d:4,5-d']bis(oxazole) (7)

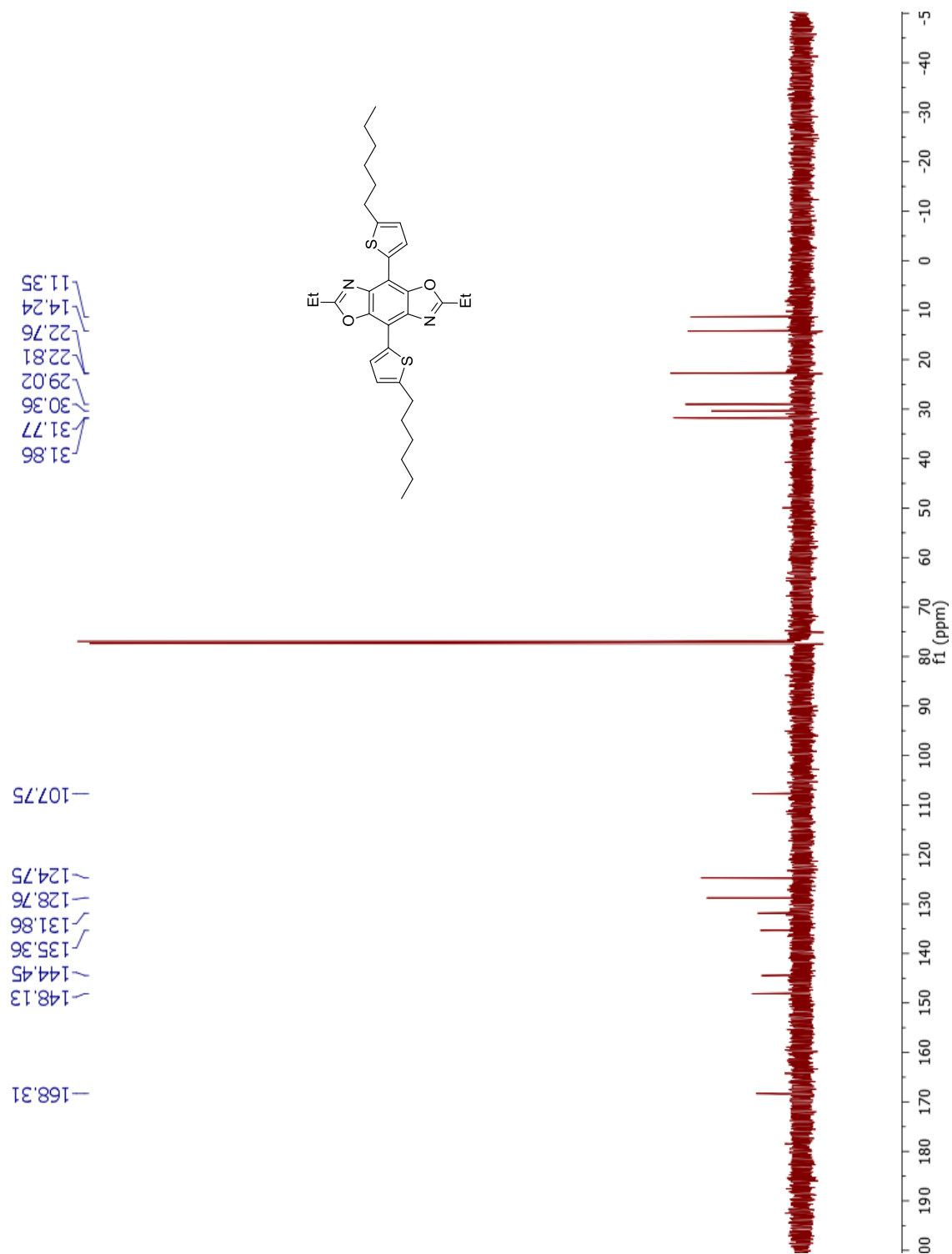


Figure 4.13. ^{13}C NMR of 2,6-diethyl-4,8-bis(5-hexylthiophen-2-yl)benzo[1,2-d:4,5-d']bis(oxazole) (**8**)

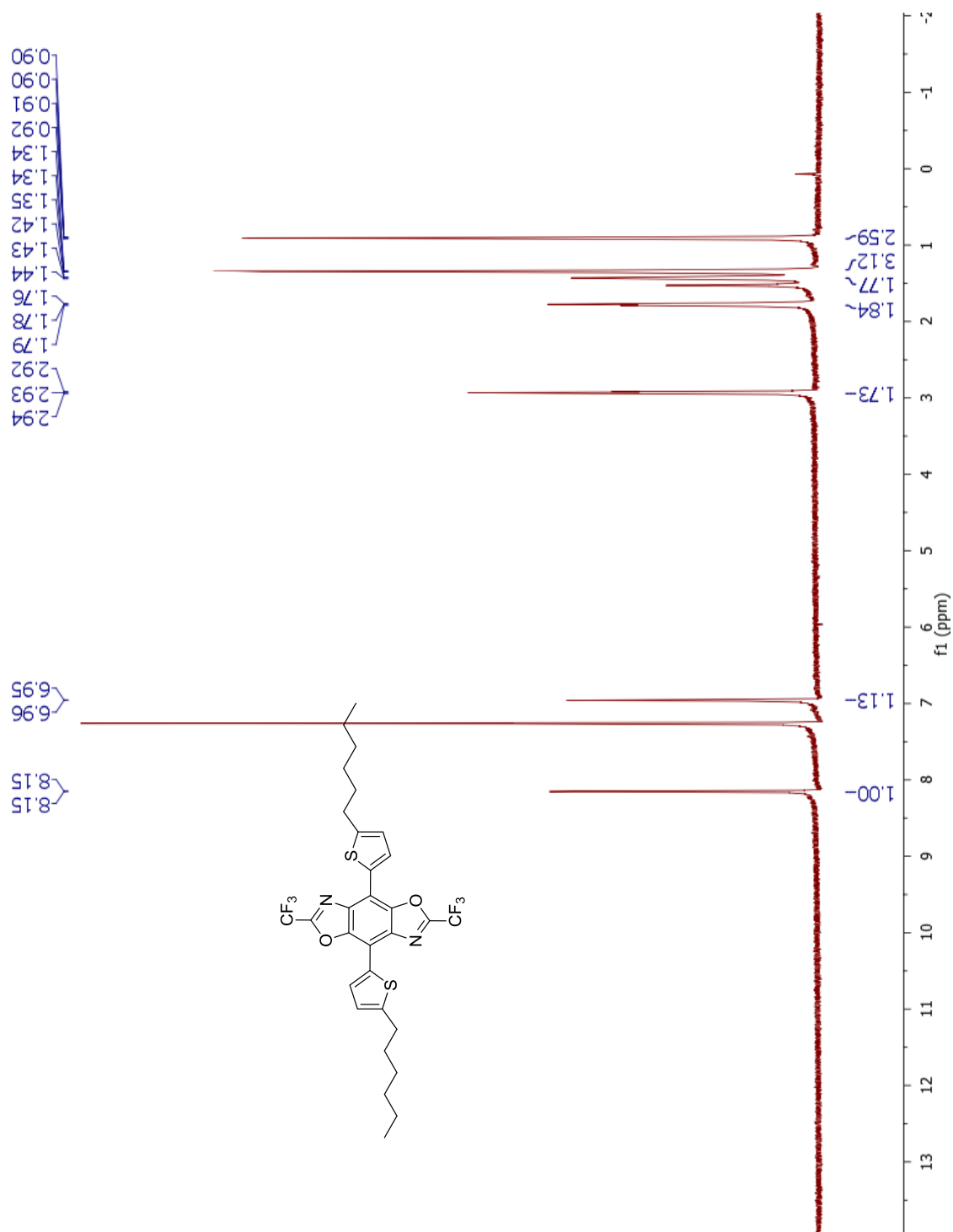


Figure 4.14. ^1H NMR of 4,8-bis(5-hexylthiophen-2-yl)-2,6-bis(trifluoromethyl)benzo[1,2-d:4,5-d']bis(oxazole) (**9**)

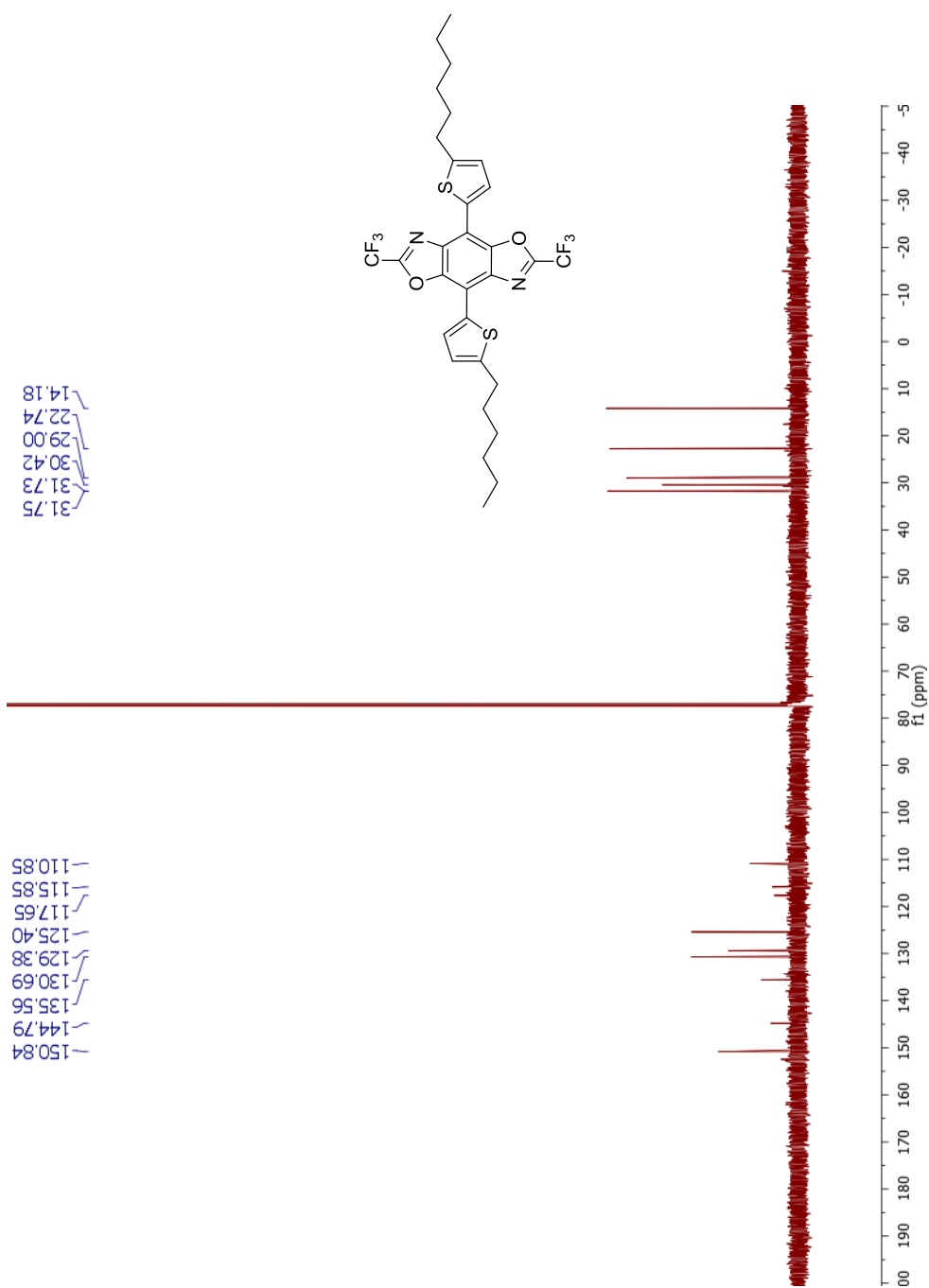


Figure 4.15. ^{13}C NMR of 4,8-bis(5-hexylthiophen-2-yl)-2,6-bis(trifluoromethyl)benzo[1,2-d:4,5-d']bis(oxazole) (9)

4.6. References

1. (a) Bredas, J.-L.; Durrant, J. R., Organic Photovoltaics. *Accounts of Chemical Research* **2009**, *42* (11), 1689-1690; (b) Boudreault, P.-L. T.; Najari, A.; Leclerc, M., Processable Low-Bandgap Polymers for Photovoltaic Applications†. *Chemistry of Materials* **2011**, *23* (3), 456-469; (c) Facchetti, A., π -Conjugated Polymers for Organic Electronics and Photovoltaic Cell Applications†. *Chemistry of Materials* **2010**, *23* (3), 733-758.
2. (a) Horowitz, G., Organic Field-Effect Transistors. *Advanced Materials* **1998**, *10* (5), 365-377; (b) Tsao, H. N.; Cho, D. M.; Park, I.; Hansen, M. R.; Mavrinskiy, A.; Yoon, D. Y.; Graf, R.; Pisula, W.; Spiess, H. W.; Müllen, K., Ultrahigh Mobility in Polymer Field-Effect Transistors by Design. *J Am Chem Soc* **2011**, *133* (8), 2605-2612.
3. (a) Friend, R. H.; Gymer, R. W.; Holmes, A. B.; Burroughes, J. H.; Marks, R. N.; Taliani, C.; Bradley, D. D. C.; Santos, D. A. D.; Bredas, J. L.; Logdlund, M.; Salaneck, W. R., Electroluminescence in conjugated polymers. *Nature* **1999**, *397* (6715), 121-128; (b) Tang, C. W.; VanSlyke, S. A., Organic electroluminescent diodes. *Applied Physics Letters* **1987**, *51* (12), 913-915; (c) Veinot, J. G. C.; Marks, T. J., Toward the Ideal Organic Light-Emitting Diode. The Versatility and Utility of Interfacial Tailoring by Cross-Linked Siloxane Interlayers. *Accounts of Chemical Research* **2005**, *38* (8), 632-643.
4. (a) Intemann, J. J.; Mike, J. F.; Cai, M.; Bose, S.; Xiao, T.; Mauldin, T. C.; Roggers, R. A.; Shinar, J.; Shinar, R.; Jeffries-El, M., Synthesis and Characterization of Poly(9,9-dialkylfluorenevinylene benzobisoxazoles): New Solution-Processable Electron-Accepting Conjugated Polymers. *Macromolecules* **2011**, *44* (2), 248-255; (b) Ahmed, E.; Kim, F. S.; Xin, H.; Jenekhe, S. A., Benzobisthiazole–Thiophene Copolymer Semiconductors: Synthesis, Enhanced Stability, Field-Effect Transistors, and Efficient Solar Cells. *Macromolecules* **2009**, *42* (22), 8615-8618.
5. Fukumaru, T.; Fujigaya, T.; Nakashima, N., Extremely High Thermal Resistive Poly(p-phenylene benzobisoxazole) with Desired Shape and Form from a Newly Synthesized Soluble Precursor. *Macromolecules* **2012**, *45* (10), 4247-4253.
6. (a) Mike, J. F.; Inteman, J. J.; Ellern, A.; Jeffries-El, M., Facile synthesis of 2, 6-disubstituted benzobisthiazoles: Functional monomers for the design of organic semiconductors. *The Journal of Organic Chemistry* **2009**, *75* (2), 495-497; (b) Mike, J. F.; Makowski, A. J.; Jeffries-El, M., An Efficient Synthesis of 2,6-Disubstituted Benzobisoxazoles: New Building Blocks for Organic Semiconductors. *Organic Letters* **2008**, *10* (21), 4915-4918.
7. (a) Bhuwarka, A.; Mike, J. F.; He, M.; Intemann, J. J.; Nelson, T.; Ewan, M. D.; Roggers, R. A.; Lin, Z.; Jeffries-El, M., Quaterthiophene–Benzobisazole Copolymers for Photovoltaic Cells: Effect of Heteroatom Placement and Substitution on the Optical and Electronic Properties. *Macromolecules* **2011**, *44* (24), 9611-9617; (b) Ahmed, E.; Subramaniyan, S.; Kim, F. S.; Xin, H.; Jenekhe, S. A., Benzobisthiazole-Based Donor–Acceptor Copolymer Semiconductors for Photovoltaic Cells and Highly Stable Field-Effect Transistors. *Macromolecules* **2011**, *44* (18), 7207-7219.

8. M. C. Scharber, D. M., M. Koppe, P. Denk, C. Waldauf, A. J. Heeger and C. J. Brabec, Design Rules for Donors in Bulk-Heterojunction Solar Cells—Towards 10 % Energy-Conversion Efficiency. *Advanced Materials* **2006**, *18* (6), 798-794.
9. Intemann, J. J.; Hellerich, E. S.; Tlach, B. C.; Ewan, M. D.; Barnes, C. A.; Bhuwalka, A.; Cai, M.; Shinar, J.; Shinar, R.; Jeffries-El, M., Altering the Conjugation Pathway for Improved Performance of Benzobisoxazole-Based Polymer Guest Emitters in Polymer Light-Emitting Diodes. *Macromolecules* **2012**, *45* (17), 6888-6897.
10. Brédas, J. L., Relationship between bandgap and bond length alternation in organic conjugated polymers. *Journal of Chemical Physics* **1985**, *82* (8), 3808.
11. Tlach, B. C.; Tomlinson, A. L.; Ryno, A. G.; Knoble, D. D.; Drochner, D. L.; Krager, K. J.; Jeffries-El, M., Influence of Conjugation Axis on the Optical and Electronic Properties of Aryl-Substituted Benzobisoxazoles. *The Journal of Organic Chemistry* **2013**, *78* (13), 6570-6581.
12. Heqedus, L. S.; Odle, R. R.; Winton, P. M.; Weider, P. R., Synthesis of 2,5-disubstituted 3,6-diamino-1,4-benzoquinones. *The Journal of Organic Chemistry* **1982**, *47* (13), 2607-2613.
13. (a) Zhang, Y.; Chien, S.-C.; Chen, K.-S.; Yip, H.-L.; Sun, Y.; Davies, J. A.; Chen, F.-C.; Jen, A. K. Y., Increased open circuit voltage in fluorinated benzothiadiazole-based alternating conjugated polymers. *Chemical Communications* **2011**, *47* (39), 11026-11028; (b) Zhang, Y.; Zou, J.; Cheuh, C.-C.; Yip, H.-L.; Jen, A. K. Y., Significant Improved Performance of Photovoltaic Cells Made from a Partially Fluorinated Cyclopentadithiophene/Benzothiadiazole Conjugated Polymer. *Macromolecules* **2012**, *45* (13), 5427-5435.
14. Tlach, B. C.; Tomlinson, A. L.; Bhuwalka, A.; Jeffries-El, M., Tuning the Optical and Electronic Properties of 4,8-Disubstituted Benzobisoxazoles via Alkyne Substitution. *The Journal of Organic Chemistry* **2011**, *76* (21), 8670-8681.
15. Yu, C.-Y.; Ko, B.-T.; Ting, C.; Chen, C.-P., Two-dimensional regioregular polythiophenes with conjugated side chains for use in organic solar cells. *Sol. Energy Mater. Sol. Cells* **2009**, *93* (Copyright (C) 2015 American Chemical Society (ACS). All Rights Reserved.), 613-620.
16. Yassin, A.; Jimenez, P.; Lestriez, B.; Moreau, P.; Leriche, P.; Roncali, J.; Blanchard, P.; Terrisse, H.; Guyomard, D.; Gaubicher, J., Engineered Electronic Contacts for Composite Electrodes in Li Batteries Using Thiophene-Based Molecular Junctions. *Chem. Mater.* **2015**, *27* (Copyright (C) 2015 American Chemical Society (ACS). All Rights Reserved.), 4057-4065.
17. Xu, X.; Cai, P.; Lu, Y.; Choon, N. S.; Chen, J.; Hu, X.; Ong, B. S., Synthesis and characterization of thieno[3,2-b]thiophene-isindigo-based copolymers as electron donor and hole transport materials for bulk-heterojunction polymer solar cells. *J. Polym. Sci., Part A: Polym. Chem.* **2013**, *51* (Copyright (C) 2015 American Chemical Society (ACS). All Rights Reserved.), 424-434.

CHAPTER 5

TUNING THE BANDGAP OF CONJUGATED POLYMERS BY *N*- ACYLATION OF ISOINDIGO CONJUGATED POLYMERS

5.1. Introduction

Conjugated polymers for OPV¹ applications offer the possibility of low-cost, easily fabricated² solar cells and much research has focused on how structure-property relationships³ can modulate the optoelectronic properties to achieve good performance. A low bandgap is necessary for absorption of the abundant visible portion of the solar spectrum and a deep HOMO can provide environmental stability⁴ and a high device open circuit voltage⁵. The position of the lowest occupied molecular orbital is also of consequence, as it should be at least 0.3 eV above that of the PCBM acceptor material to drive electron transfer of the exciton formed on the polymer⁶ upon absorbance of solar radiation. Synthesis of donor-acceptor copolymers⁷ is an effective strategy to establish the bandgap, wherein the LUMO is mainly determined by the acceptor and the HOMO by the donor. Further side group modifications can fine-tune the energy levels, and in an effort to reduce the bandgap by lowering the LUMO, we sought to study the effect of *N*-acylation of isoindigo.

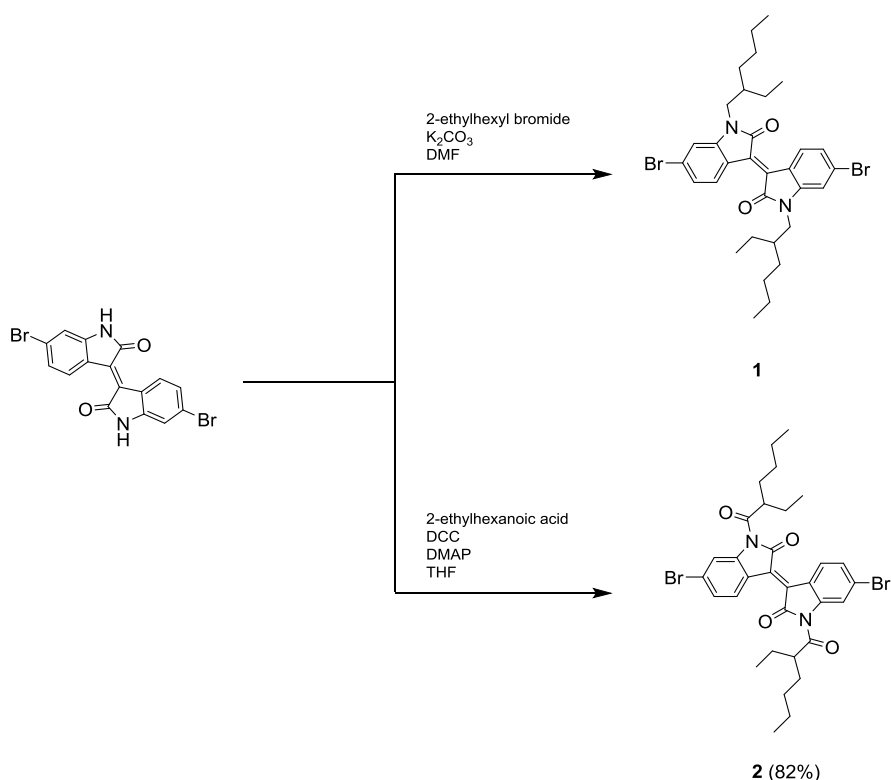
Isoindigo has become a widely studied material for the synthesis of organic transistors⁸ and OPVs, due to its facile synthesis and two lactam rings which make it a strong acceptor. It is known to produce low bandgap materials with good charge transport properties⁹. Fluorination of the 7-7' positions of the aromatic core¹⁰ has shown to reduce the LUMO and impart ambipolar transport¹¹ behavior in transistors. Another way to reduce the LUMO can be through *N*-substitution.

Isoindigo, as well as other lactam- and imide-containing units, are typically *N*-alkylated to increase solubility, but other groups such as acyl and Boc¹² can be appended to influence the electronics or self-assembly of the unit. *N*-acylation has been demonstrated with dithieno[3,2-b:2',3'-d]pyrrole¹³, to lower the HOMO of this relatively strong donor, as well as with acceptors such as benzodipyrrolidone¹⁴ and thieno[3,4-c]pyrrole-4,6-dione¹⁵ which decreased both the HOMO and the LUMO of the resulting polymers when compared to the alkylated versions. Isoindigo itself has even been *N*-acylated¹⁶ for use in conjugated polymer transistors, but has not been studied for OPVs. Herein we report a new synthesis of an *N*-acyloylisoindigo and evaluate it in donor-acceptor copolymers for OPV applications. The energy levels are further tuned by varying the donors with common alkyl vs. acyl isoindigo acceptors.

5.2. Results & Discussion

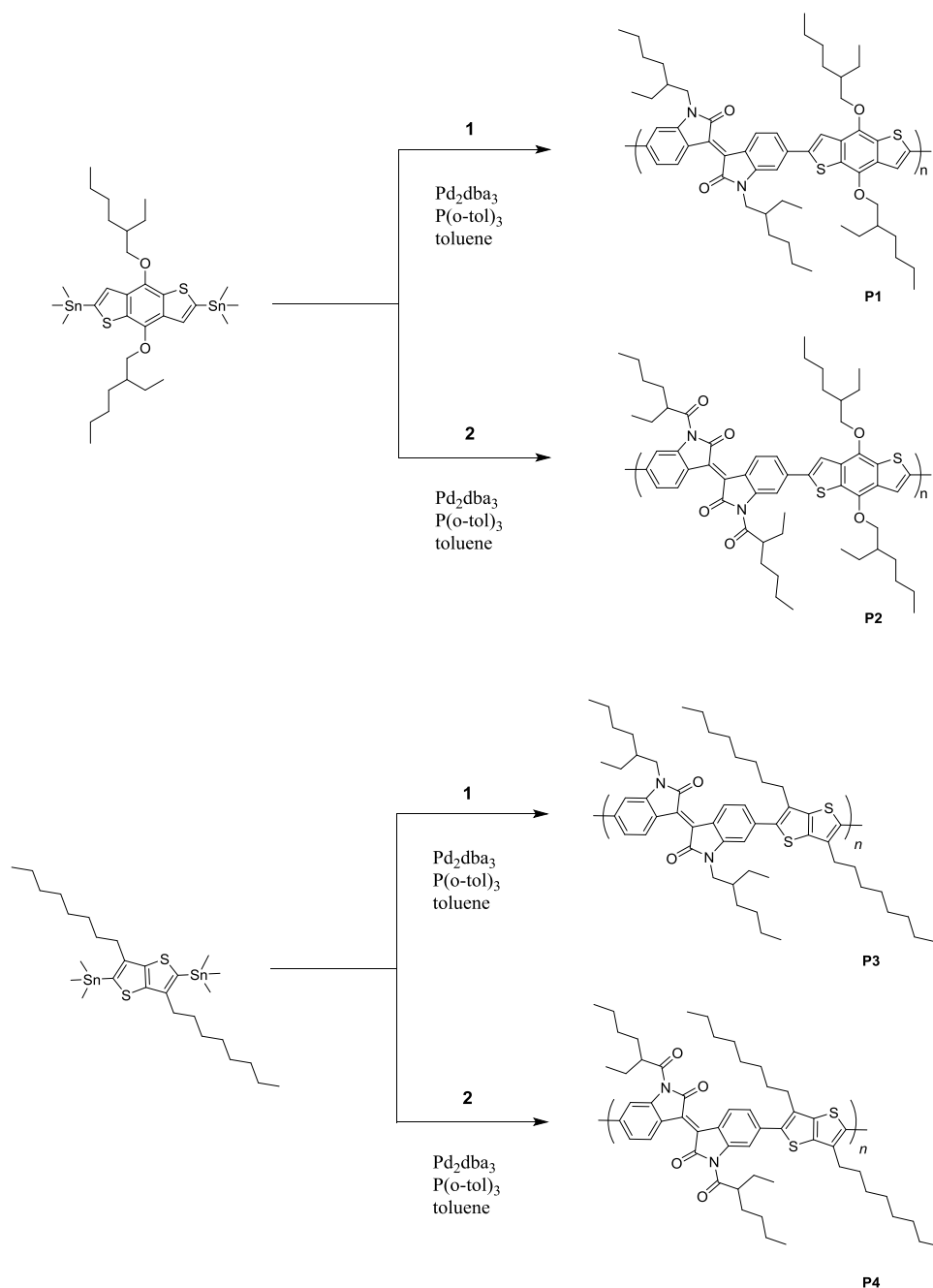
5.2.1. Synthesis

Synthesis of the isoindigo monomers is outlined in Scheme 5.1. Isoindigo was alkylated by a standard S_N2 reaction of 6,6'-dibromoisindigo with 2-ethylhexyl bromide to yield monomer **1**. Monomer **2** was synthesized by acylating 6,6'-dibromoisindigo with 2-ethylhexanoic acid with DCC and catalytic DMAP. Purification was accomplished by simply filtering to remove the DCU by-product, rotary evaporation of the filtrate and isolation of the resulting bright red solid in 82% yield.



Scheme 5.9. Synthesis of isoindigo monomers.

The electron-donating monomers 4,8-bis((2-ethylhexyl)oxy)benzo[1,2-b:4,5-b']dithiophene (BDT) and 3,6-dioctylthieno[3,2-b]thiophene (TT) were chosen due to their strong and moderate electron-donating abilities, respectively. These monomers will further fine-tune the bandgap and establish a wider scope of the effect of *N*-acylation of isoindigo, as their structural differences could also affect polymer solubility, crystallinity, and photovoltaic performance. (4,8-Bis((2-ethylhexyl)oxy)benzo[1,2-b:4,5-b']dithiophene-2,6-diyl)bis(trimethylstannane) and (3,6-dioctylthieno[3,2-b]thiophene-2,5-diyl)bis(trimethylstannane) were coupled with **1** or **2** via Stille



Scheme 5.10. Synthesis of polymers.

cross-coupling reactions (Scheme 5.2), resulting in BDT-based polymers **P1** and **P2** and thienothiophene-based polymers **P3** and **P4**. Polymer **P1** was reacted for a total of 2 days and purified by Soxhlet extraction with methanol, hexane, and chloroform. Material from the

Table 5.5. Physical properties of isoindigo polymers.

Polymer	Yield (%) ^b	Mw ^a (kDa)	PDI	Td ^c (°C)
P1	72%	5.3	1.4	376
P2	54%	4.9	1.2	331
P3	42%	5.7	2.1	
P4	34%	1.9	5.9	

^aDetermined by GPC in THF using polystyrene standards. ^bDegree polymerization calculated from the molecular weight. ^c5% weight loss temperature by TGA in air.

chloroform fraction was isolated in 72% yield. A similar reaction was conducted for **P2**, however, after 1 day the reaction solution had formed a solid film and the polymerization reaction was terminated at that point. Purification was completed in the same manner as the previous polymer, resulting in a 54% yield from the chloroform Soxhlet fraction. Both polymers were soluble in chloroform and 1,2-dichlorobenzene. Reactions to synthesize **P3** and **P4** were both conducted for 3 days, yet resulted in poor yields of 42% and 34%, respectively. Despite the low yield and low molecular weight, they were carried forward for characterization for a comparison to **P1** and **P2** as well as to determine if future optimization of these conditions would be necessary.

5.2.2. Physical properties

The molecular weight of the polymers was analyzed by GPC with chloroform as the solvent. The results, as seen in Table 5.1, show relatively low molecular weights. However, the chromatogram of each polymer also displayed another peak with a low retention time which could indicate aggregation of the polymers. Thus, the reported values might not reflect the true MWs of the polymers due to limitations of the GPC system. Despite the low MW, the polymers likely

reached their effective conjugation length, based on the similar optoelectronic properties, *vide infra*, to similar isoindigo polymers¹⁷.

N-acylation of the acceptor unit causes a lower onset of thermal decomposition, T_d , with that of **P2** being about 40 °C lower than **P1**. However, both temperatures are acceptable for normal operating conditions.

5.2.3. Optical & Electrochemical Properties

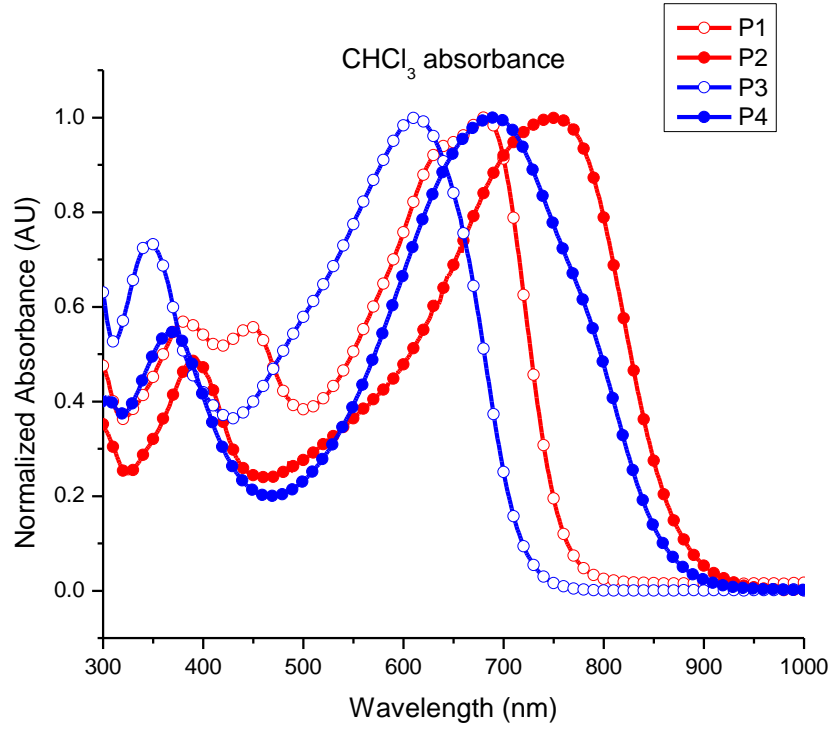
The UV-vis spectra of **P1** and **P2** are shown in Figure 5.1 and 5.2, respectively as well as summarized in Table 5.2. In solution, both polymers have a broad absorption within the visible range. The λ_{max} of **P1** is 681 nm while that of **P2** is at 747 nm, demonstrating that the side chain modification resulted in a 66 nm bathochromic shift in absorption. Interestingly, in the film state, the maximum absorption of both polymers is blue-shifted by 61 and 47 nm, respectively. While the GPC result suggested aggregation in solution, the blue-shifted absorption from solution to film might suggest less crystallinity in the solid state. **P1** also shows an increase in absorption in the higher wavelengths. With absorption values blue shifted relative to **P1** and **P4** in solution, there is a 76 nm difference between **P3** and **P4**. **P4** possesses a slight long-wavelength shoulder,

Table 5.2 Optical and electronic properties for **P1-P4**

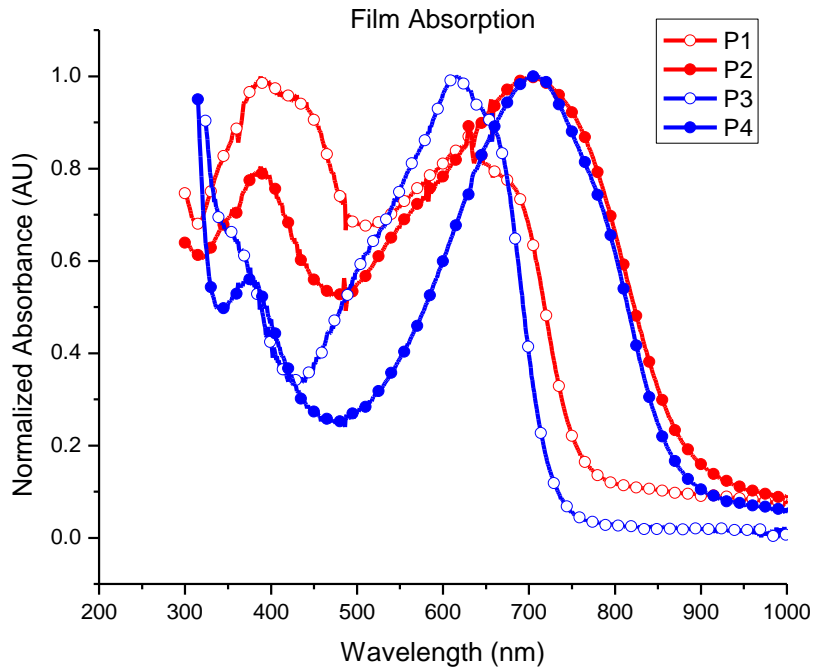
Polymer	λ_{\max} solution (nm)	λ_{\max} film (nm)	Absonset (nm)	E_g^{opt} (eV) ^a	$E_{\text{onset}}^{\text{ox}}$ (V) ^b	HOMO ^c (eV)	LUMO ^d (eV)
P1	681	379, 620	754	1.64	0.61	-5.32	-3.68
P2	747	700	872	1.42	0.62	-5.37	-3.95
P3	613	616	732	1.69	0.78	-5.44	-3.71
P4	689	705	885	1.40	0.69	-5.33	-3.93

^a Estimated from the optical absorption edge. ^a Onset of potentials (vs Fc). ^c HOMO = $-(E_{\text{onset}}^{\text{ox}} + 4.8)$ (eV). ^d LUMO = HOMO - E_g^{opt}

indicating some aggregation in solution. Despite the differences in solution, the properties in solid state between the two donor monomers become very similar in λ_{\max} , with the absorption of the BDT-based polymers being broader overall. Both **P2** and **P4** have nearly identical bandgaps of about 1.4 eV. Therefore, the difference in donor monomers ended up having little effect on the bandgap.



a..



b.

Figure 5.1. UV-Vis spectra (a) in chloroform solution and (b) in film.

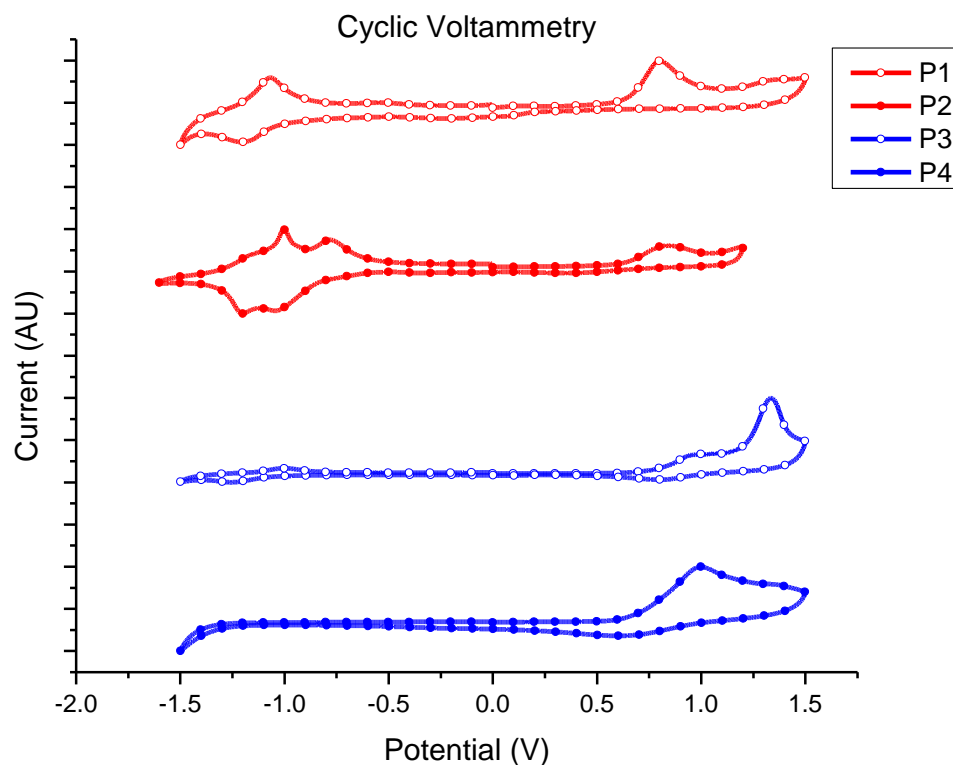


Figure 5.23. Cyclic voltammetry

The redox properties of the polymers were determined by cyclic voltammetry, as shown in Figure 5.3. Polymer solutions were drop cast onto platinum electrodes and data was obtained with an Ag/Ag^+ reference electrode and $\text{nBu}_4\text{PF}_6/\text{MeCN}$ electrolyte solution. The thienothiophene-based polymers **P3** and **P4** exhibited quasi-reversible oxidation with onsets of 0.69 V and 0.78 V, from which the HOMO was calculated to be -5.33eV and -5.44 eV, respectively. They did not show activity in the negative direction up to -1.5 V. Conversely, the BDT-based polymers were reversible upon reduction while being essentially irreversible in the positive direction.

Having determined the HOMO from the CV data, the LUMO was then calculated by subtracting the optical bandgap from the HOMO. The results among all the polymers illustrate how the *N*-acylation selectively tunes the energy levels by reducing the LUMO by more than 0.2 eV while the HOMO remained similar among common donors.

5.2.4. Photovoltaic properties

Fabrication and analysis of OPV devices containing these polymers is currently underway.

5.3. Conclusion

In conclusion, isoindigo monomers have been modified into stronger acceptors which are promising for OPV purposes. *N*-acylation selectively lowered the LUMO into the ideal range for efficient electron transfer to PCBM. Meanwhile, a small change in the HOMO level resulted in quite narrow bandgaps. As such, a large red shift of the absorption spectra of the *N*-acyl polymers when compared to their alkyl analogs, places its absorption outside the desired range for OPV applications. Because the LUMO has been selectively tuned, further studies should focus on additional donors to copolymerize with these *N*-acyl isoindigos in an effort to stabilize the HOMO and increase the bandgap such that a complementary absorption profile can be achieved. Optimization of this ideal polymer should then focus on determining the best *N*-acyl chains for solubility and self-assembly with PCBM to maximize OPV performance.

5.4. Acknowledgements

Synthetic contributions include that of Brian Tlach for the (4,8-bis((2-ethylhexyl)oxy)benzo[1,2-b:4,5-b']dithiophene-2,6-diyl)bis(trimethylstannane) and Brandon Kobilka for the (3,6-dioctylthieno[3,2-b]thiophene-2,5-diyl)bis(trimethylstannane). Benjamin

Hale performed thermal analysis studies. The author performed all other synthesis and wrote the text.

5.5. Experimental

Materials

(*E*)-6,6'-Dibromo-1,1'-bis(2-ethylhexyl)-[3,3'-biindolinylidene]-2,2'-dione¹⁸, (4,8-bis((2-ethylhexyl)oxy)benzo[1,2-b:4,5-b']dithiophene-2,6-diyl)bis(trimethylstannane)¹⁹, (3,6-dioctylthieno[3,2-b]thiophene-2,5-diyl)bis(trimethylstannane)^{18b}, and (9,9-dioctyl-9H-fluorene-2,7-diyl)bis(trimethylstannane)²⁰ were synthesized according to literature procedures. Toluene was dried using an Innovative Technology, Inc. solvent purification system. Other reagents were obtained from commercial sources and used without further purification.

Characterization

Nuclear magnetic resonance (NMR) spectra were recorded on a Varian MR (400 MHz) or a Bruker Avance III (600 MHz). Spectra were internally referenced to the residual protonated solvent peak. Chemical shifts are given in ppm (δ) relative to the solvent. Absorption spectra were obtained on a photodiode-array Agilent 8453 UV-visible spectrophotometer using sample solutions in CHCl₃ or thin films made by spin-coating 25 x 25 x 1 mm glass slides using solutions of polymer (1-3 mg/mL) in CHCl₃/chlorobenzene at a spin rate of 1200 rpm on a Headway Research, Inc. PWM32 spin-coater. Cyclic voltammetry was performed using an e-DAQ e-corder 410 potentiostat with a scanning rate of 50 mV/s. Ag/Ag⁺ was used as the reference electrode and a platinum wire as the auxiliary electrode. The reported values are referenced to Fc/Fc⁺ (-4.8 eV vs. vacuum). Polymer solutions in chlorobenzene (1-2 mg/mL) were drop-cast onto a platinum electrode. Polymer analysis was performed in deoxygenated solutions of 0.1 M

tetrabutylammonium hexafluorophosphate electrolyte in CH₃CN under an argon atmosphere. Small molecule analysis were performed by dissolving 1mg/mL of small molecule sample in 0.1 M tetrabutylammonium hexafluorophosphate in DCM and deoxygenated with argon. Gel permeation chromatography (GPC) measurements were performed on a Shimadzu Prominence UFLC instrument calibrated relative to polystyrene standards and equipped with RI and UV-Vis detectors. Measurements were conducted at 50 °C using CHCl₃ as the eluent with a flow rate of 1.0 mL/min. Thermal gravimetric analysis (TGA) and differential scanning calorimetry (DSC) measurements were performed with a Netzsch STA449 F1 instrument. TGA were conducted at a heating rate of 20 °C/min under ambient atmosphere. DSC was performed using a heat/cool/heat method at 15 °C/min under nitrogen.

Synthesis

(E)-6,6'-dibromo-1,1'-bis(2-ethylhexanoyl)-[3,3'-biindolinylidene]-2,2'-dione (2). 6,6'-dibromoisindigo (0.92 g, 2.2 mmol), 2-ethylhexanoic acid (0.69 g, 4.8 mmol), and a few crystals of DMAP were mixed in 10 mL THF. DCC (0.99 g, 4.8 mmol) was added to the solution and the mixture was stirred at room temperature for 24 h. The bright red solution was filtered with a Büchner funnel, washed with hexanes and the filtrate was concentrated by rotary evaporation. The red solid was suspended in hexanes and filtered to yield the product (1.20 g, 82%) ¹H NMR (400 MHz, Chloroform-d) δ 8.72 (d, *J* = 8.7 Hz, 1H), 8.52 (d, *J* = 1.9 Hz, 1H), 7.39 (dd, *J* = 8.8, 1.9 Hz, 1H), 3.85 (p, *J* = 6.7, 6.0 Hz, 1H), 1.82 (ddt, *J* = 10.8, 7.6, 3.6 Hz, 2H), 1.69 – 1.60 (m, 2H), 1.32 (dd, *J* = 7.8, 4.3 Hz, 4H), 0.96 (t, *J* = 7.4 Hz, 3H), 0.89 (t, *J* = 7.0 Hz, 3H). ¹³C NMR (151 MHz, CDCl₃) δ 11.73, 14.11, 23.03, 25.34, 29.57, 31.44, 47.38, 119.65, 121.12, 128.08, 128.37, 129.81, 132.38, 142.90, 167.33, 177.47.

General polymerization procedure: To an oven dried 3-neck round bottom flask equipped with a condenser was added 5 mL of degassed toluene and placed kept under an argon atmosphere. The isoindigo monomer (0.25 mmol, 1 eq), aryl bisstannane (0.25 mmol, 1 eq), tris(dibenzylideneacetone)dipalladium(0) (4.5 mg, 0.005 mmol), and tris-*o*-tolylphosphine (6 mg, 0.02 mmol) were added to the flask and the solution was degassed for 10 more minutes by bubbling argon through the solution. The flask was heated to 110 °C for the specified amount of time and then cooled and the solution was precipitated into methanol. The solid was purified by Soxhlet extraction with methanol, hexanes, and chloroform. The chloroform fraction was concentrated to approximately 10mL by rotary evaporation and then the solution was passed through a silica gel plug with chloroform as the eluent. The solvent was reduced to approximately 10mL by rotary evaporation, and then poured into methanol to precipitate the polymer which was collected by filtration with a Büchner funnel. The solid was dried overnight at 40 °C in a vacuum oven.

Poly((E)-6-(4,8-bis((2-ethylhexyl)oxy)benzo[1,2-b:4,5-b']dithiophen-2-yl)-1,1'-bis(2-ethylhexyl)-[3,3'-biindolinylidene]-2,2'-dione) (P1): Heated for 45 h. Yield 173 mg, 72% as a dark blue solid.

Poly((E)-6-(4,8-bis((2-ethylhexyl)oxy)benzo[1,2-b:4,5-b']dithiophen-2-yl)-1,1'-bis(2-ethylhexanoyl)-[3,3'-biindolinylidene]-2,2'-dione) (P2): Heated for 21 h. Yield 129 mg, 54% as a dark blue solid.

Poly((E)-6-(3,6-dioctylthieno[3,2-b]thiophen-2-yl)-1,1'-bis(2-ethylhexyl)-[3,3'-biindolinylidene]-2,2'-dione) (P3): Heated for 36 h. Yield 88 mg, 42% as a dark blue solid.

Poly((E)-6-(3,6-dioctylthieno[3,2-b]thiophen-2-yl)-1,1'-bis(2-ethylhexanoyl)-[3,3'-biindolinylidene]-2,2'-dione) (P4): Heated for 36 h. Yield 60 mg, 34% as a dark blue solid.

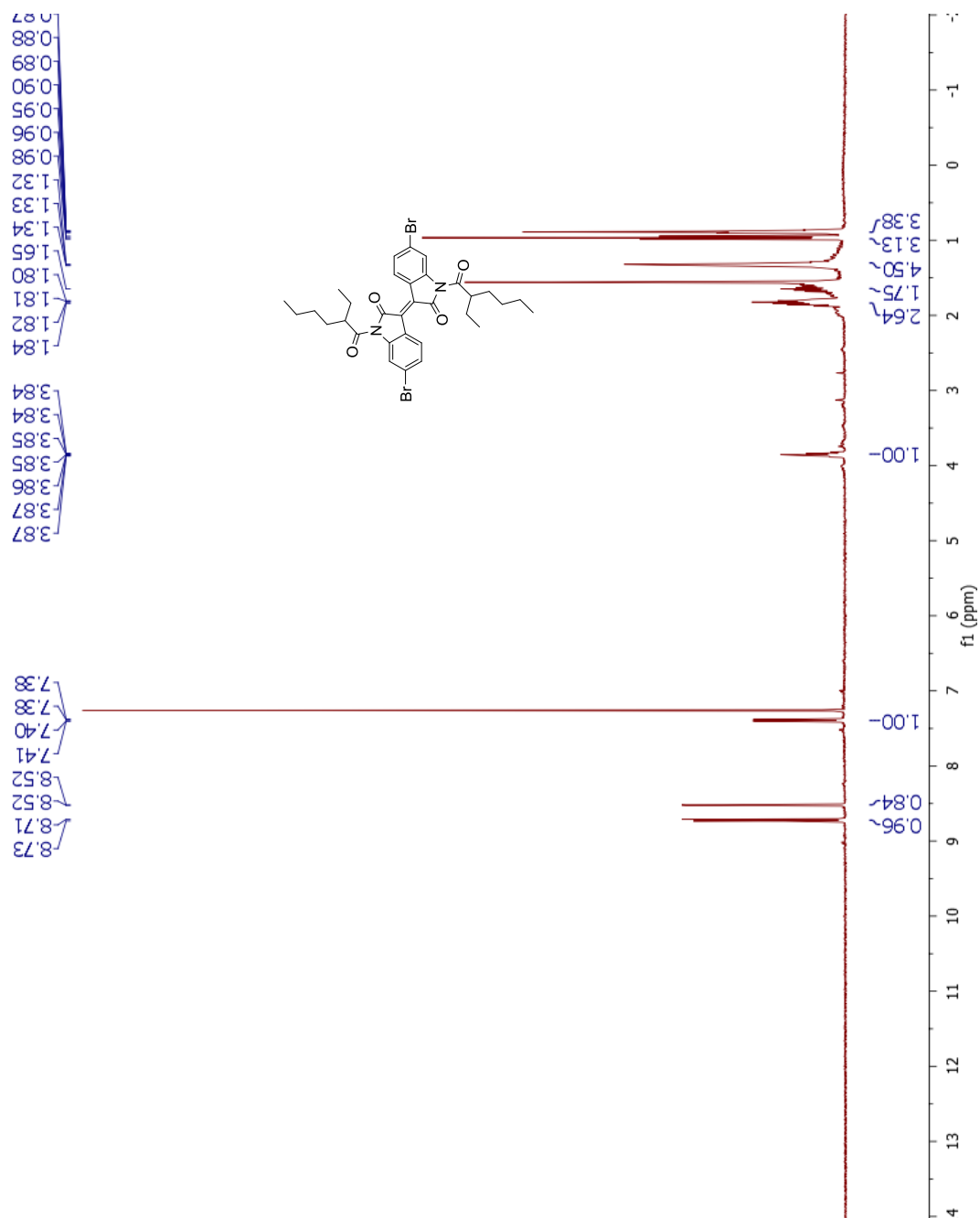


Figure 24. ¹H NMR of (E)-6,6'-dibromo-1,1'-bis(2-ethylhexanoyl)-[3,3'-biindolinylidene]-2,2'-dione (2)

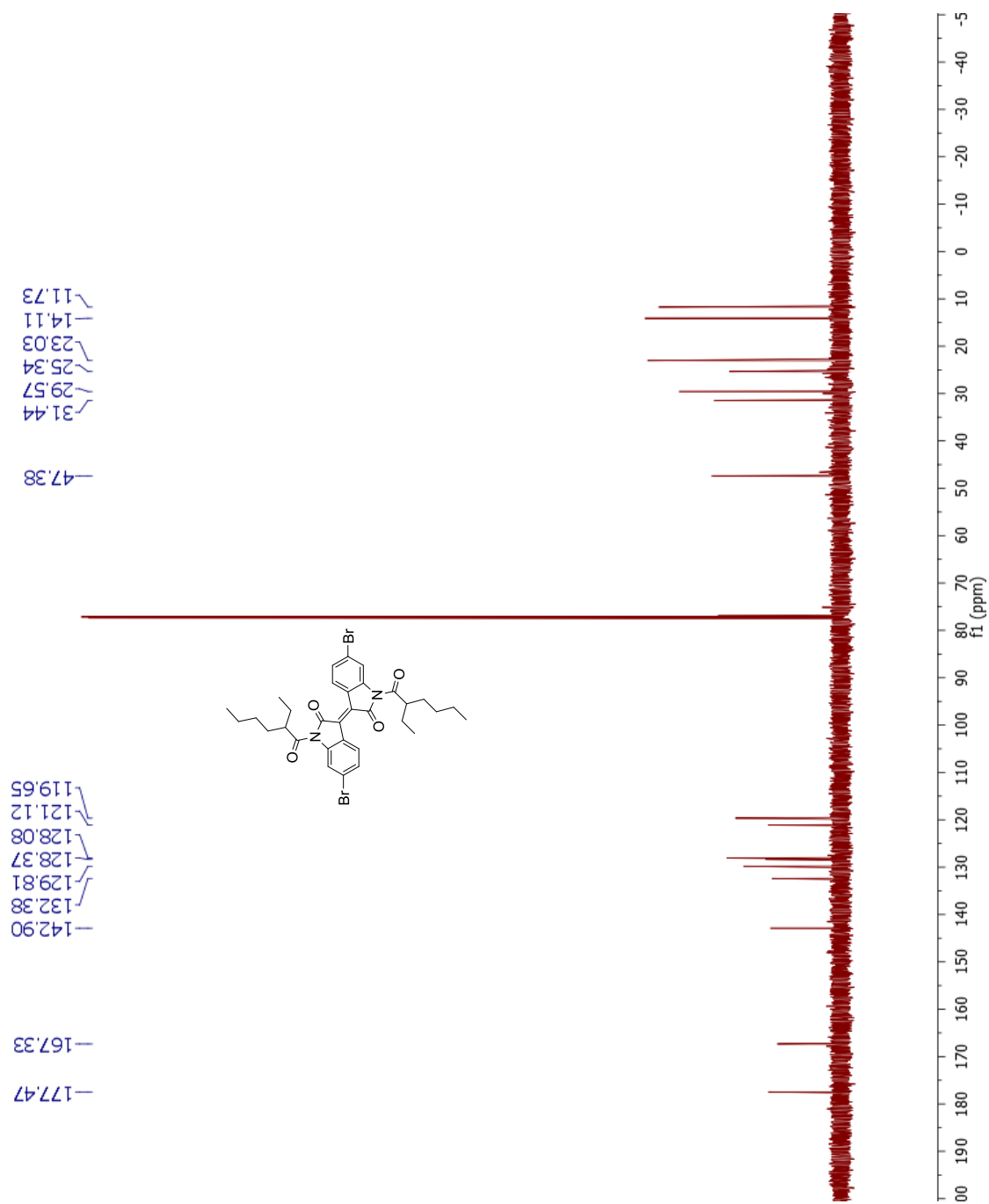


Figure 25. ^{13}C NMR of (E)-6,6'-dibromo-1,1'-bis(2-ethylhexanoyl)-[3,3'-biindolinylidene]-2,2'-dione (2)

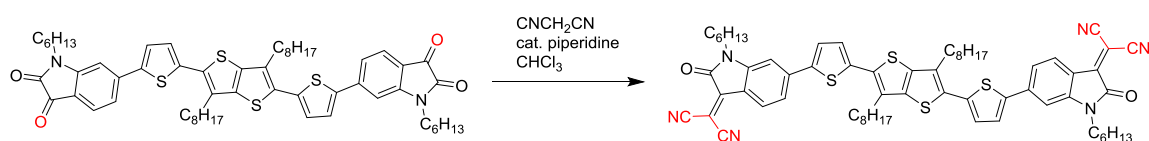
5.6. References

1. (a) Brabec, C. J.; Gowrisanker, S.; Halls, J. J. M.; Laird, D.; Jia, S.; Williams, S. P., Polymer–Fullerene Bulk-Heterojunction Solar Cells. *Advanced Materials* **2010**, *22* (34), 3839-3856; (b) Dennler, G.; Scharber, M. C.; Brabec, C. J., Polymer-Fullerene Bulk-Heterojunction Solar Cells. *Advanced Materials* **2009**, *21* (13), 1323-1338.
2. Krebs, F. C., Fabrication and processing of polymer solar cells: A review of printing and coating techniques. *Solar Energy Materials and Solar Cells* **2009**, *93* (4), 394-412.
3. Roncali, J., Molecular Engineering of the Bandgap of π -Conjugated Systems: Facing Technological Applications. *Macromolecular Rapid Communications* **2007**, *28* (17), 1761-1775.
4. de Leeuw, D., Stability of n-type doped conducting polymers and consequences for polymeric microelectronic devices. *Synthetic metals* **1997**, *87* (1), 53.
5. Scharber, M. C.; Mühlbacher, D.; Koppe, M.; Denk, P.; Waldauf, C.; Heeger, A. J.; Brabec, C. J., Design Rules for Donors in Bulk-Heterojunction Solar Cells—Towards 10 % Energy-Conversion Efficiency. *Advanced Materials* **2006**, *18* (6), 789-794.
6. (a) Cheng, Y.-J.; Yang, S.-H.; Hsu, C.-S., Synthesis of Conjugated Polymers for Organic Solar Cell Applications. *Chem Rev* **2009**, *109* (11), 5868-5923; (b) Brédas, J.-L.; Beljonne, D.; Coropceanu, V.; Cornil, J., Charge-Transfer and Energy-Transfer Processes in π -Conjugated Oligomers and Polymers: A Molecular Picture. *Chem Rev* **2004**, *104* (11), 4971-5004.
7. Van Mullekom, H.; Vekemans, J.; Havinga, E.; Meijer, E., Developments in the chemistry and bandgap engineering of donor–acceptor substituted conjugated polymers. *Materials Science and Engineering: R: Reports* **2001**, *32* (1), 1-40.
8. Horowitz, G., Organic Field-Effect Transistors. *Advanced Materials* **1998**, *10* (5), 365-377.
9. Lei, T.; Cao, Y.; Fan, Y.; Liu, C. J.; Yuan, S. C.; Pei, J., High-performance air-stable organic field-effect transistors: isoindigo-based conjugated polymers. *Journal of the American Chemical Society* **2011**, *133* (16), 6099-101.
10. Lei, T.; Dou, J.-H.; Ma, Z.-J.; Yao, C.-H.; Liu, C.-J.; Wang, J.-Y.; Pei, J., Ambipolar Polymer Field-Effect Transistors Based on Fluorinated Isoindigo: High Performance and Improved Ambient Stability. *Journal of the American Chemical Society* **2012**, *134* (49), 20025-20028.
11. Cornil, J.; Brédas, J. L.; Zaumseil, J.; Siringhaus, H., Ambipolar transport in organic conjugated materials. *Advanced Materials* **2007**, *19* (14), 1791-1799.
12. Liu, C.; Dong, S.; Cai, P.; Liu, P.; Liu, S.; Chen, J.; Liu, F.; Ying, L.; Russell, T. P.; Huang, F.; Cao, Y., Donor–Acceptor Copolymers Based on Thermally Cleavable Indigo, Isoindigo, and DPP Units: Synthesis, Field Effect Transistors, and Polymer Solar Cells. *ACS Applied Materials & Interfaces* **2015**, *7* (17), 9038-9051.

13. Evenson, S. J.; Rasmussen, S. C., N-Acyldithieno[3,2-b:2',3'-d]pyrroles: Second Generation Dithieno[3,2-b:2',3'-d]pyrrole Building Blocks with Stabilized Energy Levels. *Organic Letters* **2010**, *12* (18), 4054-4057.
14. Deng, P.; Liu, L.; Ren, S.; Li, H.; Zhang, Q., N-acylation: an effective method for reducing the LUMO energy levels of conjugated polymers containing five-membered lactam units. *Chemical Communications* **2012**, *48* (55), 6960-6962.
15. (a) Beaupré, S.; Najari, A.; Leclerc, M., High open-circuit voltage solar cells using a new thieno[3,4-c] pyrrole-4,6-dione based copolymer. *Synthetic Metals* **2013**, *182*, 9-12; (b) Warnan, J.; Cabanetos, C.; Bude, R.; El Labban, A.; Li, L.; Beaujuge, P. M., Electron-Deficient N-Alkyloyl Derivatives of Thieno[3,4-c]pyrrole-4,6-dione Yield Efficient Polymer Solar Cells with Open-Circuit Voltages > 1 V. *Chemistry of Materials* **2014**, *26* (9), 2829-2835.
16. Li, S.; Ma, L.; Hu, C.; Deng, P.; Wu, Y.; Zhan, X.; Liu, Y.; Zhang, Q., N-acylated isoindigo based conjugated polymers for n-channel and ambipolar organic thin-film transistors. *Dyes and Pigments* **2014**, *109*, 200-205.
17. (a) Liu, B.; Zou, Y.; Peng, B.; Zhao, B.; Huang, K.; He, Y.; Pan, C., Low bandgap isoindigo-based copolymers: design, synthesis and photovoltaic applications. *Polym. Chem.* **2011**, *2* (Copyright (C) 2015 American Chemical Society (ACS). All Rights Reserved.), 1156-1162; (b) Zhang, G.; Fu, Y.; Xie, Z.; Zhang, Q., Synthesis and Photovoltaic Properties of New Low Bandgap Isoindigo-Based Conjugated Polymers. *Macromolecules* **2011**, 110204084214089.
18. (a) Stalder, R.; Mei, J.; Reynolds, J. R., Isoindigo-Based Donor-Acceptor Conjugated Polymers. *Macromolecules (Washington, DC, U. S.)* **2010**, *43* (Copyright (C) 2015 American Chemical Society (ACS). All Rights Reserved.), 8348-8352; (b) Xu, X.; Cai, P.; Lu, Y.; Choon, N. S.; Chen, J.; Hu, X.; Ong, B. S., Synthesis and characterization of thieno[3,2-b]thiophene-isoindigo-based copolymers as electron donor and hole transport materials for bulk-heterojunction polymer solar cells. *J. Polym. Sci., Part A: Polym. Chem.* **2013**, *51* (Copyright (C) 2015 American Chemical Society (ACS). All Rights Reserved.), 424-434.
19. Huo, L.; Zhang, S.; Guo, X.; Xu, F.; Li, Y.; Hou, J., Replacing Alkoxy Groups with Alkylthienyl Groups: A Feasible Approach to Improve the Properties of Photovoltaic Polymers. *Angew. Chem., Int. Ed.* **2011**, *50* (Copyright (C) 2015 American Chemical Society (ACS). All Rights Reserved.), 9697-9702, S9697/1-S9697/3.
20. Huo, L.; Hou, J.; Chen, H.-Y.; Zhang, S.; Jiang, Y.; Chen, T. L.; Yang, Y., Bandgap and Molecular Level Control of the Low-Bandgap Polymers Based on 3,6-Dithiophen-2-yl-2,5-dihydropyrrolo[3,4-c]pyrrole-1,4-dione toward Highly Efficient Polymer Solar Cells. *Macromolecules (Washington, DC, U. S.)* **2009**, *42* (Copyright (C) 2015 American Chemical Society (ACS). All Rights Reserved.), 6564-6571.

CHAPTER 6

ISATIN-BASED SMALL MOLECULES FOR ORGANIC PHOTOVOLTAIC MATERIALS



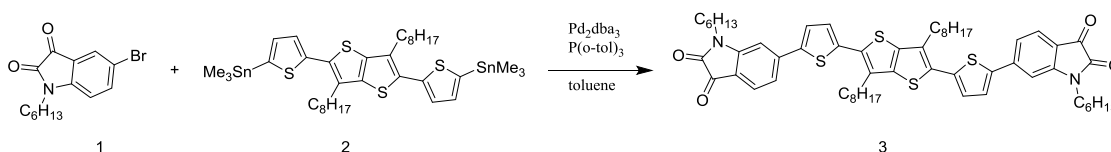
6.1. Introduction

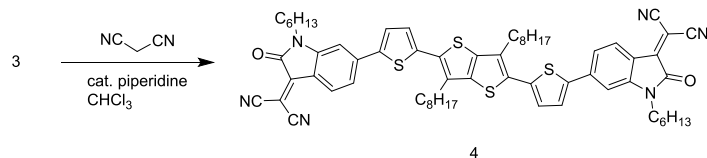
The use of small molecules¹ in the active layer of OPV devices² is gaining interest to expand the field of study which has typically focused on conjugated polymers. The development of donor-acceptor conjugated polymers³ has proven to be an effective strategy to achieve the low bandgaps needed for OPV applications. Through the development of new polymer structures and device engineering of bulk heterojunction solar cells⁴, high efficiencies have been reported. However, the high standard of reproducibility needed for industrial applications is not always possible with the polymers. Variations in molecular weight⁵ and polydispersity among batches can be detrimental to large scale production and device performance. A possible solution to these problems is the use of solution processable donor-acceptor based small molecules⁶, the design of which draws upon previous knowledge gained from their antecedent polymers, as well as push-pull dyes often used for dye-sensitized solar cells⁷. Relatively strong electron accepting units such as benzothiadiazole⁸, diketopyrrolopyrrole⁹, isoindigo¹⁰, and thieno[3,4-*c*]pyrrole-4,6-dione¹¹, are used to increase the electron affinity of the organoelectronic material. Given the demonstrated success of lactam-based acceptors, we sought to develop new A-D-A small molecules which incorporate this motif, utilizing isatin as a new acceptor.

While it is commonly used in conjugated polymers as the precursor to isoindigo, isatin itself has not been studied for organic electronic applications. Its asymmetric structure appears to lend itself well for small molecule engineering which otherwise would not be suitable for polymers. The electron deficient pyrroledione ring can lower the bandgap and its arrangement at the periphery of the molecule will help direct charge transport. Isatin also contains a site for *N*-alkylation which facilitates solubility and self-assembly. We noted that the electrophilic carbonyl of the isatin moiety provided the opportunity for further functionalization, as it is common throughout the literature to create Schiff bases or Knoevenagel condensation products thereof¹². The Knoevenagel condensation with malononitrile is often used in the synthesis of high performing conjugated materials for organoelectronic applications. It can increase the electron affinity of the compound, extend conjugation, and promote the quinoid resonance form¹³. Dicyanovinyl thiophene is a common acceptor end unit, and other variations exist such as 2-(1,1-dicyanomethylene)rhodanine¹⁴ in small molecules, as well as 3-dicyanovinyl-2-quinolone¹⁵ and similar derivatives for dye sensitized solar cells. With these structures in mind, we designed an A- π -D- π -A small molecule with *N*-hexyl isatin as the end group, 3,6-dioctylthieno[3,2-*b*]thiophene as a moderate donor, and thiophene π -spacers to increase conjugation and planarity. We studied the optoelectronic properties of this molecule as well as those after the Knoevenagel condensation of malononitrile on the isatin moiety.

6.2. Results & Discussion

6.2.1. Synthesis





Scheme 6.26. Synthesis of small molecules

Synthesis of the small molecules is illustrated in Scheme 6.1. Compound **3** was synthesized via a Stille cross-coupling reaction with 6-bromo-*N*-hexylisatin **1** and ((3,6-dioctylthieno[3,2-*b*]thiophene-2,5-diyl)bis(thiophene-5,2-diyl))bis(trimethylstannane), compound **2**. After purification by column chromatography, compound **3** was precipitated into methanol and collected by filtration. A portion of compound **3** was used to then synthesize compound **4** under mild conditions. Compound **3** was stirred at room temperature in chloroform with excess malononitrile and a drop of piperidine as a catalyst. Upon the addition of piperidine the reaction solution immediately turned from deep red to dark blue. After completion of the reaction, the product was collected by precipitation into hexanes followed by filtration to yield compound **4** in 87% yield. Both **3** and **4** were soluble in common solvents such as chloroform, chlorobenzene, toluene, and tetrahydrofuran.

6.2.2. Thermal properties

The small molecules had nearly identical T_d for **3** and **4** at 384 °C and 385 °C, respectively, as shown in Figure 6.1.

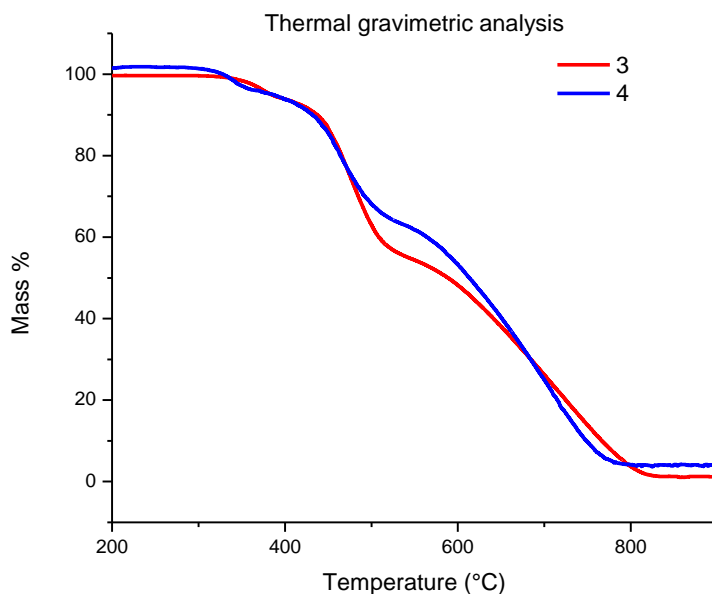


Figure 6.1. TGA of small molecules

6.2.3. Optical properties

The optoelectronic properties are summarized in Table 6.1. The UV-vis spectra, shown in Figure 6.1, show the comparison of the solution and film data for both **3** and **4**. Compound **3** forms a bright red solution and compound **4** dissolves as a deep blue solution, as shown in Figure 6.2, due to their absorption properties. Both compounds have similar molar absorptivities with that of **3** being slightly larger at $43,900 \text{ M}^{-1}\text{cm}^{-1}$ compared to $42,600 \text{ M}^{-1}\text{cm}^{-1}$ for **4**. Compound **3** absorbs mainly from 400 to 600 nm and emits the red portion of the spectrum. Its spectrum features a $\pi \rightarrow \pi^*$ transition peak at 351 nm and a stronger ICT peak at 502 nm. The solution spectrum of **4** exhibits peaks of nearly equal intensity for the $\pi \rightarrow \pi^*$ transition (401 nm) and ICT (616 nm) with a deep valley around 470 nm, which corresponds with the blue emission. Therefore, addition of the dicyanovinylene groups from **3** to **4** overall shifts the absorption by 114 nm, and the large difference is also mostly retained in the film state. The pattern of intensity is largely the same upon shifting from solution to film and both exhibit a bathochromic shift of 49 nm for **3** and 25 nm for

4, due to the increase of crystallinity and planarity in the solid state. This results in an onset of 670 nm for **3** that corresponds to an optical bandgap of 1.85 eV. While the $\pi \rightarrow \pi^*$ peak in the film of **4**, at 417 nm, is slightly larger in intensity, the ICT peak broadens out to an onset value of 827 nm and an bandgap of 1.50 eV, which is 0.35 eV lower upon addition of the dicyanovinyl units. To compare, addition of a dicyanovinyl group to a rhodanine-flanked small molecule resulted in a 0.07 eV bandgap reduction. The large difference here is mostly likely because the dicyanovinyl group is in conjugation with the rest of the molecule so it has an electronic and inductive effect in lowering the bandgap.

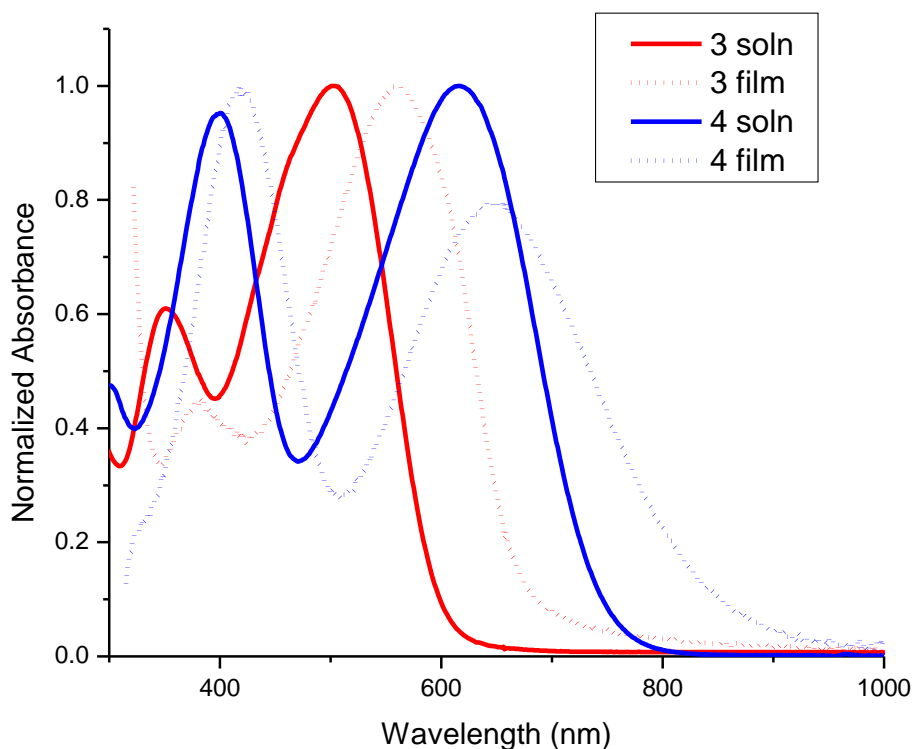


Figure 6.2. UV-vis of **3** and **4** in CHCl_3 solution and film.

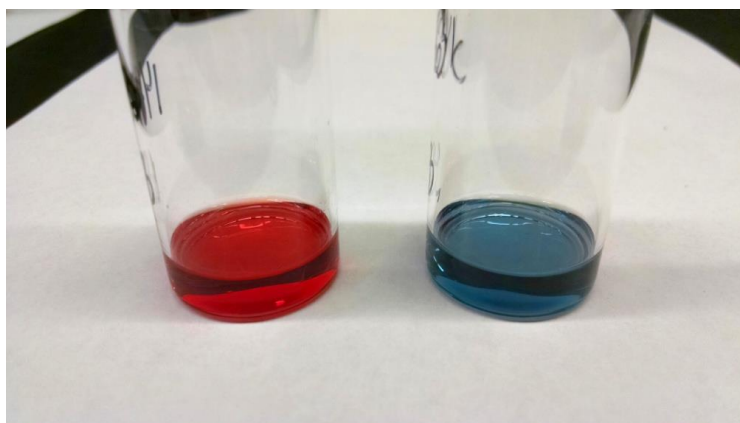


Figure 6.3. Compounds **3** (left) and **4** (right) in chloroform solution.

Table 6.1 Optical and electronic properties of small molecules

Compound	λ_{\max} solution (nm)	λ_{\max} film (nm)	Abs _{onset} (nm)	$\epsilon \times 10^4$ (M ⁻¹ cm ⁻¹)	E_g^{opt} (eV) ^a	$E_{\text{onset}}^{\text{ox}}$ (V) ^b	HOMO ^c (eV)	LUMO ^d (eV)	E_g^{EC} (eV) ^d
3	351, 502	382, 551	670	4.39	1.85	0.81	-5.30	-3.45	1.75
4	401, 616	417, 641	827	4.26	1.50	0.83	-5.32	-3.82	1.28

^a Estimated from the optical absorption edge. ^b Onset of potentials (vs Fc). ^c HOMO = $-(E_{\text{onset}}^{\text{ox}} + 4.8)$ (eV). ^d LUMO = HOMO - E_g^{opt}

6.2.4. Electrochemical properties

The electronic properties of the molecules were investigated by cyclic voltammetry which measures ionization potential and electron affinity and can be correlated to the HOMO and LUMO, respectively. The small molecule was dissolved in a Bu₄NPF₆ electrolyte/dichloromethane solution, and measurements were obtained with an Ag/Ag⁺ reference cell and platinum wire counter electrode with Fc/Fc⁺ for adjustment. The normalized data obtained is shown in Figure 6.3, which shows two nearly identical, reversible oxidation processes that occur up to 1.5V. Upon reduction, **3** exhibits one reversible peak up to -1.5 V and the addition of the dicyanovinyl groups

result in 2 reversible reduction peaks. From the onset of reduction and oxidation, the HOMO and LUMO were calculated and shown in Table 1. **3** and **4** have similar HOMOs of -5.30 and -5.32 eV, respectively, which is within an acceptable range for organic photovoltaic devices to ensure oxidative stability as well as a high V_{oc} . A greater difference among the molecules was observed in the reduction process, with **3** displaying one reversible reduction whereas **4** had two up to the range of -1.5 V. From the onset of reduction the LUMO was calculated to be -3.55 eV for **3** and -4.04 eV for **4**.

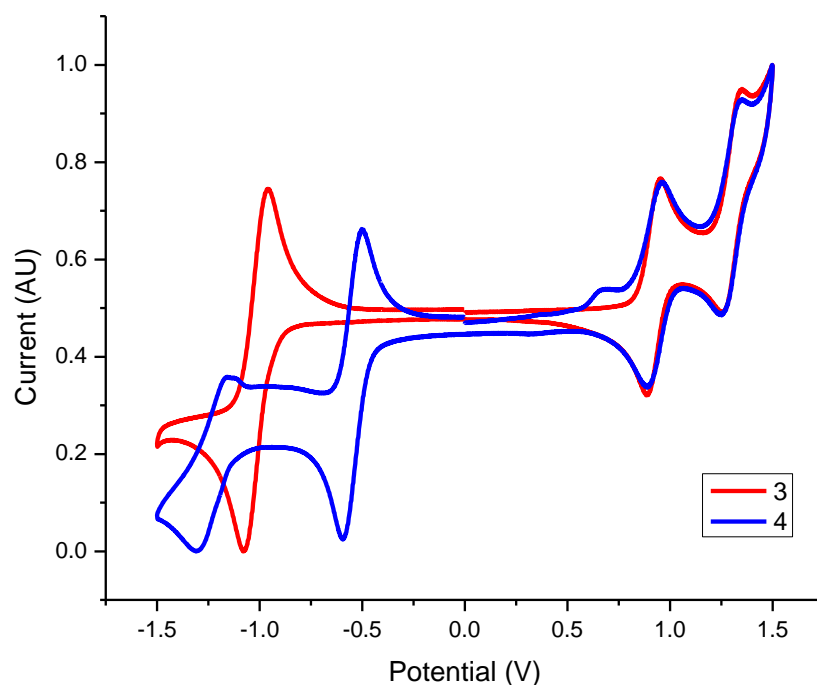


Figure 6.3. Cyclic voltammetry

6.3. Conclusion

In conclusion, novel small molecules based on isatin have been developed. A Knoevenagel condensation, resulting in the dicyanovinyl derivative **4** has been shown to possess excellent

optoelectronic properties and is a promising candidate for high performance OPVs. Fabrication of OPV devices is in progress.

6.4. Acknowledgements

Brandon Kobilka synthesized ((3,6-dioctylthieno[3,2-b]thiophene-2,5-diyl)bis(thiophene-5,2-diyl))bis(trimethylstannane), whereas the author performed all other synthesis and characterization of the small molecules. Benjamin Hale performed thermal analysis studies. The author wrote the text of this chapter.

6.5. Experimental

Characterization

Nuclear magnetic resonance (NMR) spectra were recorded on a Varian MR (400 MHz) or a Bruker Avance III (600 MHz). Spectra were internally referenced to the residual protonated solvent peak. Chemical shifts are given in ppm (δ) relative to the solvent. Absorption spectra were obtained on a photodiode-array Agilent 8453 UV-visible spectrophotometer using sample solutions in CHCl_3 or thin films made by spin-coating 25 x 25 x 1 mm glass slides using solutions of polymer (1-3 mg/mL) in CHCl_3 /chlorobenzene at a spin rate of 1200 rpm on a Headway Research, Inc. PWM32 spin-coater. Cyclic voltammetry was performed using an e-DAQ e-corder 410 potentiostat with a scanning rate of 50 mV/s. Ag/Ag^+ was used as the reference electrode and a platinum wire as the auxiliary electrode. The reported values are referenced to Fc/Fc^+ (-4.8 eV vs. vacuum). Polymer solutions in chlorobenzene (1-2 mg/mL) were drop-cast onto a platinum electrode. Polymer analysis was performed in deoxygenated solutions of 0.1 M tetrabutylammonium hexafluorophosphate electrolyte in CH_3CN under an argon atmosphere.

Small molecule analysis were performed by dissolving 1mg/mL of small molecule sample in 0.1 M tetrabutylammonium hexafluorophosphate in DCM and deoxygenated with argon. Thermal gravimetric analysis (TGA) and differential scanning calorimetry (DSC) measurements were performed with a Netzsch STA449 F1 instrument. TGA were conducted at a heating rate of 20 °C/min under ambient atmosphere.

Materials

Toluene was dried using an Innovative Technology, Inc. solvent purification system. Other reagents were obtained from commercial sources and used without further purification. 6-bromo-1-hexylindoline-2,3-dione¹⁶ and ((3,6-dioctylthieno[3,2-b]thiophene-2,5-diyl)bis(thiophene-5,2-diyl))bis(trimethylstannane)^{11a} were synthesized according to literature procedures.

6,6'-((3,6-Dioctylthieno[3,2-b]thiophene-2,5-diyl)bis(thiophene-5,2-diyl))bis(1-hexylindoline-2,3-dione) (**3**): An oven-dried 3-neck round bottom flask was equipped with a condenser and placed under an argon atmosphere. To the flask was added 5 mL degassed toluene, 6-bromo-1-hexylindoline-2,3-dione (478 mg, 1.54 mmol), ((3,6-dioctylthieno[3,2-b]thiophene-2,5-diyl)bis(thiophene-5,2-diyl))bis(trimethylstannane) (601 mg, 0.7 mmol), Pd₂dba₃ (14 mg, 0.014 mmol), and P(*o*-tol)₃ (17mg, 0.056 mmol). The mixture was heated to 110 °C for 24 h then cooled to room temperature and concentrated by rotary evaporation. The residue was purified by column chromatography with silica gel and chloroform as the eluent. The fraction containing the dark red product was concentrated to 10 mL by rotary evaporation and then precipitated into methanol. The dark purple solid was filtered with a Büchner funnel and dried in a vacuum oven overnight to yield the product (622 mg, 90%). ¹H NMR (600 MHz, Chloroform-d) δ 7.63 (d, J = 7.8 Hz, 1H), 7.51 (d, J = 3.9 Hz, 1H), 7.35 (dd, J = 7.9, 1.4 Hz, 1H), 7.24 (d, J = 3.9 Hz, 1H), 7.06 (d, J = 1.4 Hz,

1H), 3.79 (t, J = 7.3 Hz, 2H), 2.96 (t, J = 6.0 Hz, 2H), 1.85 – 1.77 (m, 2H), 1.77 – 1.68 (m, 2H), 1.49 – 1.40 (m, 4H), 1.40 – 1.33 (m, 6H), 1.33-1.23 (m, 6H), 0.91 (t, J = 7.0 Hz, 3H), 0.87 (t, J = 6Hz, 3H). ¹³C NMR (151 MHz, CDCl₃) δ 14.16, 14.27, 22.68, 22.82, 26.74, 27.51, 29.17, 29.38, 29.49, 29.87, 31.54, 32.03, 40.42, 106.41, 116.50, 120.45, 126.40, 126.83, 127.52, 131.59, 133.05, 139.49, 139.50, 142.43, 143.65, 151.98, 158.93, 182.35. HRMS (APCI): [M+H]⁺ Calcd for C₅₈H₇₀N₂O₄S₄: 987.4291; found 987.4298.

2,2'-(((3,6-dioctylthieno[3,2-b]thiophene-2,5-diyl)bis(thiophene-5,2-diyl))bis(1-hexyl-2-oxoindoline-6-yl-3-ylidene))dimalononitrile (**4**): 6,6'-(((3,6-dioctylthieno[3,2-b]thiophene-2,5-diyl)bis(thiophene-5,2-diyl))bis(1-hexylindoline-2,3-dione) (**3**) (100 mg, 0.1 mmol) and malononitrile (33 mg, 0.5 mmol) were dissolved in 10 mL chloroform at room temperature. One drop of piperidine was added and the solution immediately turned from dark red to dark blue. The solution was stirred overnight and concentrated by rotary evaporation. The residue was passed through a silica gel column with chloroform eluent. The product was concentrated by rotary evaporation and then precipitated into hexane and filtered (94 mg, 87%). ¹H NMR (600 MHz, Chloroform-d) δ 8.12 (d, J = 8.2 Hz, 1H), 7.54 (d, J = 3.9 Hz, 1H), 7.35 (dd, J = 8.3, 1.6 Hz, 1H), 7.25 (d, J = 4.0 Hz, 1H), 7.01 (d, J = 1.6 Hz, 1H), 3.77 (t, J = 7.3 Hz, 2H), 2.95 (t, J = 8.4Hz, 2H), 1.81 (p, J = 7.7 Hz, 2H), 1.73 (p, J = 7.3 Hz, 2H), 1.46 (q, J = 7.9 Hz, 2H), 1.42 – 1.23 (m, 18H), 0.91 (t, J = 7.0 Hz, 3H), 0.88 (t, J = 7.0 Hz, 3H).

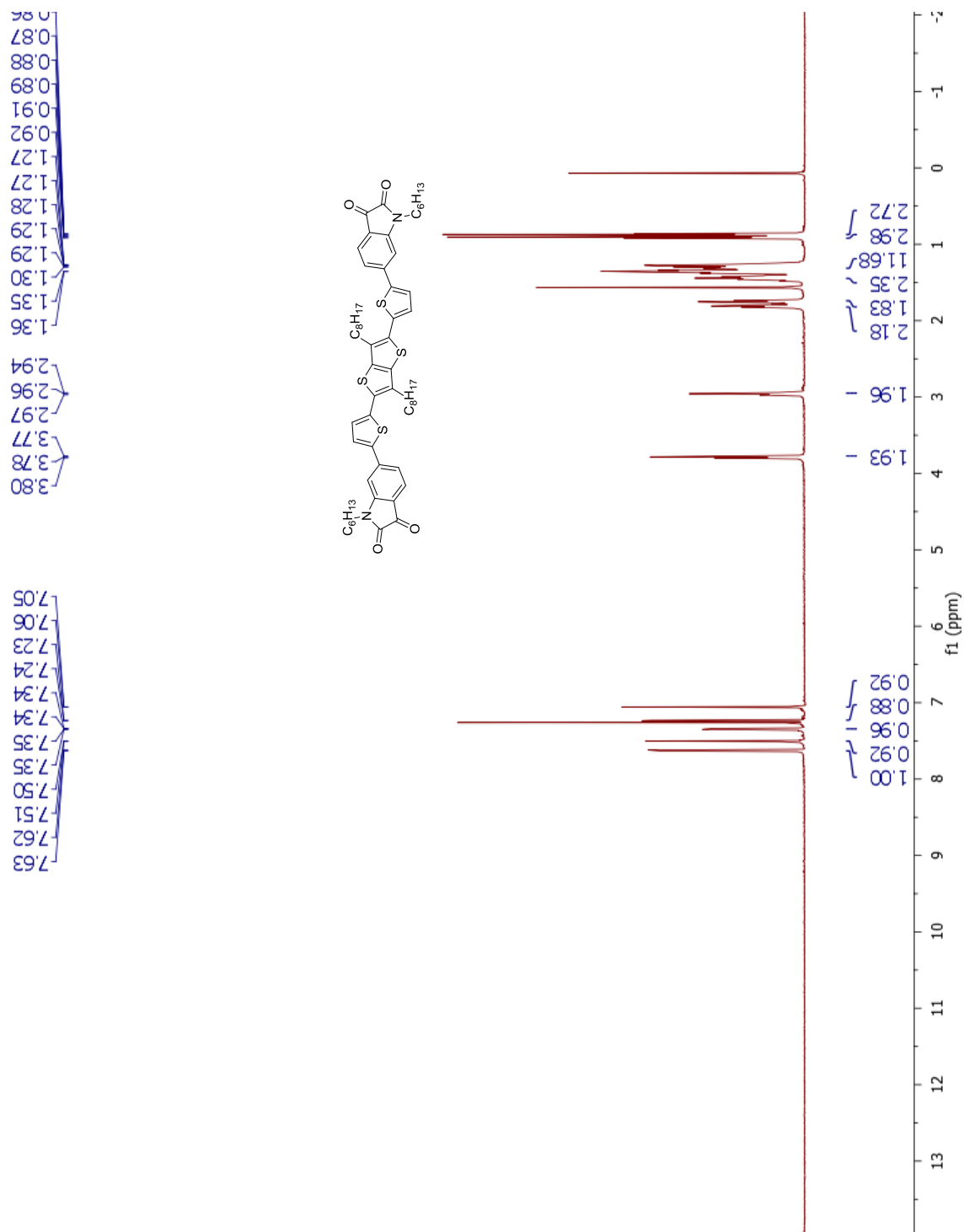


Figure 27. ¹H NMR of 6,6'-((3,6-dioctylthieno[3,2-b]thiophene-2,5-diyl)bis(thiophene-5,2-diyl))bis(1-hexylindoline-2,3-dione) (**3**)

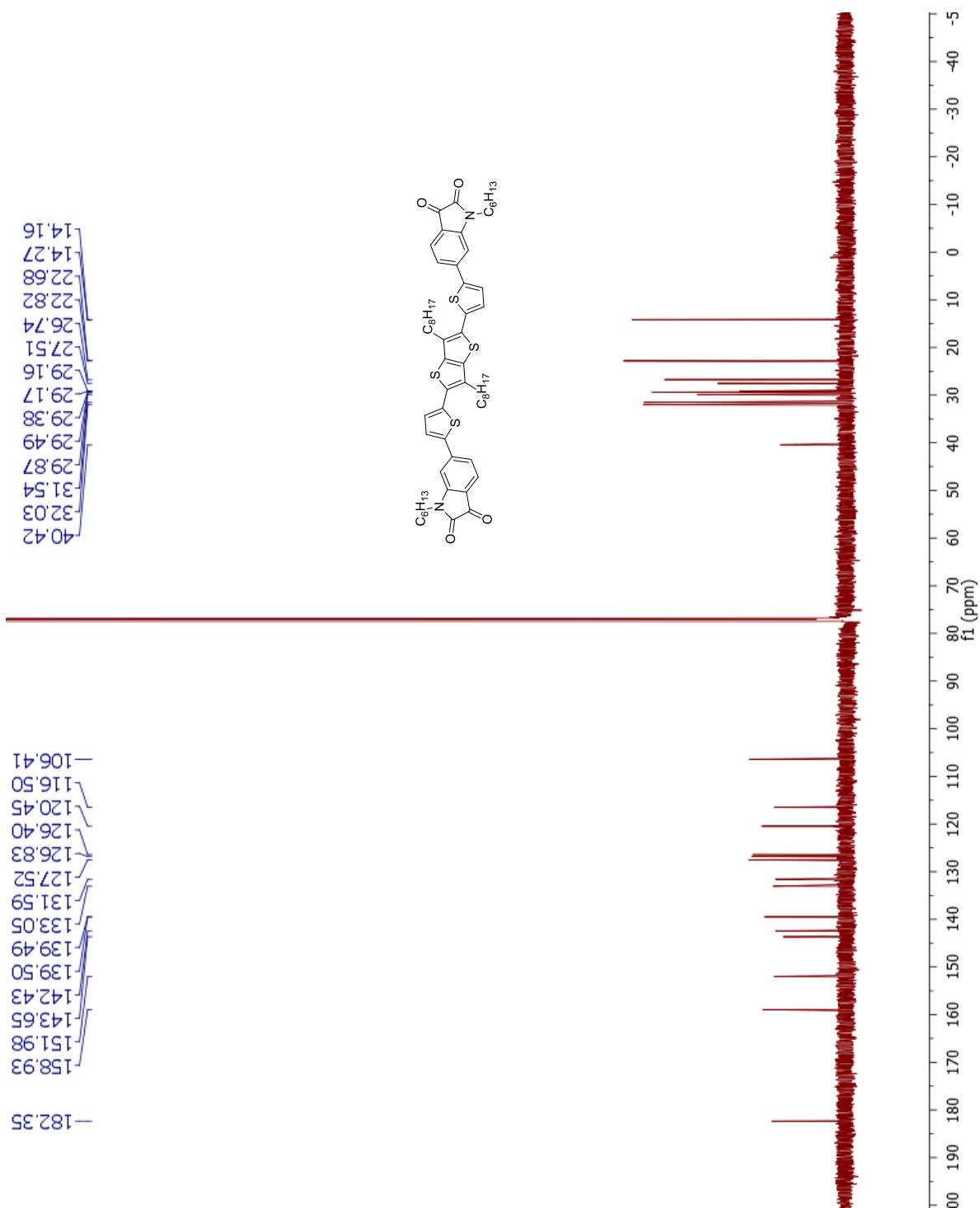


Figure 28. ^1H NMR of 6,6'-((3,6-dioctylthieno[3,2-b]thiophene-2,5-diyl)bis(thiophene-5,2-diyl))bis(1-hexylindoline-2,3-dione) (**3**)

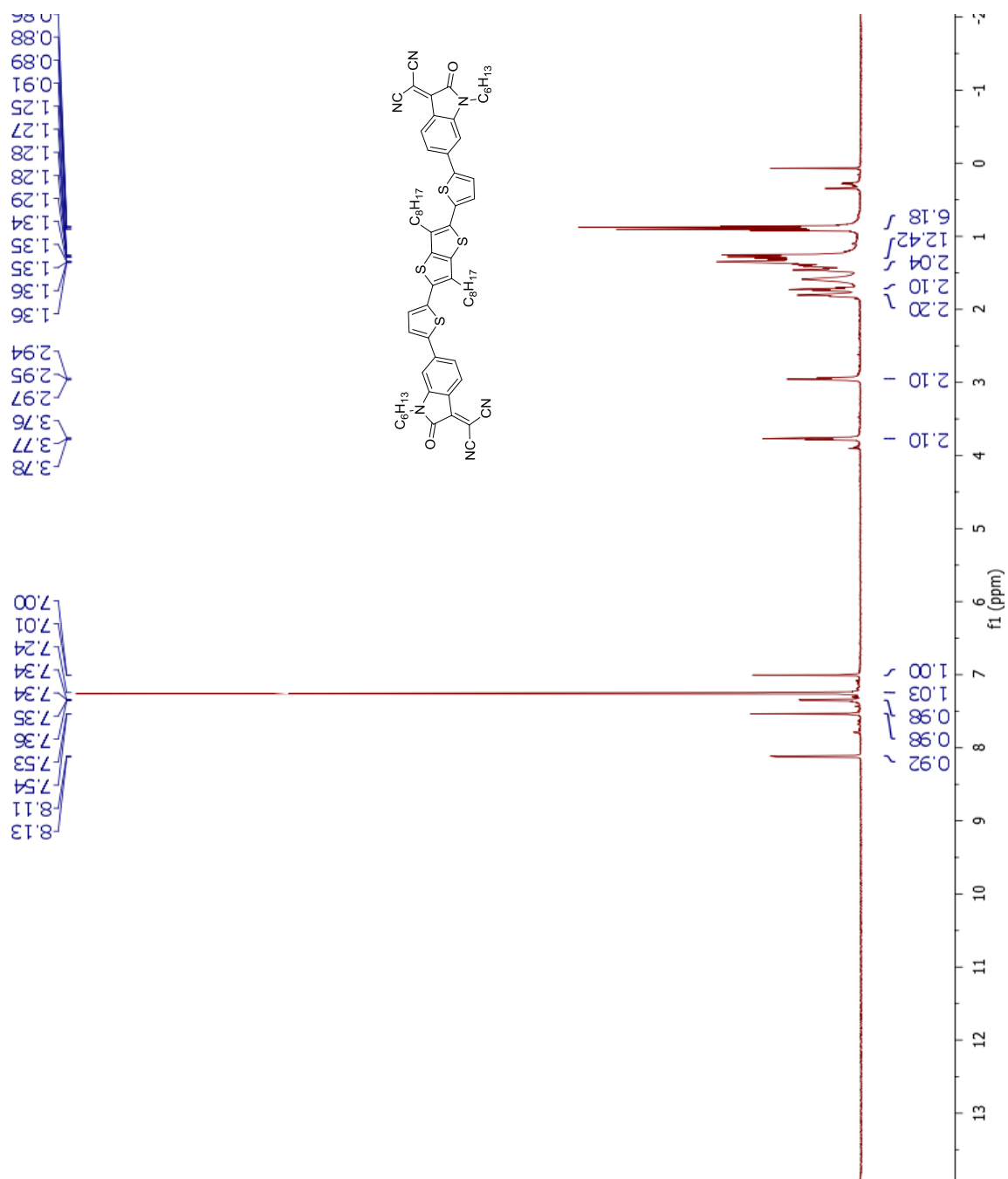


Figure 29. ¹H NMR of 2,2'-(((3,6-dioctylthieno[3,2-b]thiophene-2,5-diyl)bis(thiophene-5,2-diyl))bis(1-hexyl-2-oxindoline-6-yl-3-ylidene))dimalononitrile (**4**)

6.6. References

1. Roncali, J.; Leriche, P.; Blanchard, P., Molecular materials for organic photovoltaics: small is beautiful. *Advanced Materials* **2014**, *26* (23), 3821-3838.
2. (a) Bredas, J.-L.; Durrant, J. R., Organic Photovoltaics. *Accounts of Chemical Research* **2009**, *42* (11), 1689-1690; (b) Darling, S. B.; You, F., The case for organic photovoltaics. *RSC Advances* **2013**, *3* (39), 17633-17648.
3. (a) Havinga, E. E.; ten Hoeve, W.; Wynberg, H., Alternate donor-acceptor small-band-gap semiconducting polymers; Polysquaraines and polycroconaines. *Synthetic metals* **1993**, *55* (1), 299-306; (b) van Mullekom, H. A. M.; Vekemans, J. A. J. M.; Havinga, E. E.; Meijer, E. W., Developments in the chemistry and band gap engineering of donor-acceptor substituted conjugated polymers. *Materials Science and Engineering: R: Reports* **2001**, *32* (1), 1-40; (c) Roncali, J., Molecular Engineering of the Band Gap of π -Conjugated Systems: Facing Technological Applications. *Macromolecular Rapid Communications* **2007**, *28* (17), 1761-1775.
4. Cao, W.; Xue, J., Recent progress in organic photovoltaics: device architecture and optical design. *Energy & Environmental Science* **2014**, *7* (7), 2123-2144.
5. Coffin, R. C.; Peet, J.; Rogers, J.; Bazan, G. C., Streamlined microwave-assisted preparation of narrow-bandgap conjugated polymers for high-performance bulk heterojunction solar cells. *Nat Chem* **2009**, *1* (8), 657-661.
6. (a) Chen, Y.; Wan, X.; Long, G., High performance photovoltaic applications using solution-processed small molecules. *Accounts of chemical research* **2013**, *46* (11), 2645-2655; (b) Lin, Y.; Li, Y.; Zhan, X., Small molecule semiconductors for high-efficiency organic photovoltaics. *Chemical Society Reviews* **2012**, *41* (11), 4245-4272.
7. (a) Grätzel, M., Dye-sensitized solar cells. *Journal of Photochemistry and Photobiology C: Photochemistry Reviews* **2003**, *4* (2), 145-153; (b) Grätzel, M., Perspectives for dye-sensitized nanocrystalline solar cells. *Progress in photovoltaics: research and applications* **2000**, *8* (1), 171-185; (c) Grätzel, M., Solar energy conversion by dye-sensitized photovoltaic cells. *Inorganic chemistry* **2005**, *44* (20), 6841-6851.
8. Hou, J.; Chen, H.-Y.; Zhang, S.; Li, G.; Yang, Y., Synthesis, characterization, and photovoltaic properties of a low band gap polymer based on silole-containing polythiophenes and 2, 1, 3-benzothiadiazole. *Journal of the American Chemical Society* **2008**, *130* (48), 16144-16145.
9. (a) Zhou, E.; Wei, Q.; Yamakawa, S.; Zhang, Y.; Tajima, K.; Yang, C.; Hashimoto, K., Diketopyrrolopyrrole-Based Semiconducting Polymer for Photovoltaic Device with Photocurrent Response Wavelengths up to 1.1 μm . *Macromolecules* **2010**, *43* (2), 821-826; (b) Zhou, E.; Yamakawa, S.; Tajima, K.; Yang, C.; Hashimoto, K., Synthesis and Photovoltaic Properties of Diketopyrrolopyrrole-Based Donor-Acceptor Copolymers. *Chemistry of Materials* **2009**, *21* (17), 4055-4061.
10. (a) Deng, P.; Zhang, Q., Recent developments on isoindigo-based conjugated polymers. *Polymer Chemistry* **2014**, *5* (10), 3298-3305; (b) Stalder, R.; Mei, J.; Graham, K. R.; Estrada, L.

A.; Reynolds, J. R., Isoindigo, a Versatile Electron-Deficient Unit For High-Performance Organic Electronics. *Chemistry of Materials* **2014**, *26* (1), 664-678.

11. (a) Chen, G.-Y.; Cheng, Y.-H.; Chou, Y.-J.; Su, M.-S.; Chen, C.-M.; Wei, K.-H., Crystalline conjugated polymer containing fused 2,5-di(thiophen-2-yl)thieno[2,3-b]thiophene and thieno[3,4-c]pyrrole-4,6-dione units for bulk heterojunction solar cells. *Chemical Communications* **2011**, *47* (17), 5064-5066; (b) Zhang, Y.; Hau, S. K.; Yip, H.-L.; Sun, Y.; Acton, O.; Jen, A. K. Y., Efficient Polymer Solar Cells Based on the Copolymers of Benzodithiophene and Thienopyrroledione. *Chemistry of Materials* **2010**, *22* (9), 2696-2698.

12. (a) Solomon, V. R.; Hu, C.; Lee, H., Hybrid pharmacophore design and synthesis of isatin–benzothiazole analogs for their anti-breast cancer activity. *Bioorganic & Medicinal Chemistry* **2009**, *17* (21), 7585-7592; (b) Taghi Sharbati, M.; Soltani Rad, M. N.; Behrouz, S.; Gharavi, A.; Emami, F., Near infrared organic light-emitting diodes based on acceptor–donor–acceptor (ADA) using novel conjugated isatin Schiff bases. *Journal of Luminescence* **2011**, *131* (4), 553-558; (c) Pandeya, S. N.; Smitha, S.; Jyoti, M.; Sridhar, S. K., Biological activities of isatin and its derivatives. *Acta Pharm* **2005**, *55* (1), 27-46.

13. Wu, Q.; Li, R.; Hong, W.; Li, H.; Gao, X.; Zhu, D., Dicyanomethylene-Substituted Fused Tetrathienoquinoid for High-Performance, Ambient-Stable, Solution-Processable n-Channel Organic Thin-Film Transistors. *Chemistry of Materials* **2011**, *23* (13), 3138-3140.

14. Zhang, Q.; Kan, B.; Liu, F.; Long, G.; Wan, X.; Chen, X.; Zuo, Y.; Ni, W.; Zhang, H.; Li, M., Small-molecule solar cells with efficiency over 9%. *Nature Photonics* **2015**, *9* (1), 35-41.

15. Ganesan, P.; Chandiran, A.; Gao, P.; Rajalingam, R.; Grätzel, M.; Nazeeruddin, M. K., Molecular Engineering of 2-Quinolinone Based Anchoring Groups for Dye-Sensitized Solar Cells. *The Journal of Physical Chemistry C* **2014**, *118* (30), 16896-16903.

16. Karakawa, M.; Aso, Y., Narrow-optical-gap [small pi]-conjugated small molecules based on terminal isoindigo and thienoisindigo acceptor units for photovoltaic application. *RSC Advances* **2013**, *3* (37), 16259-16263.

CHAPTER 7

CONCLUSION

7.1. Conclusion

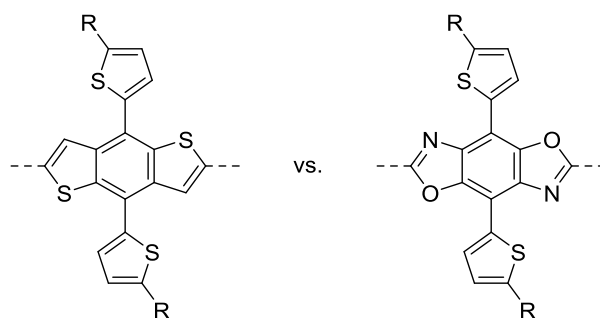
In conclusion, the research in this dissertation has made progress toward development of efficient OPV materials, in both the synthesis of new building blocks and assembly and characterization of macromolecular structures. An emphasis on structure-property relationships rationally developed novel electron accepting units to expand the array of compounds in this field. Facile yet effective synthetic steps were employed to achieve this, such as acylation, Knoevenagel condensations, and incorporation of trifluoromethyl groups. New reactions were studied with transformations of trithioorthoesters, while other synthetic challenges remain to be conquered in the case of asymmetric BBOs. The development of a 2,6-bis(trifluoromethyl)benzobisoxazole represents the pinnacle of BBO materials to date. Other studies, including acyl isoindigo and isatin-based small molecules, established the framework for future materials that have the potential to achieve excellent device performances.

7.2. Future work

New concepts pioneered in this dissertation lead the way for future research in the field of BBOs and acceptor-donor-acceptor small molecules. Studies of structure-property relationships are again the focus of these ideas toward the development of high-performance organic electronics and the following proposals are original ideas of the author of this dissertation.

7.2.1. Two dimensional BBO as a donor monomer for OPV materials

Thoughtful selection of complementary donors and acceptors is important to tune the optoelectronic properties of OPV materials, and a proven strategy is to copolymerize strong acceptors with weak/medium donors¹. This ensures a low bandgap and deep HOMO to maximize light absorption and high V_{oc} ². BBOs have proven to be weak acceptor³ components and Chapter 4 presented a new strategy for improving the electron accepting strength of BBOs by 2,6-substitution of trifluoromethyl groups and polymerization through the 4,8-axis with a moderate donor comonomer. The research of BBO cruciforms by Tlach et al⁴ demonstrated that a unique feature of BBOs is that the HOMO and LUMO are spatially separated in the molecule with the HOMO controlled by substitution of the 4,8-axis and, likewise, the LUMO controlled by the 2,6-axis. This observation provides insights into how to tune the BBO as an acceptor and, similarly, can also be utilized to make BBOs into electron-rich donor monomers.



Scheme 7.11. Structures of BDT and BBO.

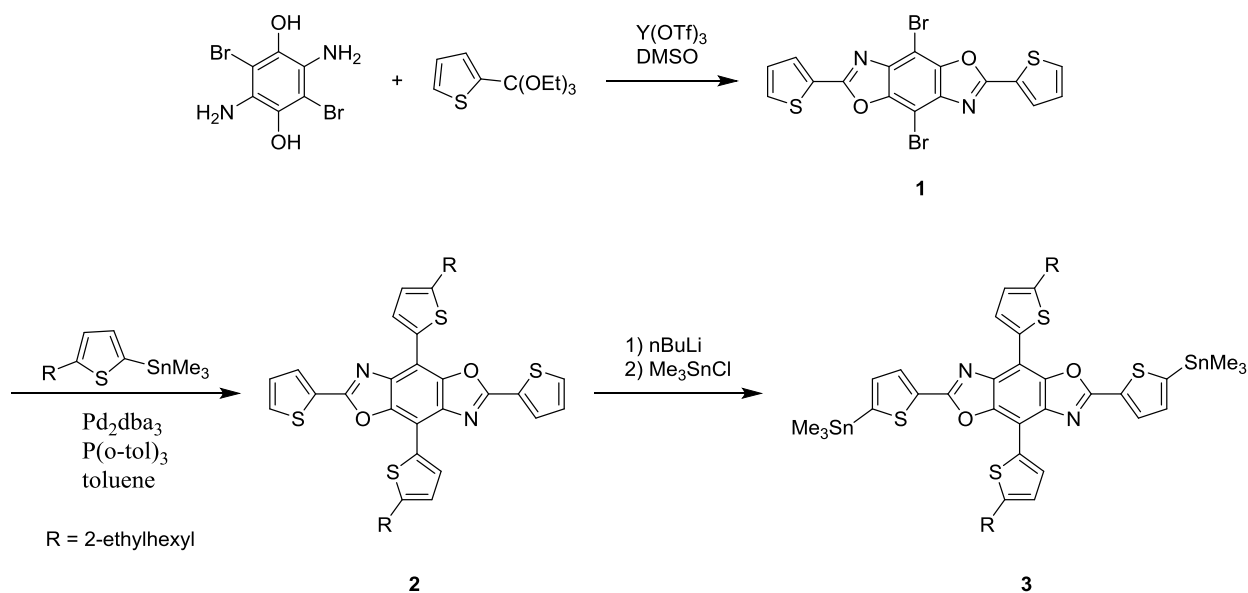
When envisioning how to incorporate BBOs into the family of known donors, a similar synthon emerges: benzo[1,2-b:4,5-b']dithiophene (BDT)⁵ (Scheme 7.1). This popular heteroaromatic species is considered to be a donor of medium strength⁶ and substitution of the 4,8-positions of BDT is accomplished in the course of its synthesis, typically with either 2-ethylhexyloxy or alkylthienyl⁷ groups, though other variations have been studied. The extra thiophene rings increase

the conjugation, hole mobility, and external quantum efficiency of the compound while having little impact on the HOMO level when compared to the alkoxy derivative. A deep HOMO is required for improved device performance, and to that end variations of BDT have been evaluated such as changing the aromatic side groups from thienyl to phenyl⁸, while another approach can involve altering the heteroatoms of the aromatic core.

The BDT-T unit is structurally similar to the BBO cruciforms and small molecules that have been studied in our group, and a direct comparison of the BBO and BDT monomers can be conducted for the purpose of developing BBO for a new donor role. The use of benzobisazoles as donors has been studied by Jenekhe⁹ with the sulfur analog, benzobisthiazole (BBTZ), wherein polymerization with diketopyrrolopyrrole resulted in a “weak donor/strong acceptor” copolymer. Variations of the polymer with different acceptors by Seki, et al, further increased the OPV performance¹⁰.

Our group has studied the optoelectronic effects when varying BBO or BBTZ as acceptors in a conjugated polymer^{3c} and shown that it has little impact on the energy levels or OPV performance. However, the smaller radii of the heteroatoms in BBO compared to BBTZ or BDT will significantly increase the planarity of two-dimensional conjugated structures. The dihedral angle between the thiophene side group and BDT core has been calculated to be 53°¹¹ and the BBO derivative will reduce steric strain for improved orbital overlap and charge transfer. The lower aromaticity and electron density of the oxazole ring¹² compared to thiophene should make BBO a weaker donor than BDT, with the potential to produce narrow bandgap donor-acceptor copolymers with a lower HOMO and therefore higher V_{oc} . Controlled experiments should be conducted by synthesizing polymers with variation of the BDT or BBO core and evaluating their physical and optoelectronic properties as well as their performance in solar cells.

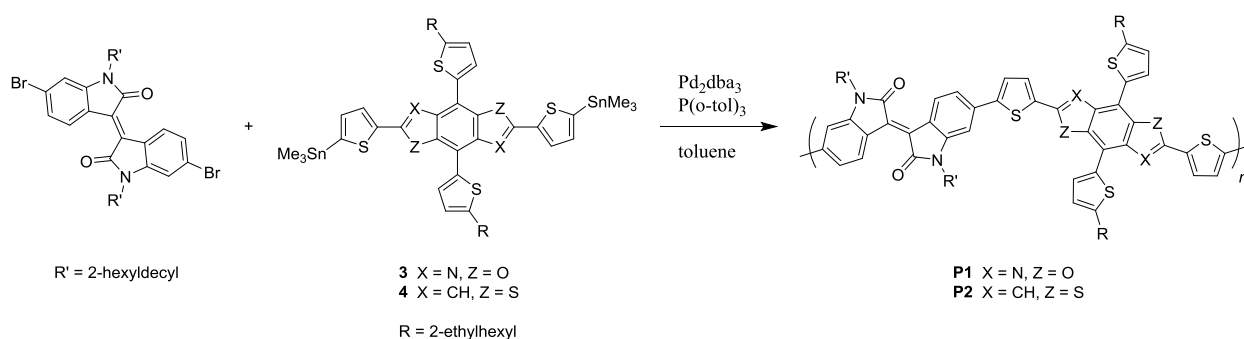
Fabrication of the BBO core, as shown in Scheme 7.2, requires synthesis of compound **1**, a 4,8-dibromoBBO with 2,6-thienyl substituents which in this case will act as pi spacers in the polymer. The thienyl groups are necessary at this point in the synthesis because, to date, there is no known method of synthesizing a BBO with either stannyl or halide substituents at the 2,6-positions to enable Stille couplings. The insolubility of **1** seemingly limits its synthetic value, yet our group has demonstrated that nevertheless a Stille cross coupling can be performed, resulting in intermediate **2**. Lastly, the flanking thiophenes can be stannylated to afford the final monomer **3** for polymerization through the 2,6-axis. Synthesis of the BDT analog **4** is plentiful throughout the literature.



Scheme 7.12. Synthesis of BBO monomer.

A strong acceptor must be chosen as the comonomer. Among the choices are benzothiadiazole¹³, diketopyrrolopyrrole (DPP)¹⁴, and isoindigo¹⁵. Benzothiadiazole is eliminated as a contender because it lacks the possibility of adding solubilizing chains. Although DPP can be alkylated, it was not chosen to avoid redundancy of the pi spacers. Flanking thiophene pi spacers

are built-in components of this monomer, and this unit was already present in the donor portion. Therefore, 5,5'-dibromoisoidigo is a practical choice, and it should be alkylated with long branched aliphatic chains (2-hexyldecyl or longer) to ensure solubility of the polymer (Scheme 7.3).



Scheme 7.13. Synthesis of BBO and BDT polymers.

The rational design of this copolymer with a two-dimensional BBO as a weak donor should lead to good efficiencies, conclusions which can be drawn by comparison to its BDT counterpart.

7.2.2. Introducing benzobisoxazinone as an electron accepting monomer for OPV materials

The Jeffries-EL group has extensively studied BBOs as an electron accepting monomer for organic semiconducting materials. The trithioorthoester condensation method discussed Chapter 2 of this dissertation developed a mild method for synthesizing novel orthoesters and successfully yielded other heterocycles such as benzoxazoles, benzoxazines, and benzoxazinones. The orthoester condensation method developed by J. Mike¹⁶, et al, has enabled the synthesis of a large family of benzobisoxazole polymers and small molecules, yet BBOs remain to be weak electron acceptors when incorporated into a polymer through their 2,6-axis. In an effort to improve their electron accepting strength, Chapter 4 of this dissertation demonstrates that introduction of

trifluoromethyl groups at the 2,6-positions and polymerization through the alternate 4,8-axis can lower the LUMO of the polymer, leading the way to narrow bandgap materials. Analysis of the similarities between the benzoxazole and benzoxazinone synthesized in Chapter 2 provides inspiration for another approach presented herein. A structural variation related to the BBO core is proposed, introducing a new heterocycle for organoelectronic studies: benzobisoxazinone (BBX).

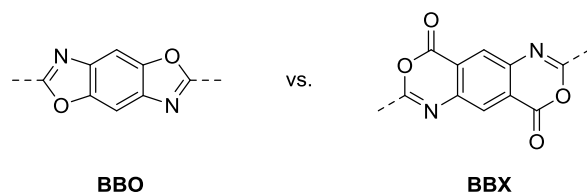


Figure 7.30. Comparison of BBO and BBX moieties.

The BBX is related to benzoxazine in the same way that BBO is related to a benzoxazole, with the heterocyclic ring attached to both sides of the core benzene ring (Figure 7.30), resulting in a symmetric species. While BBO is an aromatic compound, the introduction of the ester into the heterocycle breaks aromaticity but contributes a stronger electron accepting character to the unit. A survey of strong acceptors reveals that carbonyl groups are a common feature, such as in the popular units diketopyrrolopyrrole¹⁴ and isoindigo^{15b}. Rather than being a fused tricyclic aromatic like BBO, the BBX can be thought of as a para-phenylene vinylene derivative with linking carbonyl substituents to impart planarity and electronic effects (see Figure 7.31). As such, BBX should attain status as a strong electron acceptor.

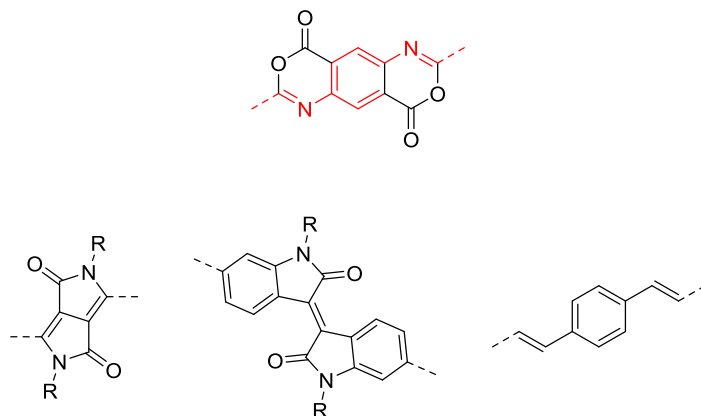
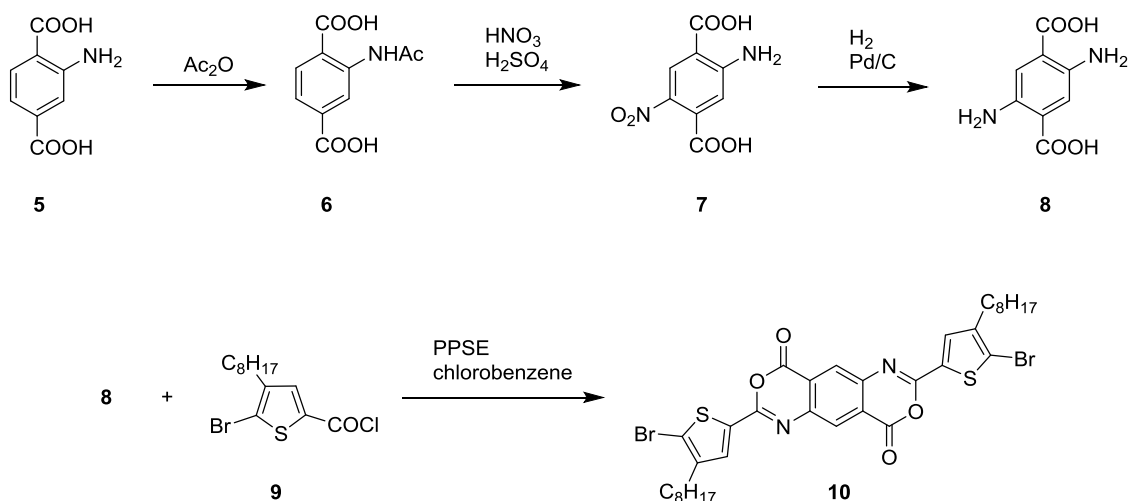


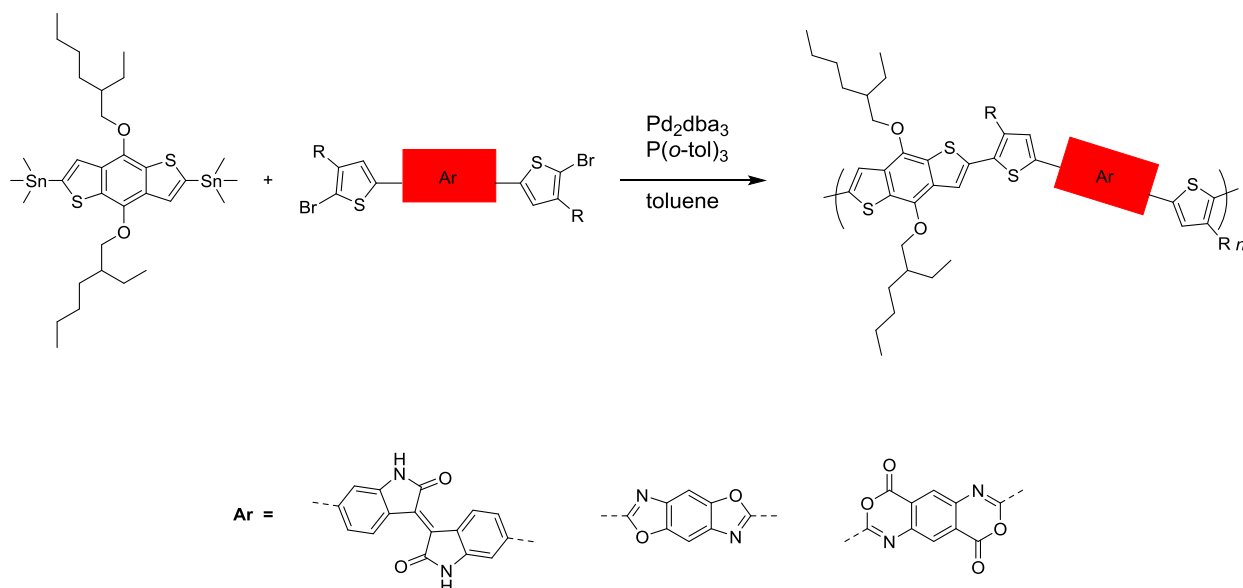
Figure 7.31. BBX bears structural similarities to other electron acceptors and para-phenylene vinylene.

Synthesis of a BBX has been reported once by Skibo & Gilchrist¹⁷ and a route toward its formation is outlined below in Scheme 7.14, beginning from the commercially available 2-aminoterephthalic acid (**5**). Acylation of **5** followed by nitration and reduction according to literature procedures affords 2,5-diaminoterephthalic acid (**8**) as the core starting material. After that, a one-step condensation is expected to yield the BBX, as demonstrated by compound **10**. Since benzoxazinones are known to be synthesized from acid chlorides¹⁸, it was chosen for this example to use an acid chloride in a PPSE solution to accomplish the ring closure. This method is often used for the synthesis of BBOs, but an orthoester condensation with catalytic $Y(OTf)_3$ is also popular and certainly these conditions could also be applied toward the synthesis of a BBX.



Scheme 7.14. Synthesis of BBX monomer.

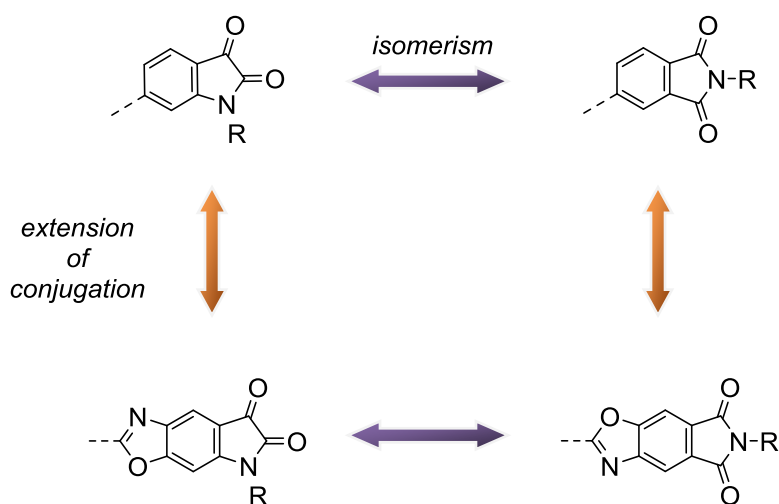
The condensation **9** with **10** yields a polymerizable pi-acceptor-pi monomer in one step, and the alkyl chains on the thiophene ensure solubility of this large pi system. At this point a donor comonomer can be selected and polymerization can be conducted via an appropriate cross-coupling reaction, such as Stille or Suzuki.



Scheme 7.15. Synthesis of donor acceptor copolymers with DPP, BBO, and BBX acceptors.

To gauge the accepting strength of the new BBX unit, side by side comparisons should also be made with BBO, and perhaps a known strong acceptor bearing some resemblance to the unit, such as the aforementioned DPP or isoindigo (Scheme 7.15). Polymers shall be synthesized with the same donor, such as 4,8-bis(2-ethylhexyloxy)BDT for example, with the only alteration being among the acceptor. Comparison of the bandgap and position of the LUMO will determine the strength of the BBX. Differences in OPV performance can be expected as well, as the morphology of the polymers could be drastically different due to their structural differences, and as a result OPV performance characteristics like J_{sc} can vary. With this format it will be possible to identify what molecular properties influence these results to gain understanding of the promising new BBX unit.

7.2.3. Oxazolophthalimide and oxazoloisatin as acceptors for solution-processable small molecule OPV materials



Chapter 6 of this dissertation introduced isatin as an acceptor moiety to the field of organic electronics by studying its properties when incorporated into an acceptor-donor-acceptor small molecule for OPV purposes. Despite the presence of two electron-withdrawing carbonyl groups, the isatin-containing small molecule had a somewhat high, yet respectable, bandgap of 1.85 eV.

Incorporation of a dicyanovinyl group by condensation of malononitrile yielded a new small molecule a greatly reduced bandgap of 1.50 eV. The following details further studies to explore isatin and related molecules as acceptor end groups to understand the role of isomerism upon the properties of the material, and offers novel compounds based on structural variations intended to enhance their semiconducting properties.

7.2.3.1. Isatin vs. phthalimide

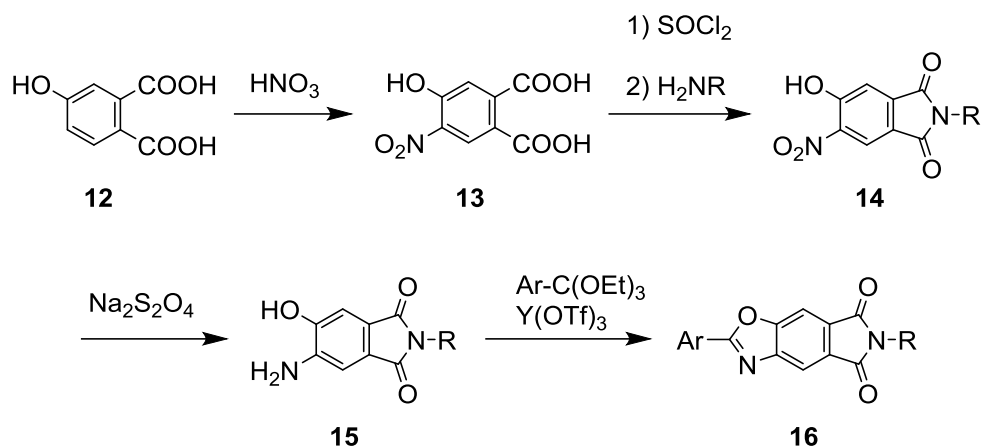
Isatin is a constitutional isomer of another electron accepting unit, phthalimide. This imide has been studied for OPV purposes in both polymers¹⁹ and small molecules^{19c, 20} and demonstrated to result in polymers with good morphology and charge transport while retaining p-type character which can be lost when the monomer is a related imide compound such as naphthalene diimide or perylene diimide²¹. To ascertain the properties of isatin as an end group, it is proposed herein to synthesize acceptor-donor-acceptor small molecules each with either isatin or phthalimide as the acceptor. Though they appear similar, the isomerism is expected to impart different effects on the optoelectronic properties and a structure-property study with these molecules has not been conducted. Given that phthalimide has two carbonyl groups directly bonded to the benzene ring, whereas isatin does not, it could be estimated that phthalimide is a stronger electron acceptor and therefore its small molecule would possess a greater electron affinity.

Another factor to consider is the morphology of the small molecules, as optimization of this parameter has a large impact on the performance of a device. Both isatin and phthalimide can be *N*-alkylated for solubility, but the orientation of these chains would be different. For isatin the chains would point along the backbone of the small molecule in the same direction as chains on other units of the molecule, while for phthalimide they would be oriented outward from each end of the backbone, resulting in different self assembled formations and different hole mobilities²².

7.2.3.2. Oxazolo derivatives

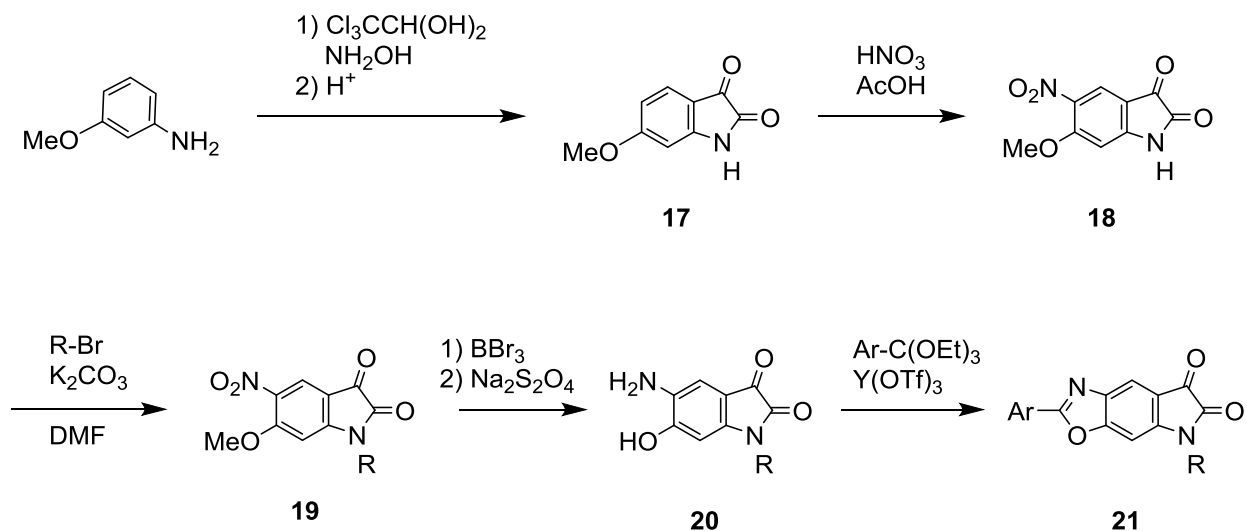
After the initial study on the effects of isomerism to provide baseline information, new molecules based on isatin and phthalimide can be synthesized and evaluated. The proposed structures expand the unit by fusing oxazole rings to the aromatic core of each unit. This electron-deficient aromatic unit is expected to increase the electron affinity of the molecule, while imparting other beneficial effects known to occur from fused ring systems: pi stacking to facilitate charge transport, planarity, and increased molar absorptivity. Connection to the rest of the small molecule through the 2-position of the oxazole ring will also alter the orientation of the acceptor unit in the small molecule in relation to their parent compounds, resulting in altered morphology. Synthesis of each oxazolo derivative is detailed below.

Synthesis of the oxazolophthalimide begins with nitration of 4-hydroxyphthalic acid, as shown in Scheme 7.6. The diacid is ring closed to the imide (**14**) by SOCl_2 and an alkylamine, a standard route to phthalimides. The nitro group is reduced, in this example with sodium dithionite, to yield the main oxazolo precursor **15**. At this point the oxazole ring can be formed with a desired aryl group, shown here as an orthoester condensation, though many other methods of oxazole formation are available in the literature as well. Most likely the Ar- group would be a thiophene pi-spacer which can be brominated and then cross coupled to the donor component of the small molecule.



Scheme 7.6. Synthesis of oxazolophthalimide.

The isatin version is synthesized (Scheme 7.7) by first forming a substituted isatin. The Sandmeyer isatin synthesis²³ is performed with 3-aminophenol, chloral hydrate, and hydroxylamine under acidic conditions to yield 6-hydroxyisatin (**17**). This is then nitrated, *N*-alkylated for solubility and demethylation followed by reduction of the nitro group results in the final aromatic core (**20**) which can be ring closed in a similar fashion as above to yield the oxazoloisatin **22**.



Scheme 7.7. Synthesis of oxazoloisatin.

Characterization of the small molecules containing these new acceptors and their device performance will be conducted in the usual way to determine the effect of this extended conjugation. It is expected that they will display greater efficiencies when compared to their parent compounds from the previous section.

7.3. Acknowledgements

I gratefully acknowledge those who have helped to support this achievement. I am thankful for the support of my family through the years by gently encouraging my academic interests. My fiancé, Nick, has done an excellent job helping me deal with the challenges of grad school, and without whom I could not have accomplished this.

I am thankful for the excellent teachers I through the years that fostered a strong interest in science, like my high school chemistry teacher Mr. Hansen whose enthusiasm for science made me aspire to attain this knowledge too. My college professors, Dr. Charles Cornett and Dr. Tim Zauche in particular, helped me understand what it meant to think like a chemist and helped me believe I could succeed in graduate school. A special thank you to my graduate advisor, Dr. Malika Jeffries-EL, for helping me to develop the creativity, independence, and skills of a research chemist. Thank you to the past members of the Jeffries-EL group who were excellent mentors and helped me better understand the scientific content and lab techniques to achieve such research. To James Klimavicz and Kirsten Johnson, my colleagues and friends, I am grateful for your support and for our “group meetings” where many innovative new research ideas were developed.

7.4. References

1. (a) Cheng, Y.-J.; Yang, S.-H.; Hsu, C.-S., Synthesis of Conjugated Polymers for Organic Solar Cell Applications. *Chem Rev* **2009**, *109* (11), 5868-5923; (b) Zhou, H.; Yang, L.;

- Stoneking, S.; You, W., A Weak Donor–Strong Acceptor Strategy to Design Ideal Polymers for Organic Solar Cells. *ACS Applied Materials & Interfaces* **2010**, *2* (5), 1377-1383.
2. Scharber, M. C.; Mühlbacher, D.; Koppe, M.; Denk, P.; Waldauf, C.; Heeger, A. J.; Brabec, C. J., Design Rules for Donors in Bulk-Heterojunction Solar Cells—Towards 10 % Energy-Conversion Efficiency. *Advanced Materials* **2006**, *18* (6), 789-794.
 3. (a) Ahmed, E.; Subramaniyan, S.; Kim, F. S.; Xin, H.; Jenekhe, S. A., Benzobisthiazole-Based Donor–Acceptor Copolymer Semiconductors for Photovoltaic Cells and Highly Stable Field-Effect Transistors. *Macromolecules* **2011**, *44* (18), 7207-7219; (b) Klimavicz, J. S.; Mike, J. F.; Bhuwarka, A.; Tomlinson, A. L.; Jeffries-EL, M., Synthesis of benzobisoxazole-based D- π -A- π -D organic chromophores with variable optical and electronic properties. *Pure and Applied Chemistry* **2012**, *84* (4), 991-1004; (c) Bhuwarka, A.; Mike, J. F.; He, M.; Intemann, J. J.; Nelson, T.; Ewan, M. D.; Roggers, R. A.; Lin, Z.; Jeffries-El, M., Quaterthiophene–Benzobisazole Copolymers for Photovoltaic Cells: Effect of Heteroatom Placement and Substitution on the Optical and Electronic Properties. *Macromolecules* **2011**, *44* (24), 9611-9617.
 4. Tlach, B. C.; Tomlinson, A. L.; Ryno, A. G.; Knoble, D. D.; Drochner, D. L.; Krager, K. J.; Jeffries-El, M., Influence of Conjugation Axis on the Optical and Electronic Properties of Aryl-Substituted Benzobisoxazoles. *The Journal of Organic Chemistry* **2013**, *78* (13), 6570-6581.
 5. Hou, J.; Park, M.-H.; Zhang, S.; Yao, Y.; Chen, L.-M.; Li, J.-H.; Yang, Y., Bandgap and molecular energy level control of conjugated polymer photovoltaic materials based on benzo [1, 2-b: 4, 5-b'] dithiophene. *Macromolecules* **2008**, *41* (16), 6012-6018.
 6. Zhang, Z.-G.; Wang, J., Structures and properties of conjugated Donor-Acceptor copolymers for solar cell applications. *Journal of Materials Chemistry* **2012**, *22* (10), 4178-4187.
 7. (a) Huo, L.; Hou, J.; Zhang, S.; Chen, H. Y.; Yang, Y., A Polybenzo [1, 2-b: 4, 5-b'] dithiophene Derivative with Deep HOMO Level and Its Application in High-Performance Polymer Solar Cells. *Angewandte Chemie International Edition* **2010**, *49* (8), 1500-1503; (b) Huo, L.; Zhang, S.; Guo, X.; Xu, F.; Li, Y.; Hou, J., Replacing Alkoxy Groups with Alkylthienyl Groups: A Feasible Approach to Improve the Properties of Photovoltaic Polymers. *Angew. Chem., Int. Ed.* **2011**, *50* (Copyright (C) 2015 American Chemical Society (ACS). All Rights Reserved.), 9697-9702, S9697/1-S9697/3.
 8. Dou, L.; Gao, J.; Richard, E.; You, J.; Chen, C.-C.; Cha, K. C.; He, Y.; Li, G.; Yang, Y., Systematic investigation of benzodithiophene-and diketopyrrolopyrrole-based low-bandgap polymers designed for single junction and tandem polymer solar cells. *Journal of the American Chemical Society* **2012**, *134* (24), 10071-10079.
 9. Subramaniyan, S.; Kim, F. S.; Ren, G.; Li, H.; Jenekhe, S. A., High Mobility Thiazole–Diketopyrrolopyrrole Copolymer Semiconductors for High Performance Field-Effect Transistors and Photovoltaic Devices. *Macromolecules* **2012**, *45* (22), 9029-9037.
 10. (a) Tsuji, M.; Saeki, A.; Koizumi, Y.; Matsuyama, N.; Vijayakumar, C.; Seki, S., Benzobisthiazole as weak donor for improved photovoltaic performance: microwave

conductivity technique assisted molecular engineering. *Advanced Functional Materials* **2014**, *24* (1), 28-36; (b) Gopal, A.; Saeki, A.; Ide, M.; Seki, S., Fluorination of Benzothiadiazole–Benzobisthiazole Copolymer Leads to Additive-Free Processing with Meliorated Solar Cell Performance. *ACS Sustainable Chemistry & Engineering* **2014**, *2* (11), 2613-2622.

11. Du, Z.; Chen, W.; Chen, Y.; Qiao, S.; Bao, X.; Wen, S.; Sun, M.; Han, L.; Yang, R., High efficiency solution-processed two-dimensional small molecule organic solar cells obtained via low-temperature thermal annealing. *Journal of Materials Chemistry A* **2014**, *2* (38), 15904-15911.

12. Horner, K. E.; Karadakov, P. B., Shielding in and around Oxazole, Imidazole, and Thiazole: How Does the Second Heteroatom Affect Aromaticity and Bonding? *The Journal of Organic Chemistry* **2015**, *80* (14), 7150-7157.

13. Hou, J.; Chen, H.-Y.; Zhang, S.; Li, G.; Yang, Y., Synthesis, characterization, and photovoltaic properties of a low bandgap polymer based on silole-containing polythiophenes and 2, 1, 3-benzothiadiazole. *Journal of the American Chemical Society* **2008**, *130* (48), 16144-16145.

14. Qu, S.; Tian, H., Diketopyrrolopyrrole (DPP)-based materials for organic photovoltaics. *Chemical Communications* **2012**, *48* (25), 3039-3051.

15. (a) Deng, P.; Zhang, Q., Recent developments on isoindigo-based conjugated polymers. *Polymer Chemistry* **2014**, *5* (10), 3298-3305; (b) Stalder, R.; Mei, J.; Graham, K. R.; Estrada, L. A.; Reynolds, J. R., Isoindigo, a Versatile Electron-Deficient Unit For High-Performance Organic Electronics. *Chemistry of Materials* **2014**, *26* (1), 664-678.

16. Mike, J. F.; Makowski, A. J.; Jeffries-El, M., An Efficient Synthesis of 2,6-Disubstituted Benzobisoxazoles: New Building Blocks for Organic Semiconductors. *Organic Letters* **2008**, *10* (21), 4915-4918.

17. Skibo, E. B.; Gilchrist, J. H., Synthesis and electrochemistry of pyrimidoquinazoline-5,10-diones. Design of hydrolytically stable high potential quinones and new reductive alkylation systems. *J. Org. Chem.* **1988**, *53* (Copyright (C) 2015 American Chemical Society (ACS). All Rights Reserved.), 4209-18.

18. Shcherbakova, I.; Balandrin, M. F.; Fox, J.; Ghatak, A.; Heaton, W. L.; Conklin, R. L., 3H-Quinazolin-4-ones as a new calcilytic template for the potential treatment of osteoporosis. *Bioorg. Med. Chem. Lett.* **2005**, *15* (Copyright (C) 2015 American Chemical Society (ACS). All Rights Reserved.), 1557-1560.

19. (a) Chen, J.; Shi, M.-M.; Hu, X.-L.; Wang, M.; Chen, H.-Z., Conjugated polymers based on benzodithiophene and arylene imides: Extended absorptions and tunable electrochemical properties. *Polymer* **2010**, *51* (13), 2897-2902; (b) Guo, X.; Kim, F. S.; Jenekhe, S. A.; Watson, M. D., Phthalimide-Based Polymers for High Performance Organic Thin-Film Transistors. *Journal of the American Chemical Society* **2009**, *131* (21), 7206-7207; (c) Zhang, G.; Fu, Y.; Zhang, Q.; Xie, Z., Synthesis and Photovoltaic Properties of Conjugated Copolymers with Benzo[1,2-b:4,5-b']dithiophene and Bis(thiophene)phthalimide Units. *Macromolecular Chemistry and Physics* **2010**, *211* (24), 2596-2601.

20. (a) Bloking, J. T.; Han, X.; Higgs, A. T.; Kastrop, J. P.; Pandey, L.; Norton, J. E.; Risko, C.; Chen, C. E.; Brédas, J.-L.; McGehee, M. D.; Sellinger, A., Solution-Processed Organic Solar Cells with Power Conversion Efficiencies of 2.5% using Benzothiadiazole/Imide-Based Acceptors. *Chemistry of Materials* **2011**, *23* (24), 5484-5490; (b) Li, W.; Wu, Y.; Zhang, Q.; Tian, H.; Zhu, W., D-A- π -A Featured Sensitizers Bearing Phthalimide and Benzotriazole as Auxiliary Acceptor: Effect on Absorption and Charge Recombination Dynamics in Dye-Sensitized Solar Cells. *ACS Applied Materials & Interfaces* **2012**, *4* (3), 1822-1830.
21. (a) Chen, D.; Zhao, Y.; Zhong, C.; Gao, S.; Yu, G.; Liu, Y.; Qin, J., Effect of polymer chain conformation on field-effect transistor performance: synthesis and properties of two arylene imide based D-A copolymers. *Journal of Materials Chemistry* **2012**, *22* (29), 14639-14644; (b) Tatemichi, S.; Ichikawa, M.; Koyama, T.; Taniguchi, Y., High mobility n-type thin-film transistors based on N, N'-ditridecyl perylene diimide with thermal treatments. *Applied physics letters* **2006**, *89* (11), 2108; (c) Usta, H.; Facchetti, A.; Marks, T. J., Air-Stable, Solution-Processable n-Channel and Ambipolar Semiconductors for Thin-Film Transistors Based on the Indenofluorenebis(dicyanovinylene) Core. *Journal of the American Chemical Society* **2008**, *130* (27), 8580-8581; (d) Hwang, Y.-J.; Ren, G.; Murari, N. M.; Jenekhe, S. A., n-Type Naphthalene Diimide-Biselenophene Copolymer for All-Polymer Bulk Heterojunction Solar Cells. *Macromolecules* **2012**, *45* (22), 9056-9062.
22. Liu, Y.; Wan, X.; Wang, F.; Zhou, J.; Long, G.; Tian, J.; You, J.; Yang, Y.; Chen, Y., Spin-Coated Small Molecules for High Performance Solar Cells. *Advanced Energy Materials* **2011**, *1* (5), 771-775.
23. Sandmeyer, T., Über Isonitrosoacetanilide und deren Kondensation zu Isatinen. *Helvetica Chimica Acta* **1919**, *2* (1), 234-242.

APPENDIX

LIST OF ACRONYMS AND DESCRIPTIONS

Acronym	Description
A- <i>cis</i> -BBO	Asymmetric <i>cis</i> -benzobisoxazole
A-D-A	Acceptor-donor-acceptor
A- <i>trans</i> -BBO	Asymmetric <i>trans</i> -benzobisoxazole
AcOH	Acetic acid
APCI	Atmospheric pressure chemical ionization
BBO	Benzobisoxazole
BBTZ	Benzobithiazole
BBX	Benzobisoxazinone
BDT	Benzo[1,2- <i>b</i> :4,5- <i>b'</i>]dithiophene
BHJ	Bulk hetrojunction
CHCl ₃	Chloroform
<i>cis</i> -BBO	<i>cis</i> -benzobisoxazole
CV	Cyclic voltammetry
DAHQ	2,5-diamino-1,4-hydroquinone
DCC	N,N'-Dicyclohexylcarbodiimide
DCU	Dicyclohexylurea
DIO	1,8-diiodooctane
DMAP	4-(Dimethylamino)pyridine
DMF	Dimethyl formamide
DMSO	Dimethyl sulfoxide
DP	Degree of polymerization
DPP	Diketopyrrolopyrrole

Acronym	Description
DSC	Differential scanning calorimetry
E_g	Bandgap
ESI	Electron-spray ionization
eV	Electron volts
FF	Fill factor
GPC	Gel permeation chromatography
HOMO	Highest occupied molecular orbital
HRMS	High resolution mass spectrometry
ITO	Indium tin oxide
J_{sc}	Short circuit current density
LUMO	Lowest unoccupied molecular orbital
m/z	Mass to charge ratio
MeCN	Acetonitrile
M_n	Number-averaged molecular weight
MP	Melting point
M_w	Weight-averaged molecular weight
MW	Molecular weight
NMR	Nuclear magnetic resonance
OFET	Organic field-effect transistor
OLED	Organic light-emitting diode
OPV	Organic photovoltaic
P3HT	Poly(3-hexylthiophene)
PCBM	[6,6]-Phenyl-C61-butyric acid methyl ester
PCE	Power conversion efficiency

Acronym	Description
PDI	Polydispersity index
PEDOT:PSS	Poly(3,4-ethylenedioxythiophene) poly(styrenesulfonate)
PPA	Polyphosphoric acid
PPSE	Polyphosphoric acid trimethylsilyl ester
PPV	Poly(phenylenevinylene)
SCE	Standard calomel electrode
T_d	Thermal decomposition temperature
TFA	Trifluoroacetic acid
THF	Tetrahydrofuran
TGA	Thermal gravimetric analysis
<i>trans</i> -BBO	<i>trans</i> -benzobisoxazole
V_{oc}	Open circuit voltage